Title
Maximum Magnitude and Probabilities of Induced Earthquakes in California Geothermal Fields: Applications for a Science-Based Decision Framework

Author
Weiser, Deborah Anne

Publication Date
2016

Peer reviewed|Thesis/dissertation

UNIVERSITY OF CALIFORNIA

Los Angeles

Maximum Magnitude and Probabilities of Induced Earthquakes in California Geothermal Fields: Applications for a Science-Based Decision Framework

A dissertation submitted in partial satisfaction of the

requirements for the degree

Doctor of Philosophy in Geology

by

Deborah Anne Weiser

2016

ABSTRACT OF THE DISSERTATION

Maximum Magnitude and Probabilities of Induced Earthquakes in California Geothermal Fields: Applications for a Science-Based Decision Framework

by

Deborah Anne Weiser

Doctor of Philosophy in Geology

University of California, Los Angeles, 2016

Professor David D. Jackson, Chair

Induced seismicity is occurring at increasing rates around the country. Brodsky and Lajoie (2013) and others have recognized anthropogenic quakes at a few geothermal fields in California. I use three techniques to assess if there are induced earthquakes in California geothermal fields; there are three sites with clear induced seismicity: Brawley, The Geysers, and Salton Sea. Moderate to strong evidence is found at Casa Diablo, Coso, East Mesa, and Susanville. Little to no evidence is found for Heber and Wendel.

I develop a set of tools to reduce or cope with the risk imposed by these earthquakes, and also to address uncertainties through simulations. I test if an earthquake catalog may be bounded by an upper magnitude limit. I address whether the earthquake record during pumping time is consistent with the past earthquake record, or if injection can explain all or some of the

earthquakes. I also present ways to assess the probability of future earthquake occurrence based on past records. I summarize current legislation for eight states where induced earthquakes are of concern. Unlike tectonic earthquakes, the hazard from induced earthquakes has the potential to be modified. I discuss direct and indirect mitigation practices. I present a framework with scientific and communication techniques for assessing uncertainty, ultimately allowing more informed decisions to be made.

The dissertation of Deborah Anne Weiser is approved.

George Peter Bird

Edward Parson

Gilles F. Peltzer

David D. Jackson, Committee Chair

University of California, Los Angeles

2016

DEDICATION

Although not scientists by trade, my family has never failed to encourage or support my scientific curiosity. From stealthily dumping out my rock-collection-storage-cum-beef-jerky-container so I could collect more the next day, to experiencing my first earthquakes with me, or indulging my constant questioning of the natural world, the three of you have been a part of it all. Mom, Dad, and Becca, thank you for being my scientific sounding board, for always wanting to know what I've learned, and for helping me keep my eye on the ball.

Corey: thank you for your input, understanding, compassion, and unwavering support throughout this process. Perhaps you've even become a little bit more of a rock nerd along the way!

This work is dedicated to you, my favorite rocks.

Table of Contents

List of Figures

List of Tables

ACKNOWLEDGEMENTS

The United States Geological Survey supported this work. This research was also supported by SCEC, which is funded by NSF Cooperative Agreement EAR-1033462 and USGS Cooperative Agreement G12AC20038. The SCEC award number supporting this work is 13167.

I couldn't have asked for a more thoughtful, kind, and supportive advisor. Dave, your unfaltering positive attitude always made for pleasant meetings and discussions. Your untiring advocacy for your students and for the greater good of science has served as a wonderful example to those of us lucky enough to work with you. Thank you for your insightful contributions to my work, and especially for your comments during the home stretch.

The members of my dissertation committee, Peter Bird, Gilles Peltzer, and Edward Parson, have generously given their time and expertise to better my work. I thank them for their contributions and their good-natured support.

I want to acknowledge the many friends, colleagues, teachers, and fellow students who assisted, advised, and supported my research and writing efforts over the years. I would especially like to thank Lucy Jones, for hiring an energetic 20-year-old college student as an intern. I am eternally grateful for your dedication to me as a budding scientist, and for all you have done to support my career development. Without Bob Dollar's a-R-tful leadership and guidance, I would still be using Excel! Thank you for teaching me how to code with R, and for always encouraging me to ask the right question before seeking an answer. Kathy, thank you for your enduring support and uncanny ability to send encouraging words at the just right moment. Thanks to my SAFRR and USGS colleagues for your intellectual support, and for helping create the "special sauce" in the disaster science world.

I am grateful to my fellow graduate students and peers who have persevered with me throughout this process. Thank you for your writing and coding help, moral support, high fives, and cute animal videos. I would especially like to thank Anne, Britney, Carolyn, Carrie, Dalal, Emily, Ivy, Jen, Jess, Lindsay, Michelle, Mike, Ricky, and Shayna.

Finally, to all my friends and family who have supported me and encouraged me through this process, thank you.

CURRICULUM VITAE

EDUCATION EXPERIENCE

2008-2016 University of California, Los Angeles
Geology Ph.D., expected, Department of Earth, Planetary, and Space Sciences

2004-2008 Occidental College
B.A. Geology, Cum Laude

PROFESSIONAL EXPERIENCE

2006-Present **U.S. Geological Survey** Pasadena, CA
Student Trainee-Geology

Served on steering Committee for the 2008 Great Southern California ShakeOut, the largest earthquake drill in US History, with over 5 million participants. The ShakeOut has grown to include +20 million participants worldwide. Contributed to the scientific development and organization of the ShakeOut Scenario for the USGS Multi-Hazards Demonstration Project.

Prepare and deliver presentations to represent the USGS in local schools regarding geology and geology-based careers and educating students on how to respond in an earthquake.

Organize and deliver science-based presentations on topics including: earthquake safety, local hazards, mitigation, disaster preparedness, and earthquake early warning.

2008-2016 **University of California, Los Angeles** Los Angeles, CA
Teaching Assistant, Teaching Associate, and Teaching Fellow

Prepare material for, teach, and evaluate 60-100 undergraduate students for general education Earth, Planetary and Space Science courses.

Guest lecture, grade, administer exams, and assist the course professor with crucial tasks.

Hold twice-weekly office hours to assist students experiencing difficulties in the course.

2007 **Southern California Earthquake Center** Los Angeles, CA
SURE (Summer Undergraduate Research Experience) Intern

Awarded competitive summer internship.

Performed and completed self-guided research study investigating the influence of fracture patterns on precariously balanced rocks (PBRs), and how PBRs serve as paleo-earthquake ground motion indicators.

Field team assistant on three trenches in the Bidart Fan section of the San Andreas Fault. Prepared and mapped trench walls, used Adobe Illustrator and Photoshop to digitize maps, collected and analyzed C-14 samples, took aerial photographs, and analyzed field work results.

HONORS AND AWARDS

2014 Seismological Society of America Geosciences Congressional Visits Day Student Travel Grant Winner

2009-2012 Four-time Excellence in Teaching award: UCLA Dept. of Earth and Space Sciences

2009 Certificate of Recognition from City of Los Angeles for service to southern California and work on the ShakeOut Steering Committee

2004-2008 Dean's List, Occidental College

SAMPLE RESEARCH EXPERIENCE

2009-2016	Ph.D. Research on Induced Seismicity: Compare spatiotemporal correlations between geothermal pumping and earthquake occurrence. Determine if a population maximum magnitude can be identified from a sample of earthquakes. Develop and present quantitative toolkit for mitigating and preparing for induced seismicity
Spring 2009	Ph.D. Field Research in Tangshan, China, trenching along the Guye Fault
Summer-Fall 2005	As Occidental College Research Field Assistant, paleomagnetic studies on northern San Andreas Fault.

PROFESSIONAL ASSOCIATION MEMBERSHIPS

Seismological Society of America

American Geophysical Union

Southern California Earthquake Center

SELECT PUBLICATIONS

Weiser, D.A. and D.D. Jackson, in review, Observed and possible maximum magnitudes of induced earthquakes?, Journal of Geophysical Research: Solid Earth.

van der Elst, N.J, M.T. Page, D.A. Weiser, T.H.W. Goebel, and S.M Hosseini, in press, Induced earthquake magnitudes are as large as (statistically) expected.

Weiser, D.A. and D.D. Jackson, 2016, Science-based decision making in a high-risk energy production environment, Abstract presented at 2016 Seismological Society of America Annual Meeting, Reno, Nevada, April 20-22.

Weiser, D.A. and D.D. Jackson, 2015, Relative Contributions of Tectonic Strain and Pumping to Seismicity at California Geothermal Fields, Abstract presented at 2015 Seismological Society of America Annual Meeting, Pasadena, California, April 21-23.

Weiser, D.A., Mar/Apr 2015, Lessons I learned while attending the 2014 Geosciences Congressional Visits Day. Seismological Research Letters 86.2A (2015): 305-306.

Weiser, D.A., D.D. Jackson, and L.M. Jones, 2014, Maximum magnitudes of earthquakes in geothermal fields? Abstract presented at 2014 American Geophysical Union Annual Meeting, San Francisco, CA, Dec. 15-19.

Weiser, D.A., D.D. Jackson, and L.M. Jones, 2014, Geothermal pumping and induced seismicity in California geothermal fields, Abstract presented at 2014 Seismological Society of America Annual Meeting, Anchorage, Alaska, April 30-May 2.

Weiser, D.A., L.M. Jones, and E. Hauksson, 2012, Aftershock Decay with Distance from a Fault, Abstract presented at 2012 Southern California Earthquake Center Annual Meeting, Palm Springs, California, Sept. 9-12.

Red Cross Multi-Disciplinary Team, 2011, Report on the 2010 Chilean earthquake and tsunami response: U.S. Geological Survey Open-File Report 2011-1053, v. 1.1, 68 p., available at http://pubs.usgs.gov/of/2011/1053/.

Weiser, D.A., 2011, Relationships Between Earthquakes and Mapped Faults, Abstract presented at 2011 XXV International Union of Geodesy and Geophysics General Assembly, Melbourne, Australia, June 28-July 7.

1 Dissertation introduction

Geothermal energy will continue to develop around the world as reliance on alternative energy grows, including expansion into more seismically active areas. Pumping fluids in and out of the ground, as done in geothermal fields, has been shown to induce earthquakes (e.g. McGarr et al. 2002, Brodsky and Lajoie 2013). This dissertation is the first study that examines all of California's major geothermal fields for induced seismicity.

In California, a decades-long earthquake record exists, in some places beginning in the early 1900s. Geothermal pumping began at The Geysers in 1960, and elsewhere around the state in the 1980s. The earthquake record has been improving with the advent of more advanced technology, and areas of seismic concern have been identified. Are these earthquakes caused by geothermal activities? In the past, some geothermal activities have been aborted because of perceived earthquake risk, so it is an important issue that merits investigation.

The process of differentiating natural and induced earthquakes may be challenging, but methods I present here begin to address this, and can be also applied to other areas such as those with extensive pumping under high pressures. I examine magnitude frequency relationships and compare prior earthquake rates to those during the pumping interval both near and far from the well. This work can help constrain earthquake activity as likely induced or not.

The decision making process in an environment of uncertainty is not unique to the geothermal industry. There are parallels with other energy production endeavors that may generate earthquakes; therefore I include examples from oil and gas production (including fracking and wastewater disposal), enhanced geothermal systems (EGS), and more traditional geothermal production. Here, I introduce my dissertation work and summarize the main results.

1.1 Observed and possible maximum magnitudes of induced earthquakes?

I investigate the hypothesis that an observed earthquake magnitude distribution provides information on the upper magnitude limits at California geothermal fields and at other fluid injection sites around the world. I assume that earthquakes occur as a temporal Poisson process with a doubly-truncated Gutenberg-Richter magnitude distribution. Confidence limits on the expected largest magnitude can be inferred from the lower and upper magnitude limits, the b-value, and the number of earthquakes in the catalog. McGarr (2014) suggested that maximum magnitudes for injection-induced earthquakes are constrained by the volume of injected fluid. For appropriate catalogs, I evaluate whether McGarr's data may be explained instead by the random occurrence of events with a much higher magnitude limit. For the cases studied, the observed maximum earthquake is within the 95% confidence limits, such that I cannot refute an assumed upper magnitude limit of 10 or larger. In other words, the largest observed magnitudes at those sites are consistent with those expected from random samples of a population with a virtually unlimited upper magnitude. Nevertheless, catalog properties can be useful in estimating the probability of the largest event in a specified future time interval. I expect that at California geothermal fields, magnitude 5 and larger earthquakes can occur within four years with substantial probability.

1.2 Relative contributions of induced earthquakes, and examination of temporal correlation of earthquakes and injection with time

Previous studies of induced seismicity in California geothermal fields investigate only one or two fields or a few wells, and an examination of all of the state's geothermal fields has yet not been performed until now. I subject each geothermal field to three approaches designed to

characterize possible induced seismicity. Two approaches, exploring spatiotemporal correlations between earthquakes and pumping and using criteria checklists, are already widely used. For the third approach, I have developed a linear combination of two hypotheses, and determine the maximum likelihood fit between yearly earthquake rate and yearly injected volume. Results indicate the proportion of the total earthquake catalog that is induced. Finally, all evidence is summarized, and I classify each field as having strong, moderate to strong, or poor evidence for induced earthquakes.

1.3 Science-based decision making in a high-risk energy production environment

When beginning energy production practices that may induce earthquakes, decisions must be made about acceptable risk. How much ground shaking, structural damage, infrastructure damage, or delays of geothermal power and other operations is tolerable? I review current and past mitigation strategies as well as existing protocol. A framework for making decisions in the case of (potentially) risky earthquakes is presented. Timely and accurate scientific information can assist in determining the costs and benefits of changing production parameters. Helpful information includes a probability estimate of adverse effects ("costs"), frequency of earthquakes of different sizes, and associate impacts of different magnitude earthquakes.

Mitigation efforts benefit from risk management decisions based on robust science, which are well communicated to stakeholders. Valuable elements to communicate include risks and benefits of different actions (such as a traffic light protocol), factors considered when deciding what is acceptable risk, and the probability of specific magnitude events. Effective communication requires disseminating information to multi-lingual communities and those with

low science-literacy, and it should include non-traditional end-product delivery methods such as using social media, and other forms of digital interfaces.

I present a case example for The Geysers geothermal field to discuss locally "acceptable" and "unacceptable" earthquakes, and share nearby communities' responses to smaller and larger magnitude earthquakes. What magnitude earthquake is tolerable (to both local residents and operators)? I use the USGS's "Did You Feel It?" data archive to sample how often felt events occur and how many of those are above acceptable magnitudes.

Using methods developed in Chapters 2 and 3, I develop a science-based framework for lessening seismic risk and other negative consequences. This includes assessing future earthquake probabilities based on past earthquake records. One of my goals is to help characterize uncertainties in a way that they can be managed; to this end, I present simple and accessible approaches that can be used in the decision making process.

1.4 References cited

Brodsky, E. and L. Lajoie, 2013, Anthropogenic Seismicity Rates and Operational Parameters at the Salton Sea Geothermal Field. Science, vol. 341, p. 543-546.

McGarr, A., D. Simpson, and L. Seeber, 2002, Case histories of induced and triggered seismicity, *International Handbook of Earthquake and Engineering Seismology*, Part A, W.H.K. Lee et al., eds., Academic Press, 647-661.

McGarr, A., 2014, Maximum magnitude earthquakes induced by fluid injection, J. Geophys. Res.: Solid Earth, vol. 119. 12pp.

2 Observed and possible maximum magnitudes of induced earthquakes?

2.1 Introduction

A recent boom in the production of oil, gas, and geothermal energy has led to unprecedented increases in earthquake rates at many locations in the United States and around the world (e.g. Ellsworth 2013; Ellsworth et al. 2015; Rubinstein and Mahani 2015). In most cases earthquakes have been small or moderate, but is there a maximum magnitude for future earthquakes?

"Maximum magnitude," without qualifiers, is often used to describe the largest observed earthquake (e.g. McGarr 2014, Yeck 2015), the largest earthquake based on fault parameters or physical properties (e.g. Wells and Coppersmith 1994; Zoback and Gorelick 2012), a statistical confidence limit for the largest earthquake in a specified time interval (e.g. Holschneider et al. 2014), etc. Many authors attempt to predict, test for, or determine an upper bound for future magnitude at sites with reported induced seismicity (e.g. Hallo et al. 2014; Yeck et al. 2015; Holschneider et al. 2014; McGarr 2014). Here I distinguish the magnitude of the largest observed earthquake, M_{obsmax}, from $M_{possmax}$, the largest possible. My analogy is that $M_{possmax}$ is the largest earthquake (upper bound) in a population of events with a doubly truncated Gutenberg-Richter (G-R) magnitude distribution (Holschneider et al. 2011), and M_{obsmax} is the largest in a sample of N events from that population. As long as the magnitude scale is consistent in comparing sites, the details of the magnitude scale do not matter much. Most specific magnitudes, M, to which I refer in the text, are moment magnitudes.

The largest possible earthquake has strong practical implications for building codes, engineering standards, insurance rates, and public safety; thus accurate estimation of $M_{possmax}$ could be quite valuable. The largest observed earthquake is often taken as an estimate of $M_{possmax.}$ However, the

largest event in any future time interval will of course depend on the number of events, and M_{obsmax} will approach $M_{possmax}$ statistically only as the sample size, and thus the specified time interval, approaches infinity. The sample size needn't be strictly proportional to a specified time interval because the earthquake rate may vary, perhaps in a predictable way. Zöller and Holschneider (2014) postulated a two-parameter relationship between pumping rate and earthquake rate for a fluid-injection site at Paradox Valley, Colorado. They estimated the two parameters and a uniform b-value from catalog and pumping data. Assuming a doubly truncated G-R magnitude distribution, they then estimated confidence intervals for the expected largest magnitude in a sample of a given size. In a doubly truncated G-R model, the probability density function of observed magnitudes (M) between M_c and $M_{possmax}$ is given by

$$P_{\beta M_{poss\max}}(M) = \frac{\beta e^{(-\beta M)} \chi_{[Mc, M_{poss\max}]}(M)}{e^{(-\beta M_c)} - e^{(-\beta M_{poss\max})}}, \tag{2.1}$$

where $\beta = \log(10) \times b$ represents the G-R b-value and the value of $\chi_{[Mc, M_{poss\max}]}(M)$ is equal to 1 between M_c and $M_{possmax}$, and 0 outside of those magnitudes (modified from Holschneider et al. 2011). With Zöller and Holschneider's (2014) assumed relationship between pumping and earthquake rate, they could then estimate the maximum pumping rate likely to produce a given magnitude with given probability.

Holschneider et al. (2011) showed that a typical earthquake catalog contains very little information about a limiting magnitude. However, a catalog with many earthquakes may in principle provide a useful limit on the absolute maximum. Holschneider et al. (2015) hint at this by using the word "almost" in their title. Kagan (2002) provides a mathematical basis. His equation 26 gives the likelihood function for the truncated Pareto distribution (the equivalent of the doubly truncated G-R distribution expressed in seismic moment instead of magnitude, and assumed to be related to a physical limit). The upper moment limit M_{xc}, analogous to the absolute

upper magnitude limit, appears explicitly in that equation. Kagan emphasizes that the influence of M_{xc} is weak, so that it can be estimated only under special circumstances. The difference between a truncated and tapered earthquake distribution is only important for earthquakes near the upper limit ($M_{possmax}$ in the truncated version and M_{corner} in the tapered version). In this case, it makes little difference, and the truncated version is easier to deal with in computations. Here I examine the available catalogs for California geothermal zones to see if circumstances allow an upper magnitude limit to be constrained for any of the zones.

Recent induced seismicity literature includes correlations between the largest observed magnitude (M_{obsmax}) and various measures of pumping activity. McGarr (2014) plotted M_{obsmax} vs. the volume of injected fluid at several sites around the world (Figure 2.1), finding that M_{obsmax} is generally less than or equal to a value proportional to the injected volume. He further suggested that the maximum magnitude ($M_{possmax}$) is physically limited by injected volume if certain standard conditions hold, such as increase of pore pressure due to saturation of pores in brittle rock. Unfortunately, his paper did not clearly define the procedures that he used to set time and space windows for his calculations of injected volume associated with each earthquake (or study area). Clarification of this in future publications would be helpful, if his method persists. I ask whether McGarr's findings may be explained instead by the number of earthquakes in the catalog drawn from a population with a much larger magnitude limit.

2.2 Data and study locations

2.2.1 Geothermal field locations and data sources

I focus on the nine large geothermal fields in California with active injection wells: Brawley, Casa Diablo, Coso, East Mesa, Geysers, Heber, Salton Sea, Susanville, and Wendel (e.g. Weiser

et al. 2014). I also examine the case studies in McGarr (2014), and I present new interpretations for Basel, Switzerland and the Raton basin in Colorado and New Mexico. I examine earthquakes within close proximity to nearby injection wells for each site (see example in Figure 2.2).

I have made use of many different earthquake catalogs in this paper. For northern and southern California, I selected the most regionally comprehensive and widely available double difference catalogs. For northern California, I use the Waldhauser and Schaff (2008) catalog, for which data are available from 1984 to 2012. From 2012-present I use Waldhauser's double-difference catalog (2009). The Waldhauser and Waldhauser and Schaff catalogs were accessed via the Northern California Earthquake Data Center (NCEDC) website (http://ncedc.org/ncedc/catalog-search.html). For southern California earthquake data, I utilize the Hauksson, Yang, and Shearer (2012) catalog (1981 – June 30, 2011); for data from July 1, 2011 – present, I use the Southern California Seismic Network (SCSN) catalog (Hutton et al. 2010; SCEDC 2013). I also examine earthquake catalogs for Raton basin (Rubinstein et al. 2014), Soultz-Sous-Forêts (BCSF 2009), and Basel (Fäh et al. 2011; http://hitseddb.ethz.ch:8080/ecos09/query). Data are current through March 22, 2015. Catalogs were last accessed on March 25, 2015.

2.2.2 Data choices and assumptions

In most of the figures presented, curves are calculated from the inferred values of the magnitude higher than that which I have determined the catalog is complete (M_c), $N(M_c)$, the number of earthquakes above that completeness threshold, the Gutenberg-Richter (G-R) b-value (b), the largest historically observed earthquake (M_{obsmax}), and an assumed value of $M_{possmax}$ (arbitrarily large limiting magnitude). As described above, I make a subjective choice of the time period of the analyzed catalog and completeness threshold M_c such that the G-R b-value is stable. An

example of how I choose M_c is shown in Figure 2.3 and summarized briefly here: I plot the magnitude frequency diagram (MFD) and the variation of b-value with M_c. I determine the magnitude at which roll-off begins on the MFD diagram (Figure 2.3A); this can be found by examining the stable-slope portion of the line. When the slope of the line changes as magnitudes decrease (usually to a shallower slope), this can be taken as a lower bound of M_c. The start of this roll-off represents the minimum earthquake magnitude at which all earthquakes were recorded by the network. I compare this to a plot showing how b-values fluctuate with different M_c values. As seen in Figure 2.3B, the curvature of the points level off around the same M_c as the one I determine by looking at the slope on the MFD plot. The second plot does not always flatten out, in which case I only use the M_c determined from the MFD. In all cases, if there was more than one defensible value for M_c, the conservative option was selected.

I limit my analysis to locations with 30 or more earthquakes. With fewer earthquakes the estimated b-values have unacceptably large uncertainties. Thus I did not analyze confidence limits for the Wendel and Soultz-Sous-Forêts (from McGarr's 2014 paper) geothermal fields, even though the earthquake catalogs are available.

Since I am using McGarr's (2014) work as an example to evaluate hypotheses that place a limit on maximum magnitude, and his work examines injection-induced earthquakes, I focus on earthquakes near injection wells. I choose to select earthquakes hypocenters that occurred within 10 km of active injection wells. In some cases (e.g. Basel), the wells are no longer active; however, they were active at the time the majority of earthquakes were occurring.

Geysers introduced two new water sources in the last two decades, the second of which is called the Santa Rosa Geysers Recharge Program (SRGRP). It began carrying water to The Geysers for injection in November 2003. As seen in Figures 2.4 and 2.5, seismicity rates increased after the

increase in injection from these new water sources. I analyzed b-value and M_c for four time intervals (the start of the earthquake catalog – 1997; 1997 – 2003; 2003 – present; and the start of the catalog – present), based on the timing of increases in injection from the new water sources. The most conservative option was to use only data from after Nov. 1, 2003. I chose to focus on the recent past (earthquakes after Nov. 1, 2003) in order to estimate better the earthquake rate in the near future. Another choice is deciding which earthquake catalog to use.

There are catalogs of varying completeness and duration. One catalog may have more accurate hypocenter locations than another, but not have as long of a temporal duration or as low a completeness threshold. I examined different widely accessible catalogs (e.g. ComCat vs. Hauksson, Yang, and Shearer 2012) and determined that my findings would not change by varying which catalogs I use for California.

McGarr's hypothesis focuses on the relationship between fluid injection and earthquake magnitude. Therefore, I chose to concentrate my study around injection wells, rather than both injection and production sites. For California, I retrieved a list of active injection wells from the California Department of Oil, Gas, and Geothermal Resources (DOGGR 2011). Justin Rubinstein provided locations of Raton basin injection wells within New Mexico. Locations of the Raton basin wells in Colorado were found in Rubinstein et al. (2014). Markus Häring of Geo Explorers, Ltd. provided proprietary injection well locations for Basel, Switzerland and Soultz-Sous-Forêts, France. Figures were generated using R, Microsoft Excel, and Adobe Illustrator.

2.3 Methods

In any magnitude-based study it is helpful to examine the entire catalog rather than just the largest observed event. I assume a doubly truncated Gutenberg-Richter (G-R) magnitude

distribution and a uniform earthquake rate above the lower magnitude threshold. A doubly truncated G-R model restricts the well-known Gutenberg-Richter magnitude-frequency relation (Gutenberg-Richter 1956) between an upper and lower magnitude bound. Typically the lower threshold is near the magnitude of completeness, and the upper threshold is at or above an assumed upper magnitude limit. Once these assumptions are confirmed, (e.g. Figure 2.6) my results depend only on the magnitude of completeness (lower bound) M_c, the number of events, N, above that magnitude, and the b-value. I illustrate my methods using The Geysers geothermal field, as seen in Figures 2.2 and 2.4-2.8. It is the largest geothermal field in the world and has a large earthquake catalog. Following McGarr's focus on injection-induced earthquakes I include all earthquakes above the completeness magnitude within 10 km of active injection wells.

2.3.1 Catalog simulations

Simulated earthquake catalogs from an ideal doubly truncated G-R distribution can help to put a catalog of real events in context. These simulations choose random realizations of the G-R process and scale by the total number of earthquakes. I show the simulations for illustration only; my quantitative results come from analytical calculations presented below.

Random samples from the same G-R distribution exhibit a range of behaviors especially at upper magnitudes. I display cumulative magnitude distributions for five thousand simulated earthquake catalogs in Figure 2.7A. Doubling the number of simulated catalogs did not affect the results substantially, implying that further simulations were unnecessary. I employ a random number generator to simulate these catalogs, with input parameters derived from real data at each site. Inputs include the b-value, the magnitude of completeness, and the number of earthquakes greater than the completeness threshold, M_c. I also set an arbitrarily large value of 10 for the

limiting magnitude $M_{possmax}$. I am not advocating that a M10 earthquake could happen at any of the sites I discuss; rather I select that value to show that the largest observed earthquake is practically independent of the large limiting magnitude. If a magnitude 10 earthquake cannot be excluded, then no smaller limit can be determined with the available data.

Random samples drawn from the same GR distribution exhibit considerable scatter at the upper ends of the magnitude distribution, as can be seen in Figure 2.7A. The largest simulated earthquake in Figure 2.7 (A and B) had a magnitude of about 8.5, even though $M_{possmax}$ equals 10. As illustrated by the simulated catalogs, one can determine the probability (Figure 2.7B) that the largest earthquake in a sample of a given size would exceed a given magnitude. At present, the largest observed earthquake at The Geysers geothermal field is M4.7, well within the scatter predicted from these randomly generated catalogs. Thus the largest observed magnitude at The Geysers is quite consistent with the value expected if the population has a limiting magnitude of 10 or greater.

2.3.2 Assumptions

The completeness magnitude M_c and the uncertainty of earthquake magnitudes generally decrease with time as the number and quality of seismographs increase. Thus judgment is required to choose a beginning time and lower magnitude threshold of the catalog used for analysis. I choose a value for M_c such that using the methods described in Section 2.1; I ignored earthquakes smaller than this threshold and calculated the b-value using the maximum likelihood method (Aki 1965). This method does not account for the finite upper magnitude limit, but a correction for $M_{possmax}$ would be negligible for the relevant range of $M_{possmax}$. I assume a maximum possible magnitude and derive a cumulative density function for the largest

earthquake in a random sample of given size, lower threshold, b-value, and $M_{possmax}$. Similarly, I could derive a cumulative density function of the largest possible earthquake from the largest observed, but, as I show below, the largest observed depends very weakly on the largest possible unless it is very small or the number of events is exceptionally large.

I make three main assumptions about each observed or simulated catalog. 1) Earthquake data are described by a G-R magnitude distribution. 2) The marginal magnitude distribution within each test area is truncated to zero above magnitude $M_{possmax}$. 3) Earthquakes occur as a time-varying Poisson process, in which the rate of earthquakes can be assumed constant over short durations. Once I have a model for induced earthquakes as a function of pumping, I would be able to use a non-homogeneous Poisson model to estimate induced seismicity. I am asking what conditions are necessary to identify $M_{possmax}$. If $M_{possmax}$ cannot be identified in this special case with a Poisson process, one certainly would be unable to determine $M_{possmax}$ assuming the more general case of a non-homogeneous Poisson process. For forward projections, I assume the rate of earthquakes for the projection time window is the same as the average rate from the observed catalog.

2.3.3 Theory and application

For the doubly truncated Gutenberg-Richter distribution (equation 2.1), the probability that a single earthquake magnitude exceeds M is

$$P(M) = \frac{((10^{-bM}) - (10^{-bM_{poss\max}}))}{((10^{-bM_c}) - (10^{-bM_{poss\max}}))} \quad for\ M_c \le M \le M_{poss\max} \tag{2.2}$$

where b is the G-R b-value, $M_{possmax}$ is an assumed upper magnitude bound, M_c is the magnitude of completeness, and $M_c \le M \le M_{poss\max}$. By assumption P($M_{possmax}$) = 0, and because of the

normalization, P(M_c) = 1. Seismologists commonly refer to P(M) as the "normalized cumulative magnitude distribution". In conventional statistical notation, P(M) would be labeled the complementary distribution, and 1–P(M) would be the regular cumulative distribution. The "survival function"

$$S(M_{obs\max}) = 1 - (1 - P(M_{obs\max}))^N \tag{2.3}$$

is the probability that in a sample of N events, at least one event will be greater than M_{obsmax}. For chosen lower and upper critical values, SL and SU respectively, the confidence interval is defined by $SL \le S(M) \le SU$. I chose SL = 0.025 and SU = 0.975 to describe a two-sided 95% confidence interval.

Using simple algebra and replacing M by M_{obsmax}, I combine equations (2.2) and (2.3) to relate the parameters M_{obsmax}, $M_{possmax}$, M_c, N, b, and P: any one of them can be estimated if the others are known or assumed. S, the survival function, depends uniquely on P, the normalized cumulative G-R distribution, and N, the number of earthquakes. To estimate confidence limits for expected maximum magnitude in a random sample of N earthquakes, I choose critical values of S, estimate the corresponding P values from equation (2.3), and solve equation (2.2) for M_{obsmax} as a function of b, M_c, and $M_{possmax}$. The result is

$$M_{obs\max} = -\frac{1}{b}\log(P \times 10^{-bM_c} + (1 - P) \times 10^{-bM_{poss\max}}), \tag{2.4}$$

where P is computed from S using equation (2.3). Solving for P requires extreme numerical precision for large N, so it is useful to compute $\log(1 - P)$ first.

Figure 2.8 shows results using a suite of hypothetical $M_{possmax}$ values; b, M_c, and N from the catalog of events near injection wells at the Geysers geothermal field in California, and S values of 0.025 and 0.975, as described above. Any pair of M_{obsmax} and $M_{possmax}$ values not between the two curves can be rejected with 95% confidence. For the Geysers field M_{obsmax} is about 4.7, and

as shown in the figure any $M_{possmax}$ between 4.7 and a limiting magnitude of 10 cannot be rejected. The slopes of the critical curves are negligible, so $M_{possmax}$ values much larger than 10 could not be rejected either. The shape of the contours indicates why M_{obsmax} provides little information about $M_{possmax}$; for M_{obsmax} between about 4.4 and 6.2, any $M_{possmax}$ between M_{obsmax} and 10 would not be rejected.

The curves in Figure 2.8 depend on the sample size N, and the expected largest event M_{obsmax} should approach $M_{possmax}$ as N approaches infinity.

Given that a realistic sample provides no meaningful limit on $M_{possmax}$, is any forecast hopeless? Surely not. Given the observed rate of events at the lower threshold M_c, one can estimate the expected number of events in a future sample of any fixed time interval and use the equations above to estimate confidence limits for M_{obsmax} in that interval. I estimate the rate of $M \geq 5$ earthquakes, using the equation

$$N(M) = N(M_c) \times 10^{b(M_c - 5)}, \tag{2.5}$$

which assumes that the earthquake rates do not change with time. I summed the yearly rates over all the California geothermal fields, finding that the yearly rate of *M*5+ earthquakes within 10 km of any active geothermal injection well is about 0.25. The individual rates, as well as the values for M_c, $N(M_c)$, b, M_{obsmax}, and 95% confidence windows for M_{obsmax}, are listed for each field in Table 2.1. For a Poisson process with rate parameter λ, the probability of no events over time T is given by the equation

$$P(n = 0) = e^{-\lambda T} \tag{2.6}$$

(Evans et al. 1993), where λ = 0.25 per year, the probability of having no *M*5.0 within T = 4 years is 0.36, where T is taken from the above rate of 0.25 $M \geq 5$/year. Therefore, at least one earthquake would be expected within from the start of 2015 until the end of 2018 (four years) at

64% probability. In the last 34 years, there have been six $M \geq 5$ within 10 km of presently existing geothermal injection wells in California (those used in this study), corresponding to a rate of 0.18 per year. Unless conditions change substantially, I expect an earthquake of *M*5.0 or larger near an injection well within the same four year period with 64% probability, and expect an earthquake with the same stipulations within 12 years at 95% probability. I would withdraw my estimate if the rate of small events, or the b-value, were to decrease substantially.

Shaded in gray in Table 2.1 are results from two sites from McGarr's (2014) paper. I determine M_c, N(M_c), b, and M_{obsmax}. Wendel and Soultz have fewer than 30 earthquakes, and therefore are not included in this table or the rest of my study, as I chose to limit my analysis based on a minimum $N(M_c)$ and M_c. Testing magnitude limits of 10 and larger, I calculate 95% confidence bounds for expected maximum observed earthquakes. As is the case for each site, if M_{obsmax} falls between M_{low} and M_{high} (the values of M_{obsmax} at $M_{possmax} = 10$), $M_{possmax} \geq 10$ cannot be refuted.

2.4 Results

I confirm the general results of Holschneider et al. (2011) and, using data from California geothermal fields, I am in search of exceptions. I tested limiting magnitudes of 10 and larger, and present 95% confidence bounds for expected maximum observed earthquakes at each California geothermal field (Table 2.1). McGarr's (2014) paper shows the least upper bound for the examples he presents. I select a few data points from his paper (Basel, Soultz, Raton basin), and subject them to the same methods I developed for California. In all of the examples I have analyzed, I have found no defensible *upper bound* for earthquake magnitudes.

The bad news is that, from the available earthquake catalogs, one cannot expect to get any limiting information on the maximum possible earthquake size. The good news is that the

random process can be extrapolated forwards, and one can make a pretty good estimate of the range of earthquake sizes to expect in a finite time.

I expect an earthquake of *M5*.0 or larger within 10 km of an injection well in California within the four years from 2015-2018 with 64% probability. I expect such an event to occur with 95% probability during the 12 years from 2015-2026.

2.5 Discussion

One popular hypothesis is that earthquake magnitudes may be limited by the geometry of faults on which they occur. Wells and Coppersmith, (1994), Hanks and Bakun, (2014), and many others have shown correlations between fault rupture length, area, displacement, and other size measures as a function of earthquake magnitude. There is temptation to assume that fault dimension may impose an upper magnitude limit. However, the correlations referenced above are based on rupture length inferred after an earthquake, which is fundamentally different from the pre-existing fault length. Induced earthquakes frequently occur on previously unmapped faults (Yeck et al. 2014). Even for earthquakes that occur on known faults, some ruptures begin on unmapped faults and rupture onto previously mapped faults, or extend beyond mapped fault traces. Examples include the Landers (Hauksson et al. 1993), Denali (Haeussler et al. 2004), and El Mayor-Cucapah (Wei et al. 2011) earthquakes. Therefore, when attempting to pre-assign a maximum possible magnitude for a specific geothermal field or region, which fault should you consider? As mentioned, one may be tempted to use fault geometry (e.g. Wells and Coppersmith 1994 or Hanks and Bakun 2014). If a 300 km-long fault is only 20 km away, could an earthquake on a small nearby fault grow into a larger rupture? For the Salton Sea, which is less than 20 km from the mapped trace of the San Andreas Fault (SAF), should one assume $M_{possmax}$ for the

Salton Sea geothermal field is the same as the entire length of the SAF? I challenge the notion that magnitude-fault area scaling relations should be predictors of magnitude based on mapped fault length, and instead suggest a statistical approach to determine if maximum magnitude can be constrained given an earthquake catalog.

2.6 Conclusions

There are, in principle, conditions such that a sample catalog reveals useful information about the maximum magnitude of the population from which it is drawn. Those conditions require large numbers of events with magnitudes near the population maximum. None of the cases I examined satisfied those conditions. An upper magnitude limit of 10 or greater could not be refuted at any of the California geothermal sites I test, nor at the few sites I test from McGarr's (2014) study, based on current earthquake catalogs.

From the b-value of the earthquake population, it is possible to put confidence limits on the largest magnitude in a future sample of a given size and lower magnitude threshold. If the earthquake rate at the lower threshold can be estimated, then confidence limits can also be applied to a given future test period. These methods and results are applicable to both natural and induced earthquakes. I provide a general result that has broad implications when approaching the concept of maximum magnitude.

I retrieved sufficient earthquake data to apply my analysis for two sites (Basel and Raton basin) from McGarr's (2014) study. I found that the maximum observed magnitudes can be explained just as well by sampling a random process with an arbitrarily large upper limit, rather than a physically imposed limit based on the volume of injected fluids. This is an alternative explanation to that proposed in McGarr's (2014) paper.

Chapter 2 Figures

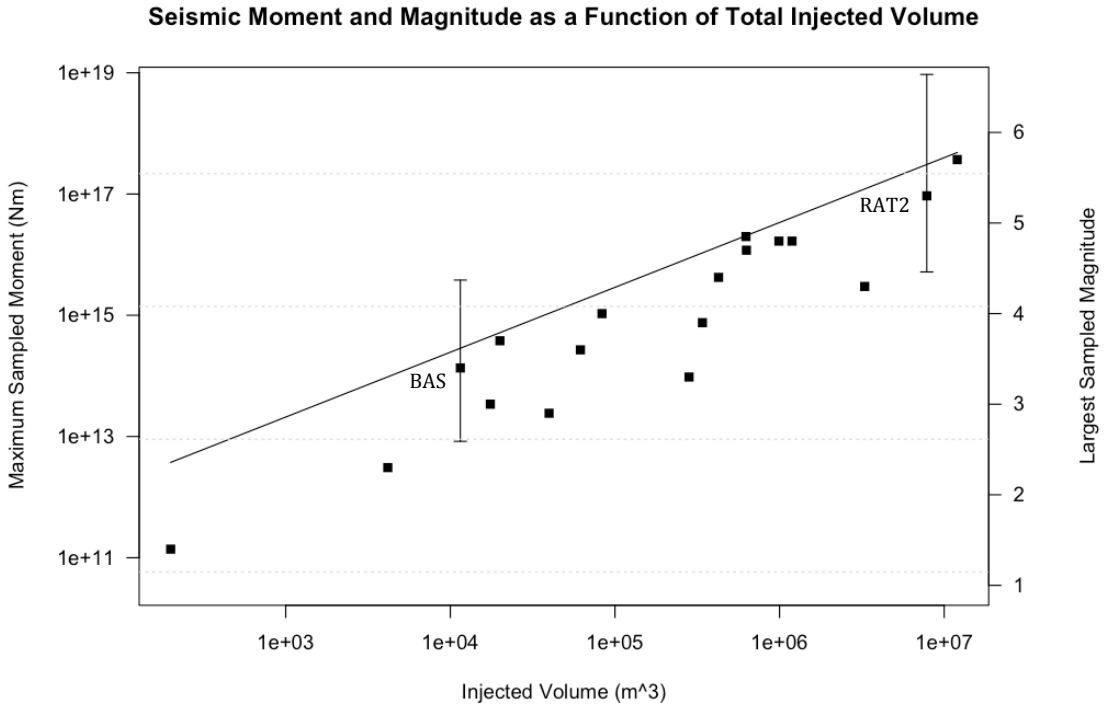

Figure 2.1

Relationship between seismic moment (and magnitude) of largest observed events from McGarr (2014), and injected volume thought to have induced them. McGarr described an upper bound for earthquake magnitudes induced by fluid injection; this relationship is represented by the diagonal line, and by the equation: $M_0 = G\Delta V$, where M_0 is moment, ΔV is injected volume, and G is the modulus of rigidity. I examine catalogs for Basel (BAS) and Raton basin (RAT2); the vertical lines demonstrate that the actual M_{obsmax} lies within the expected range of M_{obsmax} with $M_{possmax} \geq 10$. Soultz-Sous-Forêts had too few earthquakes to obtain results, and I've not yet obtained injection and catalog data for the other sites.

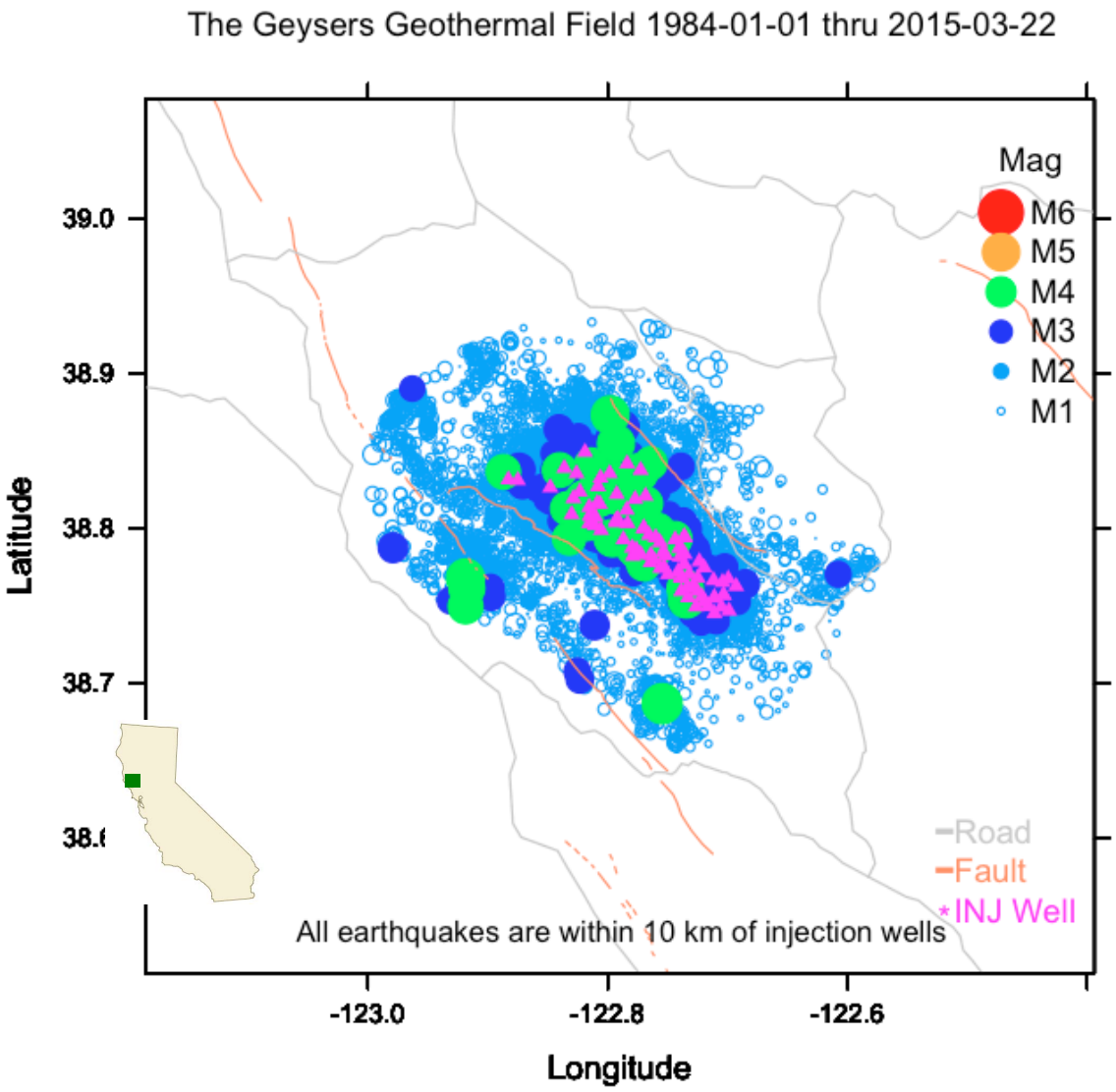

Figure 2.2

An example of the way I select seismic data, from The Geysers geothermal field. Earthquakes are shown as circles, the sizes and colors of which vary by magnitude. I consider all earthquakes within 10 km of the nearest active injection well (pink triangles). California well locations are from the California Department of Oil, Gas, and Geothermal Resources (2011). Inset map of California: California Energy Commission.

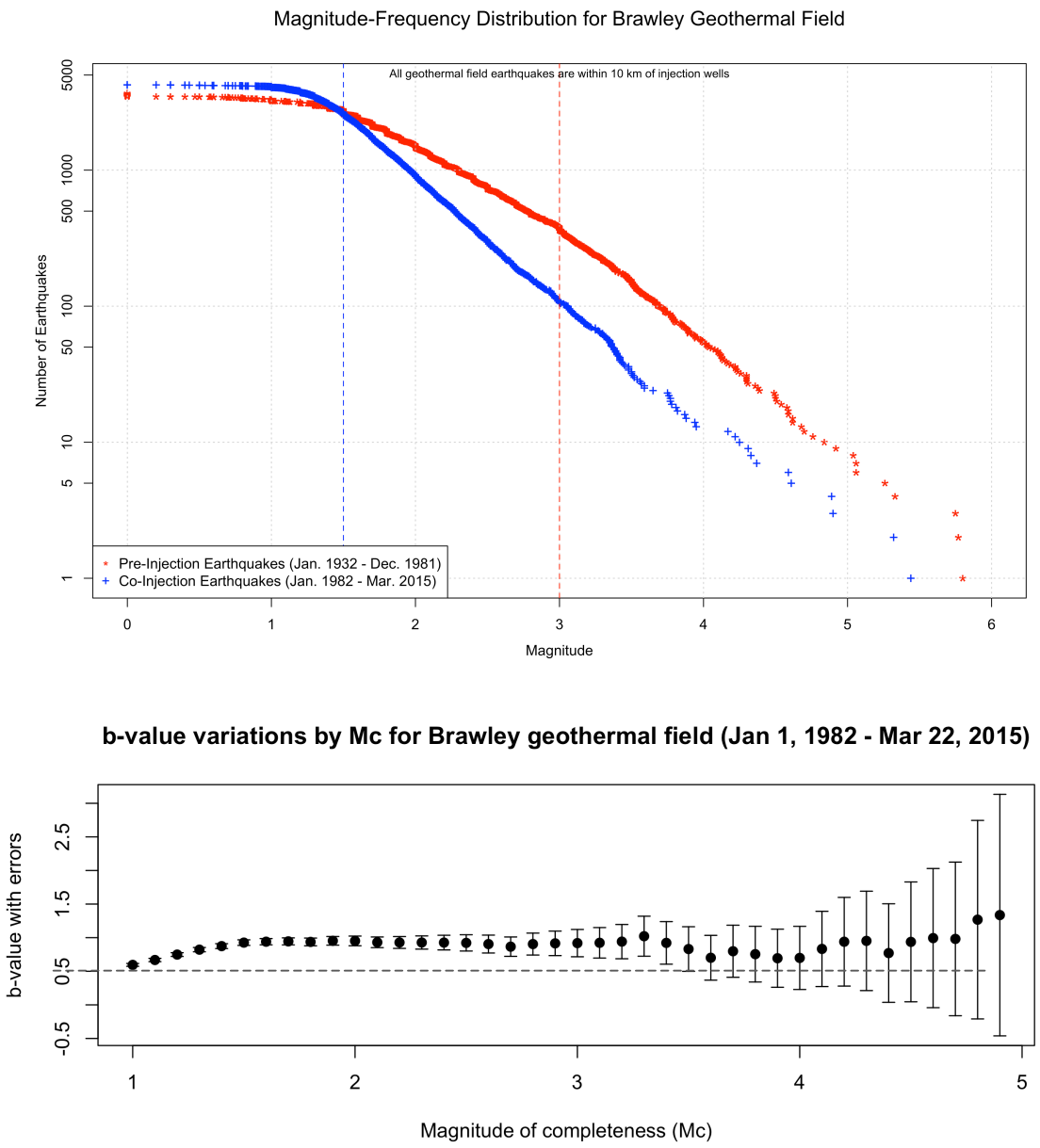

Figure 2.3

(A) I plot a magnitude-frequency diagram (MFD) and examine of the roll-off. Both pre- and co-pumping earthquakes are shown. These values are shown for earthquakes occurring within 10 km of active injection wells at the Brawley geothermal field. **(B)** Variations in estimated b-values as a function of assumed lower cutoff magnitude, M_c. Errors are shown as 98% confidence limits. b-value appears to stabilize around $M1.5$ and $b \sim 1.0$, so I take $M_c = 1.5$.

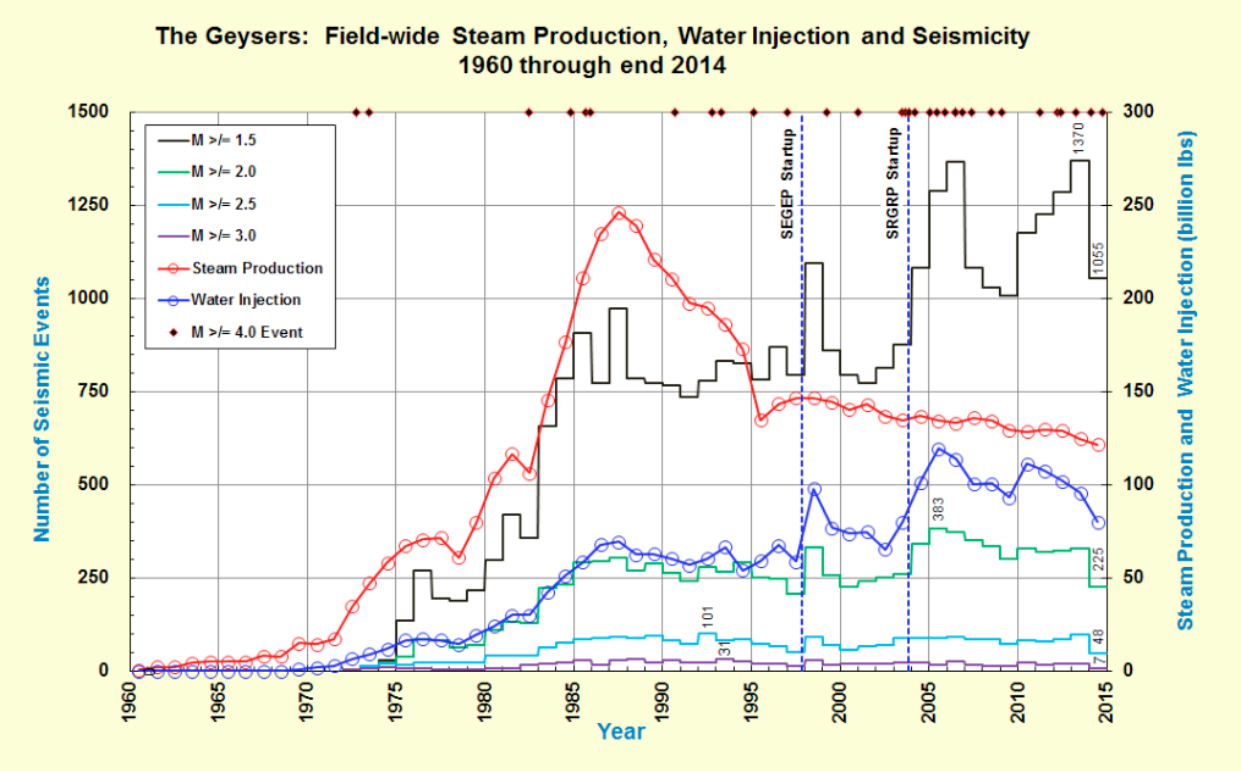

Figure 2.4

Production, injection and seismicity levels at The Geysers geothermal field, from 1960 through the end of 2014 (Hartline, 2015). Note the initiation of the SEGEP (South-east Geysers Effluent Pipeline) and SRGRP (Santa Rosa Geysers Recharge Project) water sources. In agreement with the data shown in this figure, Beall et al. (2010) confirm that in the years following the introduction of the new water sources The Geysers experienced new peak numbers of $M \geq 1.2$ earthquakes. Printed with permission from Calpine.

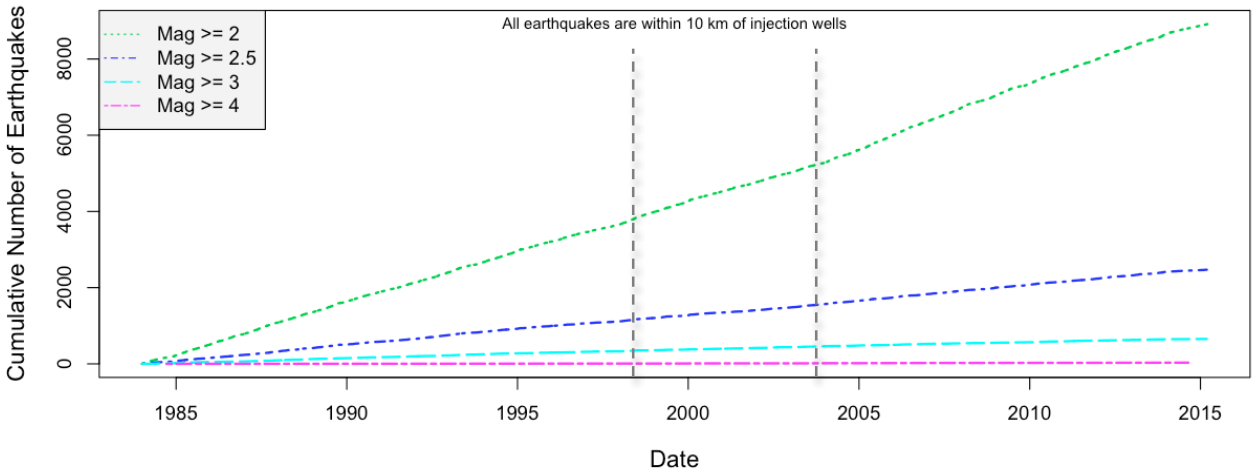

Figure 2.5

Cumulative number of earthquakes at The Geysers Geothermal field from 1984-2015, separated by magnitude. There is an observable rate change of $M \geq 2$ earthquakes around 1997 and late 2003. The dashed vertical lines indicate the arrival of water from the SEGEP (left) and SRGRP (right) sources. The increases in injection volumes correlates well with long-term seismicity rate increases.

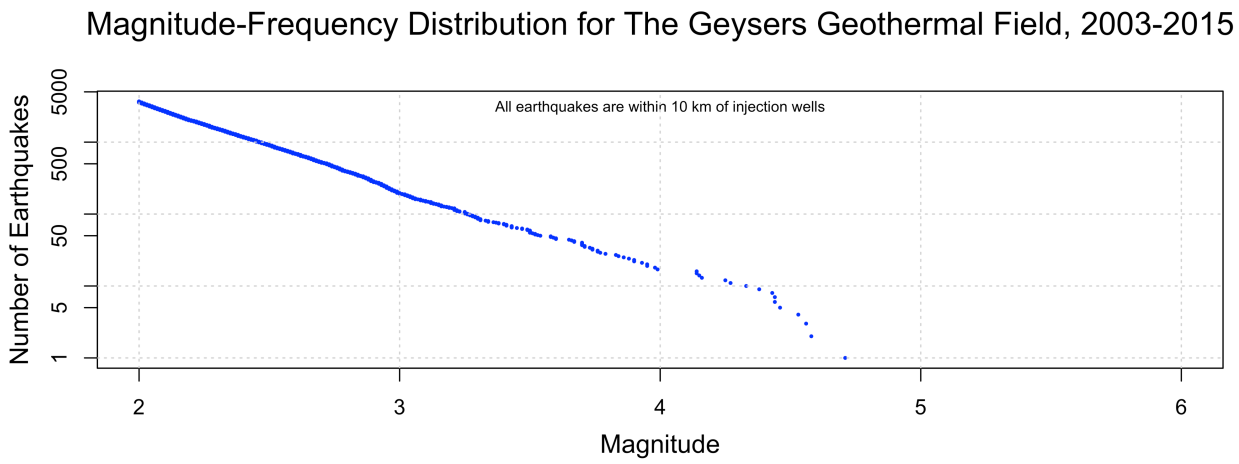

Figure 2.6

Observed magnitude-frequency distribution (MFD) for The Geysers Geothermal Field. I display data from 2003-2015, for which the catalog is complete above magnitude 2.

2.7A

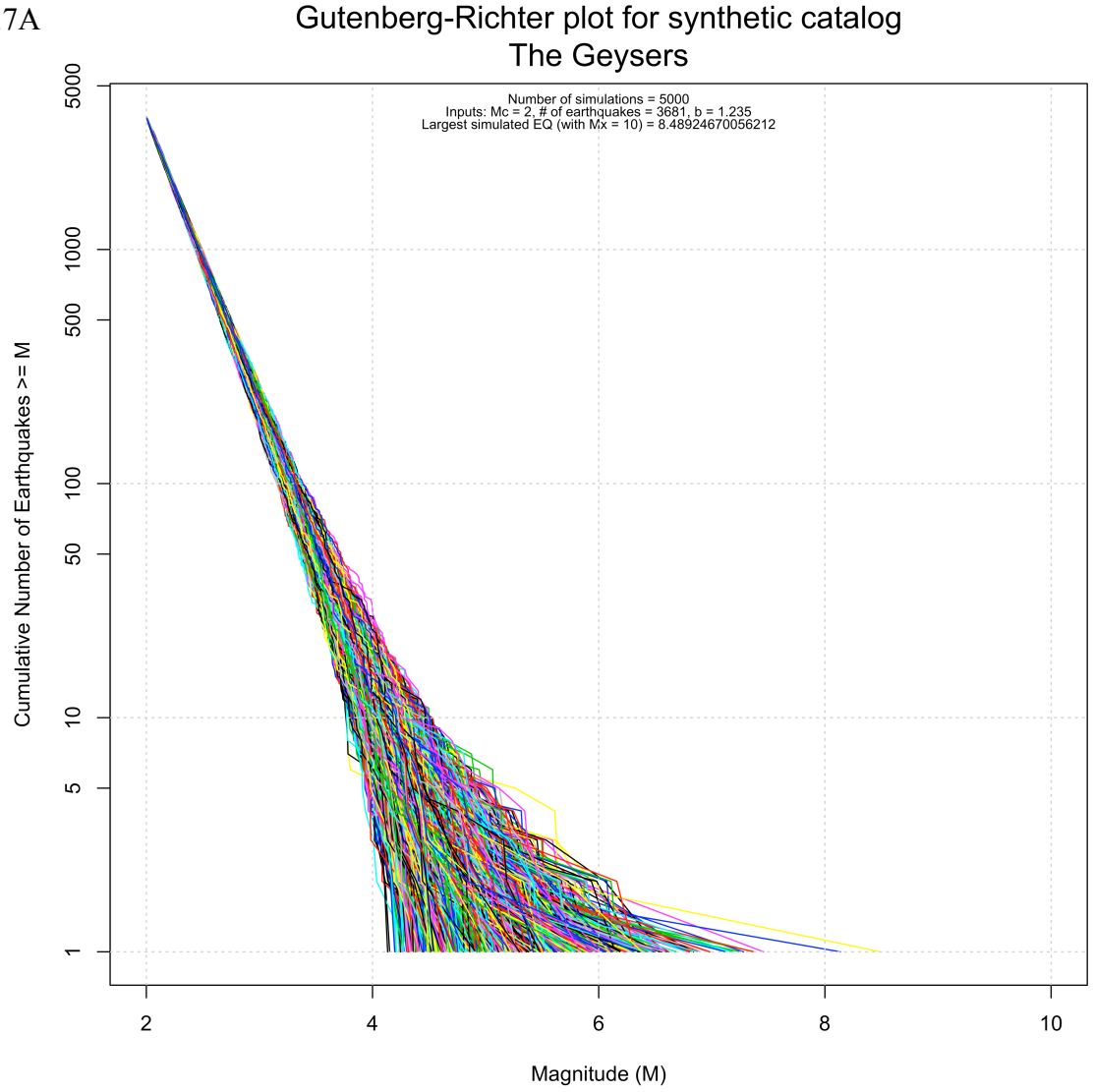
Gutenberg-Richter plot for synthetic catalog
The Geysers
Number of simulations = 5000
Inputs: Mc = 2, # of earthquakes = 3681, b = 1.235
Largest simulated EQ (with Mx = 10) = 8.48924670056212
Cumulative Number of Earthquakes >= M
5000
1000
500
100
50
10
5
1
2
4
6
8
10
Magnitude (M)

2.7B

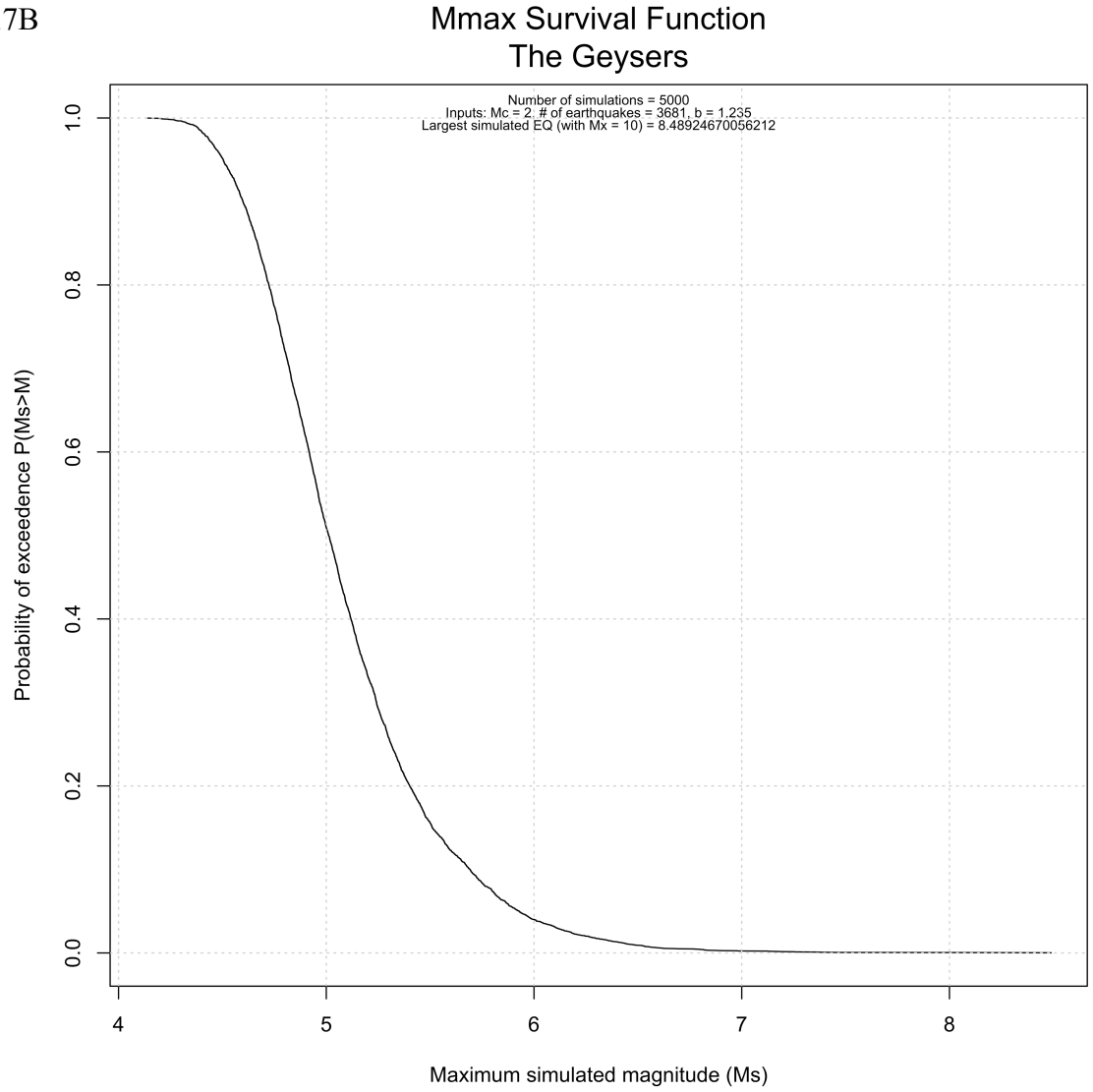
Mmax Survival Function
The Geysers
Number of simulations = 5000
Inputs: Mc = 2, # of earthquakes = 3681, b = 1.235
Largest simulated EQ (with Mx = 10) = 8.48924670056212
Probability of exceedence P(Ms>M)
0.0
0.2
0.4
0.6
0.8
1.0
4
5
6
7
8
Maximum simulated magnitude (Ms)

Figure 2.7

I calculate cumulative magnitude distributions for five thousand simulated earthquake catalogs **(A)**. I employ a random number generator to simulate these catalogs, with inputs derived from real data at each site. Inputs include the b-value, the magnitude of completeness, and the number of earthquakes greater than the completeness threshold, M_c. The example presented here is based on the number of earthquakes above M_c, within 10 km of injection wells at The Geysers geothermal field in northern California, from November 1, 2003 - March 22, 2015. I also selected an arbitrarily large magnitude ($M_{possmax}$) as the maximum possible magnitude; in these cases I selected a magnitude of 10. My deliberate selection of this magnitude is notated on the figure as "*Mx*" instead of $M_{possmax}$.

The largest observed earthquake (M_{obsmax}) at The Geysers (from 2003-2015) is *M*4.71. As seen here, this M_{obsmax} of 4.71 is consistent with $M_{possmax}$ = 10 given the number of events in the catalog. Other analytical results are consistent with an $M_{possmax}$ no smaller than 10 (Figure 2.8).

The large scatter at tail end of the magnitude distribution illustrates the wide range of earthquake magnitudes that can occur with the same numerical inputs. It is likely that I will neither simulate nor observe the true maximum magnitude. **(B)** The probability of exceeding each of the maximum simulated magnitudes (M_s) at The Geysers from November 1, 2003 - March 22, 2015.

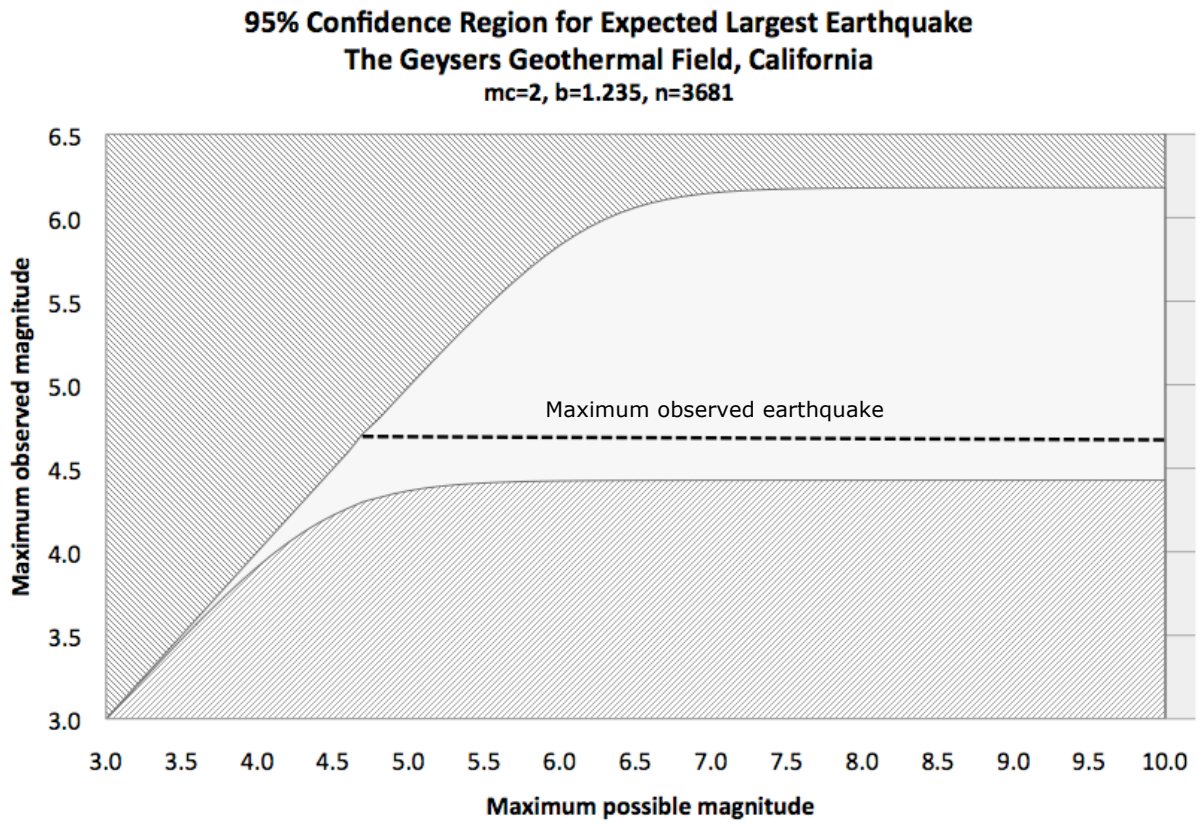

Figure 2.8

Confidence intervals for expected magnitude of the largest observed earthquake, conditioned on a truncated Gutenberg-Richter magnitude distribution with parameters described below, in a sample of 3681 quakes as a function of assumed maximum possible magnitude of the population. The lower magnitude threshold (2.0), the Gutenberg-Richter b-value (1.235), the earthquake count (3681), and the observed maximum magnitude are those estimated for The Geysers geothermal field in California, from November 1, 2003 to March 22, 2015. The white area is within the confidence intervals 0.025 to 0.975. The largest observed earthquake is consistent with any population maximum larger than M4.7; for lower values, the observed maximum would exceed the maximum possible earthquake. The upper and lower magnitude thresholds are essentially independent of the population maximum, and do not continue to

increase, because the expected number of large earthquakes is so small according to the Gutenberg-Richter distribution and the model saturates at these high magnitudes. With only a small sample size, the full magnitude distribution will not be observed.

Site	*Date Range*	M_c	$N(M_c)$	*b*	M_{obsmax}	M_{low}	M_{high}	*P(M5 in 5yrs)*
Brawley	1981/01/11-2015/03/17	1.7	2245	0.982±0.048	5.75	4.54	6.74	3.77×10^{-2}
Casa Diablo	1984/01/01-2015/03/22	1.7	9155	1.102±0.0268	4.88	4.78	6.74	6.77×10^{-2}
Coso	1981/01/20-2015/03/22	1.7	5462	1.13±0.036	5.17	4.51	6.42	2.98×10^{-2}
East Mesa	1982/2/2-2012/3/21	1.6	31	1.688±0.706	2.7	2.16	3.43	1.65×10^{-6}
The Geysers	2003/11/01-2015/03/22	2	3681	1.235±0.047	4.71	4.43	6.18	5.63×10^{-2}
Heber	1981/1/15-2015/3/16	2	739	1.251±0.107	4.13	3.84	5.57	3.81×10^{-3}
Salton Sea	1981/01/11-2015/03/17	1.9	2962	1.023±0.043	5.75	4.74	6.85	5.84×10^{-2}
Susanville	1985/10/23-2014/2/20	1.7	41	1.050±0.382	3.66	2.71	4.76	4.50×10^{-4}
Basel, Switzerland	2006/11/10-2007/11/30	1.2	173	1.209±0.214	3.4	2.59	4.37	4.17×10^{-3}
Raton basin, CO/NM	1963/6/6-2013/12/10	3	101	0.988±0.229	5.3	4.46	6.64	2.65×10^{-2}

Table 2.1

Parameters used to obtain magnitude and probability results for geothermal fields in California with active injection. Two sites from McGarr's (2014) study, Basel, Switzerland and Raton basin, CO and NM, are included (highlighted in gray). The table is based on earthquakes within 10 km of active injection wells. The date range is the date of the first earthquake after pumping began until the last earthquake (prior to or on 2015/03/22). M_c is the magnitude of completeness; $N(M_c)$ is the number of earthquakes with magnitudes greater than or equal to M_c; *b* is the GR b-value; M_{obsmax} is the largest observed earthquake during the specified date range; M_{low} and M_{high} represent the lower and upper 95% confidence bounds for the expected M_{obsmax} assuming $M_{possmax}$ = 10. For all fields in this study, M_{obsmax} falls between M_{low} and M_{high}, confirming that a limiting magnitude of 10 cannot be refuted based on catalog and input parameters. P(*M*5 in 5yrs) is the probability that within the next 5 years, a M≥5 larger earthquake will occur within 10 km of an active injection well at the specified field assuming the recent earthquake rate is maintained.

2.7 References cited

Aki, K., 1965, Maximum likelihood estimate of b in the formula log(N) = a − bM and its confidence limits, Bull. Earthq. Res. Inst. Tokyo Univ., 43, 237–239.

BCSF, Central Seismological Bureau of France (1960-2009), 2009, Seismicity Catalog of Metropolitan France, www.seisme.prd.fr/sismicite.html.

Beall, J., M. Wright, A. Pingol, and P. Atkinson, 2010, Effect of High Rate Injection on Seismicity in The Geysers, GRC Transactions, vol. 34, p. 1203-1208.

California Department of Oil, Gas, and Geothermal Resources (DOGGR), 2011, GeoSteam - Query Geothermal Well Records, Production and Injection Data, http://geosteam.conservation.ca.gov/WellSearch/GeoWellSearch.aspx.

California Energy Commission, California Clean Energy Tour: The Geysers. http://www.energy.ca.gov/tour/geysers/.

Ellsworth, W.L., 2013, Injection-induced earthquakes, Science, vol. 341, is. 6142, p. 1225942 1-7.

Ellsworth, W., A. Llenos, A. McGarr, A. Michael, J. Rubinstein, C. Mueller, M. Petersen, and E. Calais, 2015, Increasing seismicity in the U.S. midcontinent: Implications for earthquake hazard, The Leading Edge, vol. 34, no. 6, p. 618-626.

Fäh, D., Giardini, D., Kästli, P., Deichmann, N., Gisler, M., Schwarz-Zanetti, G., Alvarez-Rubio, S., Sellami, S., Edwards, B., Allmann, B., Bethmann, F., Wössner, J., Gassner-Stamm, G., Fritsche, S., Eberhard, D., 2011, ECOS-09 Earthquake Catalogue of Switzerland Release 2011 Report and Database, Public catalogue, 17. 4. 2011, Swiss Seismological Service ETH Zurich, Report SED/RISK/R/001/20110417.

Hartline, C., 2015, Calpine Corporation presentation to the Seismic Monitoring Advisory Committee Meeting (SMAC). http://www.geysers.com/media/Calpine%20Presentation%2005.11.15.pdf, Geothermal Visitors Center Middletown, California, May 15.

Hanks, T.C. and W.H Bakun, 2014, M-logA Models and Other Curiosities, Bulletin of the Seismological Society of America, vol. 104, p. 2604–2610.

Hauksson, E., W. Yang, and P.M. Shearer, 2012, Waveform Relocated Earthquake Catalog for Southern California (1981 to 2011), Bulletin of the Seismological Society of America, vol. 102, no. 5, p. 2239-2244.

Hauksson, E., L.M. Jones, K. Hutton, and D. Eberhart-Phillips, 1993, The 1992 Landers Earthquake Sequence: Seismological Observations, Journal of Geophysical Research, vol. 98, no. B11, p. 19835-19858.

Hallo, M., I. Oprsal, L. Eisner, and M. Ali, 2014, Prediction of magnitude of the largest potentially induced seismic event, J. Seismol., vol. 18, p. 421-431.

Haeussler, P.J., D.P. Schwartz, T.E. Dawson, H.D. Stenner, J.J. Lienkaemper, F. Cinti, P. Montone, B. Sherrod, and P. Craw, 2004, Surface Rupture of the 2002 Denali Fault, Alaska, Earthquake and Comparison with Other Strike-Slip Ruptures, Earthquake Spectra, vol. 20, p. 565–578.

Holschneider, M., G. Zöller, R. Clements, and D. Schorlemmer, 2014, Can we test for the maximum possible earthquake magnitude?, Journal of Geophysical Research: Solid Earth, vol. 119, p. 2019-2028, doi: 10.1002/2013JB010319.

Holschneider, M., G. Zöller, and S. Hainzl, 2011, Estimation of the Maximum Possible Magnitude in the Framework of a Doubly Truncated Gutenberg-Richter Model, Bulletin

of the Seismological Society of America, vol. 101, no. 4, p. 1649-1659, doi: 10.1785/0120100289.

Hutton, K., J. Woessner, and E. Hauksson, 2010, Earthquake Monitoring in Southern California for Seventy-Seven Years (1932–2008), Bulletin of the Seismological Society of America, vol. 100, no. 2, p. 423–446.

McGarr, A., 2014, Maximum magnitude earthquakes induced by fluid injection, J. Geophys. Res.: Solid Earth, vol. 119. 12pp.

Rubinstein, J.L. and A. B. Mahani, 2015, Myths and Facts on Wastewater Injection, Hydraulic Fracturing, Enhanced Oil Recovery, and Induced Seismicity, Seismological Research Letters, vol. 86, no. 4, 8pp.

Rubinstein, J.L., W.L. Ellsworth, A. McGarr, and H.M. Benz, 2014, The 2001–Present Induced Earthquake Sequence in the Raton Basin of Northern New Mexico and Southern Colorado, Bulletin of the Seismological Society of America, vol. 104, no. 5, p. 2162–2181.

SCEDC, 2013, Southern California Earthquake Center, Caltech, Dataset, http://service.scedc.caltech.edu/eq-catalogs/date_mag_loc.php, doi:10.7909/C3WD3xH1.

Waldhauser, F. and D.P. Schaff, 2008, Large-scale relocation of two decades of Northern California seismicity using cross-correlation and double-difference methods, J. Geophys. Res., vol. 113, p. B08311.

Waldhauser, F., 2009, Near-real-time double-difference event location using long-term seismic archives, with application to Northern California, Bulletin of the Seismological Society of America, vol. 99, p. 2736-2848.

Wei, S., E. Fielding, S. Leprince, A. Sladen, J.-P. Avouac, D. Helmberger, E. Hauksson, R. Chu, M. Simons, K. Hudnut, T. Herring, and R. Briggs, 2011, Superficial simplicity of the 2010 El Mayor-Cucapah earthquake of Baja California in Mexico, Nature Geoscience, no. 4, p. 615–618.

Weiser, D., D.D. Jackson, and L.M. Jones, 2014, Geothermal pumping and induced seismicity in California geothermal fields, Abstract presented at 2014 Seismological Society of America Annual Meeting, Anchorage, Alaska, April 30-May 2.

Wells, D. L., and K. J. Coppersmith, 1994, New Empirical Relationships among Magnitude Rupture Length, Rupture Width, Rupture Area, and Surface Displacement, Bulletin of the Seismological Society of America, vol. 84, no. 4, p. 974-1002.

Yeck, W.L., L.V. Block, C.K. Wood, and V.M. King, 2015, Maximum magnitude estimations of induced earthquakes at Paradox Valley, Colorado, from cumulative injection volume and geometry of seismicity clusters, Geophys. J. Int., vol. 200, p. 322-336.

Zoback, M. and S. Gorelick, 2012, Earthquake triggering and large-scale geologic storage of carbon dioxide, Proceedings of the National Academy of Sciences, vol. 109, no. 26, p. 10164-10168.

Zöller, G. and M. Holschneider, 2016, The Earthquake History in a Fault Zone Tells Us Almost Nothing about m_{max}, Seismological Research Letters, vol. 87, no. 1, p. 132-137.

Zöller, G. and M. Holschneider, 2014, Induced Seismicity: What is the Size of the Largest Expected Earthquake?, Bulletin of the Seismological Society of America, vol. 104, no. 6, p. 2736-2848.

3 Relative contributions of induced earthquakes, and examination of temporal correlation of earthquakes and injection with time

3.1 Introduction

Geothermal energy is an important source of power, however geothermal production and other energy-production technologies can induce earthquakes, as observed in France, Germany, Switzerland, the U.S. and elsewhere. Induced earthquakes in California could potentially trigger damaging earthquakes on the San Andreas and other major faults. Thus, it is critical to better understand the relationship between geothermal production and induced seismicity.

I examine spatiotemporal correlations between seismicity and fluid volume. Time series are also examined for periods prior to and including pumping. Results suggest that seismicity often increases when a new geothermal field begins pumping, and that there are temporal correlations between fluctuations in net fluid volume and seismicity. Relationships between pumping and seismicity hold true for multiple factors (injection, production, or net volume injected); I do not perform an analysis of each factor, as was done by Brodsky and Lajoie (2013). When I say "pumping" this broadly refers to fluid leaving or entering the ground, and not specifically to the direction of pumping. (For example, a relationship between pumping and earthquakes at the Salton Sea exhibits spatiotemporal correlations between earthquakes and injection, production, and the net fluid volume.) Below, I consider the effect of injection, production, and net volume.

Davis and Frohlich (1993) proposed a series of criteria that examine possible connections between seismicity and fluid injection. Davis, Nyffenegger, and Frohlich (1995) updated this work to assess effects of fluid withdrawal. I examine the relation between fluid volume change

and seismicity for each geothermal field, using the criteria appropriate when either production and/or injection activities are involved.

I present a new method of determining the proportion of induced earthquakes, given a population of earthquakes near geothermal injection wells. I use a linear combination of two end-member hypotheses: that earthquakes are evenly distributed in time, and that earthquake occurrence is directly controlled by injection volume. For each field, I find the maximum likelihood of the linear relationship between the two hypotheses, and use that as an indication of the proportionality of the population that is induced. Finally, I summarize the findings of each method to determine if a population of earthquakes is induced, and group California geothermal fields into those that have strong, moderate to strong, or little to no evidence for induced seismicity. An individual assessment of seismicity in some geothermal fields has taken place; however, a side-by-side examination of California's geothermal fields has not been performed until now.

3.2 Background

3.2.1 Historic geothermal energy production in California

Geothermal energy production in California began at The Geysers. The first geothermal power plant was constructed in the 1930s, but was only in operation for a few years (Lund 2004), On October 30, 1958, the Magma-Thermal Company signed the first modern commercial contract to supply steam for energy production with Pacific Gas and Electric (Koenig 1991). The first power plant in the US to generate electricity from geothermal steam power production, The Geysers' Unit 1, came online in June 1960 (Lund 2004). By 1965, production wells had been drilled along a 10 km stretch of the Big Sulphur Creek Canyon, some reaching depths as great as 1.5 km

(Koenig 1991). Fluid injection began at the field in 1968, when the Regional Water Quality Control Board banned surface disposal of geothermal fluid, and operators injected produced water and steam condensate (Koenig 1991). At the time Koenig (1991) published his historical review of activity at The Geysers, over 600 wells had been drilled and the field had reached the status of being the world's foremost energy producing geothermal field (California Energy Commission 2010). Today, the field is home to the largest network of geothermal power plants in the world, and provides nearly 60% of the energy needs of California's North Coast region (http://www.geysers.com/geothermal.aspx).

The development of geothermal energy in the Imperial Valley near the Salton Sea can be seen as nothing less than triumphant. Energy production efforts began as early as 1927 and continued into the 1970s (Howard and Towse 1977). The region's hyper-saline brines posed a significant challenge to geothermal power production; according to Elders and Cohen (1983), the brines contain some of the highest naturally occurring concentrations of dissolved metals in the world. The first well expressly for steam production was dug in 1961, with 10 more wells drilled nearby by 1964; these wells were abandoned within a few years due to high costs (Elders and Cohen 1983). Injection of produced brine was not commonplace at the time, and costs to drill injection wells were high. Therefore, discussions were held about the possibility of dumping produced fluids into the Salton Sea, and what the resulting adverse regional impacts may have been (Goldsmith 1976). Goldsmith (1976) envisioned a tumultuous path forward for geothermal development in the region, and that options for produced brine disposal could result in a range of results from "near-catastrophic through neutral to beneficial." Ultimately, re-injecting produced brine was decided upon as the optimal solution. Further exploratory attempts to develop cost-effective geothermal production began again in the 1970s, but the first geothermal power plant

was not successfully operational and economically viable until 1982 (Elders and Cohen 1983). All four Imperial Valley geothermal fields, Brawley, East Mesa, Heber, and Salton Sea, were operating by 1985 (Department of Oil Gas and Geothermal Resources, DOGGR, 2015).

California's eleven major geothermal fields (defined as those having monthly pumping volume data available through DOGGR 2015) had all initiated operations by the end of 1988. The following dates are the first available monthly pumping data from DOGGR, and are taken as the first occurrences of injection and production (reliable records do not exist for testing periods prior to these dates). In the Imperial Valley, Brawley's first power plant launched in January 1982, with the Salton Sea next in February 1982, followed by East Mesa in January 1983, and Heber in April 1985. As mentioned before, The Geysers started production in June 1960. In the northeast corner of California, there are four geothermal fields near the town of Susanville. The Susanville geothermal field began operations in December 1982. Litchfield started up in January 1984, Wendel in June 1985, and Amedee in September 1988. Located near Mammoth Mountain, the Casa Diablo geothermal field started up in July 1984. The Coso Geothermal field, in eastern California, commenced pumping in May 1986.

3.2.2 Geothermal energy production methods in California

Geothermal energy production requires a heat source close enough to earth's surface for exploitation to be economically viable. There are many methods used to generate geothermal energy, but they all require the basic ingredients: capturing the earth's natural heat to generate steam that can drive a turbine to produce electricity. There are three main classifications of geothermal systems: steam-dominated systems, liquid-dominated systems, and enhanced geothermal systems (EGS) (National Research Council 2012). The Geysers is one of only a few examples of a steam-dominated system (e.g. Eberhart-Phillips and Oppenheimer 1984). The

other major geothermal fields in California are liquid-dominated systems (http://energyalmanac.ca.gov/renewables/geothermal/types.html). The Coso geothermal field may have evolved from a liquid-dominated field to a partly steam-dominated field after injection was introduced in the 1980s (NRC 2012). In both steam- and liquid-dominated geothermal systems, steam or hot water is extracted (produced) from wells that penetrate into naturally occurring fractures in the hot rock. Cold water is usually injected to replenish the fluid supply (NRC 2012). Liquid-dominated power plants rely on flash technologies, since produced fluid does not come up to the surface as steam. Once extracted from the earth, extremely hot water is "flashed" into steam within the power plant (DiPippo 2012). The vapor turns a turbine, which drives a generator to create electricity. The goal of an EGS system is to allow for production in a high-temperature zone with either low permeability or a lack of fluid; high-pressure fluid injection is often used to enhance permeability by opening existing fractures or creating new ones (e.g. DiPippo 2012, Rutqvist et al. 2013). There are a few EGS wells at The Geysers, but the project is in its demonstration phase. The viability of EGS for commercial production is still being tested, but a few countries around the world have pilot projects, like that at The Geysers (NRC 2012).

3.2.3 Previous work characterizing induced seismicity in California geothermal fields

Previous studies have suggested that there is induced seismicity in at least some of California's geothermal fields (e.g. Eberhart-Phillips and Oppenheimer 1984, Kaven et al. 2011, and Lajoie 2012), however an analysis of all the fields in the state had not been performed prior to this work. In order to determine if earthquakes have been induced or not, authors often have

compared pumping parameters and seismicity (e.g. Brodsky and Lajoie 2013, Martínez-Garzón et al. 2014, and Kwiatek et al. 2015).

Understanding the mechanism of induced earthquakes has been the topic of much research. Fluid injection can increase pore pressure, in turn reducing effective stresses; this may lead to motion on faults and fractures (e.g. Majer et al. 2007, Ellsworth 2013). As fluid pressure spreads through the rock matrix or along fractures and perturbs a larger volume, the probability increases of encountering a large fault and inducing a larger earthquake (Keranen et al. 2014). Contraction has also been suggested as a mechanism for geothermal-induced earthquakes. Geothermal energy production inherently occurs in high-temperature environments. Cold water is injected into hot rock; this causes contraction, which may produce sufficient thermoelastic stress changes to induce seismicity (e.g. Rutqvist et al. 2013). Rutqvist et al. (2013) have proposed this as the dominant cause of induced earthquakes at The Geysers. Fluid extraction can also induce earthquakes through processes like subsidence-driven pore pressure increases (McGarr et al. 2002). Martínez-Garzón and her co-authors (2014) proposed that more than one physical mechanism for induced seismicity (such as pore pressure diffusion encountering a fault and contraction) can operate within the same field and depends on fluid injection rate.

3.2.4 Study area: geothermal fields in California

California is home to eleven geothermal fields, some near seismically active areas (Figure 3.1). In northern California, fields include Amedee, Casa Diablo, The Geysers, Litchfield, Susanville, and Wendel. Southern California geothermal fields include Coso, and four in the Imperial Valley: Brawley, East Mesa, Heber, and Salton Sea. Induced seismicity has already been recognized at The Geysers, Salton Sea, and Coso Geothermal Fields, and has likely occurred at

other California fields (e.g. Allis 1982, Brodsky and Lajoie 2013, and Fialko and Simons 2000). Before geothermal pumping ever started, many of these areas were already seismically active. I will present evidence that can be used to estimate what proportion of seismicity is induced in each of the state's geothermal fields.

3.3 Characterizing induced seismicity

3.3.1 Definitions

A large body of literature exists which explores the details of induced seismicity, but a clear and precise definition is not universally agreed upon. This is evidenced by the plethora of ways authors have described induced seismicity over the last few decades. According to Kisslinger (1976), induced events are natural earthquakes set off by a relatively small perturbing stress, while Peppin and Bufe (1980) describe induced earthquakes as "possessing a definite relation to activities of man." Other definitions are very specific, such as that in the Illinois Hydraulic Fracturing Regulatory Act: "'Induced seismicity' means an earthquake event that is felt, recorded by the national seismic network, and attributable to a Class II injection well used for disposal of flow-back and produced fluid from hydraulic fracturing operations" (225 ILCS 732/1-96 2013). This type of description may be legally binding in Illinois, but does not accurately describe all induced earthquakes. Some choose to define induced seismicity using a set of criteria to examine characteristics of an earthquake or earthquake sequence (Davis and Frohlich 1993). Induced seismicity from fluid injection at depth is often identified by spatial proximity and multiple temporal correlations between fluid injection parameters and earthquake occurrence (e.g. Evans 1966; Bardwell 1966; Healy et al. 1968; Raleigh et al. 1976; Ake et al. 2005; Majer et al. 2007). Specifically with respect to earthquakes in geothermal fields, Lajoie

(2012) wrote that, “Production of geothermal power is shown to induce seismicity as water is pumped into or out of a reservoir, both altering fluid pressure and creating thermal perturbations that may lead to fracturing of the reservoir rock.”

As shown by this collection of explanations, the quest to define this special set of earthquakes is not new and does not yet have an authoritative answer. One may never be able to definitively provide proof that a single earthquake is induced. Even with a mountain of evidence, it will likely be a difficult judgment call. The work in this chapter aims to reduce the subjectivity of that decision.

A commonly used tool by statistical seismologists, epidemic-type aftershock (ETAS) modeling, may shed light on this philosophical debate over distinguishing induced and natural seismicity (Llenos and Michael 2013). ETAS, a stochastic model based on aftershock scaling laws, explores the probability of earthquake rate changes being due to an increase in background seismicity rate, aftershock activity, and a combination of those two effects (Ogata 1988). If one term dominates at much higher probability, it can be considered to be the governing factor (e.g. Wang et al. 2010). However, one may not know the rates of both terms. I do not pursue ETAS modeling in this work.

Within this dissertation, I define induced earthquakes as those that would not have occurred at that magnitude, time, and location without human activity. To show that an event is likely induced, one could demonstrate that the observational probability an earthquake likely would have occurred was low under preexisting conditions (e.g. the probability of a $M5$ earthquake in a given area within one year was greatly increased with the onset of human energy development activities). One induced earthquake can trigger other earthquakes, which would also be considered induced.

3.3.2 Data

When an earthquake occurs, it is possible to determine some information without technical equipment, however much more can be known about an earthquake if detailed data have been recorded. Similarly, understanding of induced earthquakes increases with more information obtained.

To understand potential impacts of geothermal injection and production on earthquakes, it is useful to examine time series detailing production parameters. Although data are not continuous as with (most) earthquake catalogs, monthly injection and extraction totals for geothermal fields in California are freely available from the California Department of Oil, Gas, and Geothermal Resources (DOGGR) (DOGGR 2015; last accessed February 24, 2016). Data are uploaded sporadically, and may not be publicly available for a few months after they are collected (at the time of writing, the last five to six months of data were not available).

Throughout this chapter, I employ multiple earthquake catalogs, taking advantage of their various strengths to enhance this work. For example, when examining criteria to determine if earthquakes are likely induced, location is a very important factor. Double-difference catalogs place special emphasis on earthquakes locations. Locations errors are reduced by using correlations in travel times for seismic waves that travel along similar paths (Waldhauser and Ellsworth 2000). For my work analyzing criteria checklists, I utilize continuous seismicity data from the Waveform Relocated Earthquake Catalog for Southern California (Hauksson et al. 2012), and the Double Difference Earthquake Catalog for Northern California (Waldhauser and Schaff 2008). Since the southern California double-difference catalog only extends to forward to 2011, Southern California seismicity data are supplemented with Southern California Seismic Network (SCSN) data (Hutton et al. 2010; SCEDC 2013).

Lengthy earthquake catalogs are desirable. Southern California data (available 1932-present) are taken from the SCSN catalog (Hutton et al. 2010; SCEDC 2013; last accessed January 12, 2015), and northern California data are extracted from the Northern California Seismic Network (http://ncedc.org/ncedc/catalog-search.html; available 1967-present; last accessed January 12, 2015). For pre-NCSN northern California seismicity, I use Berkeley Seismic Network (BSN) data (BDSN 2014; available 1910-2003; last accessed November 19, 2015).

It is a challenge comparing old and new earthquake data. In California, earthquake detection capabilities have improved over time, but there are catalog variations associated with network upgrades, station outages, and other technical challenges. When comparing old and new data, the completeness level has to be one for which both are complete; this is limited by the older data.

3.4 Methods and approaches for examining possible induced seismicity

When exploring if an earthquake sequence may have been induced, associations between human activity and earthquakes are often examined. Unlike an explosion, and earthquake caused by injection or withdrawal of fluids does not appear to create a definitive seismic signature. Peppin and Bufe (1980) studied seismicity in the Geysers Geothermal Field; they could not determine a distinct seismic signal when looking at focal mechanism, spectral corner frequency, seismic moment, or Richter magnitude. Their results imply that there is a strong similarity between natural and induced earthquakes. This supports the hypothesis that induced events are natural earthquakes set off by a relatively small perturbing stress (Kisslinger 1976). If potentially induced earthquakes are the first of their kind for a region, and obvious relationships can be drawn between the timing and location of the earthquakes and some external forcing agent (such as fluid injection or withdrawal), the earthquakes were likely induced (Healy et al. 1968).

In seismically active regions with potentially induced seismicity, determining the cause of the earthquake is less straightforward. Complications may include time delays and/or large distances between the earthquakes and the potential cause (Keranen et al. 2014). I scrutinize two commonly used methods for determining if earthquakes may have been induced (analysis of spatiotemporal relationships between pumping and earthquakes and criteria checklists), to California geothermal fields. Advantages and shortcomings for each approach are presented.

3.4.1 Spatiotemporal relationships between earthquakes and geothermal pumping

Much of California sits on or near an active plate boundary and experiences high natural levels of seismicity. Among the state's eleven major geothermal fields is The Geysers, which is home to the largest single source of geothermal electricity in the world (California Energy Commission 2010). My results provide further evidence that many California geothermal fields exhibit increased rates of seismicity with the onset of geothermal activities, and that there may be a correlation between seismicity and the difference between the fluid volume injected and extracted.

Some hypotheses that link geothermal production and earthquakes include the relationship between seismic moment and cumulative injected volume, the volume difference between fluid injection and production and seismicity rate, and diffusion of fluids into areas with pre-existing stress (e.g. McGarr 2014, Brodsky and Lajoie 2013). I ask whether these results are confirmed by geothermal pumping records for the entire state and qualitatively comparing those to local and regional seismicity records. To do this, I analyze spatiotemporal relationships between seismicity and monthly pumping volumes. I contrast observed seismic behavior for time windows before and after pumping initiation in order to determine if seismicity may be induced. Seismic analysis

will not only include changes in seismicity rate, but also changes in the number of earthquakes of a given magnitude over time.

Induced seismicity has already been recognized at a few of California's geothermal fields, including the Salton Sea and The Geysers Geothermal Fields (e.g. Brodsky and Lajoie 2013; Denlinger and Bufe 1982). I examine relationships between seismicity and fluid injection and production to determine if and where seismicity in California geothermal fields is likely related to geothermal pumping. California's geothermal fields are promising locations to examine; there are numerous wells with available pumping data, many of the areas experience high levels of seismicity, and seismic records pre-date the initiation of geothermal pumping.

3.4.1.1 Mohr-Coulomb failure theory

Many factors can induce seismicity, such as changes in subsurface pore-pressure, dam reservoir water levels, or subsurface temperature (e.g. Allis 1982; Hoover and Dieterich 1969). Zoback (2010) and others cited increased pore pressure as a potential source of earthquake activity in a region with injection. However, reducing pore pressures through production (depleting fluid from a reservoir) can also cause deformation leading to compaction and a subsequent permeability reduction (e.g. Allen and Mayuga 1969). This may lead to normal faulting in or around fluid-producing areas.

Increased pore pressure at depth reduces the effective normal stress, which acts perpendicular to a fault plane. Effective normal stress is a force that inhibits shearing motion, similar to the increased difficulty of pushing a weighted box across the floor. When pore pressure is increased, and the effective normal stress is reduced, elastic energy stored in rocks is released in the form of an earthquake (Zoback 2012). Zoback (2012) is among many who suggest that earthquakes

resulting from this reduction in effective normal stress would have occurred eventually, however they would have been slower to occur.

According to the Mohr-Coulomb failure criterion, the most common model for evaluating shear failure induced by pore pressure increases, slip along any plane in a rock should occur when the shear stress reaches a critical threshold dependent on the normal stress. Before being altered, the state of stress of fractured rock can be gauged by determining local stresses. Maximum and minimum principle stresses (σ_1 and σ_3, respectively) can be visualized with a Mohr Circle, which is a two-dimensional projection of a three-dimensional physical state (Figure 3.2).

When fractured rock is injected with fluid, the increase in pore pressure has the effect of shifting the Mohr circle to the left, and brings the rock closer to failure (Hubbert and Rubey 1959). Injection of fluid into the ground may cause the subsurface rock to fail, with stresses acting on individual grains caused by the difference between external normal stresses and internal fluid pressures. This stress alteration is known as effective stress. With effective stress, the Mohr-Coulomb failure criterion can be expressed by the equation:

$$\tau_{crit} = \mu(\sigma_n - P) + \tau_0 \tag{3.1}$$

where τ_{crit} is the critical shear stress needed to incite slip on a fault; this is related to the coefficient of friction μ, the normal stress across the fault plane σ_n, the fluid pressure P, and the rock's inherent shear strength with no normal stress τ_0 (e.g. Hubbert and Rubey 1959, Davis and Frohlich 1993, and Ellsworth 2013).

3.4.1.2 Analysis of spatiotemporal relationships between pumping and earthquakes

I inspect time histories of fluid volume changes and earthquake characteristics associated with geothermal pumping. Over both the short- and long-term, I compare the volumes of injected and

extracted fluids, the net difference between the two, and monthly counts of earthquakes above a determined completeness threshold (Figure 3.3A-F). A negative change in fluid volume means that more fluid was withdrawn than was injected during the month (net fluid volume = injected fluid volume – extracted fluid volume). Analyses were performed for the nine geothermal fields with continuous injection and production. Litchfield and Amedee are shut-in, injection has never taken place at either field, and they are not included in the rest of the study.

Induced earthquakes occur within close proximity to injection and production wells (see Figure 3.4; e.g. Davis and Frohlich 1993). Therefore, I consider all earthquakes within three kilometers of (presently) active injection wells, unless otherwise specified. Focusing on earthquakes at close proximity to wells should help to reduce input from natural earthquakes.

All analyses were performed using earthquakes with magnitudes above a magnitude of completeness (M_c) cutoff, the threshold at which the network likely recorded all earthquakes. When comparing earthquakes before and during pumping, I evaluate M_c for the period prior to when pumping commenced. That M_c is then applied to the entire earthquake catalog. When examining earthquakes that occurred contemporaneously with geothermal fluid perturbations, I reevaluate the M_c for earthquakes that follow the first day of pumping activity. In my analysis, the M_c for earlier time periods is always higher than for more recent time periods. This decrease in M_c values with time reflects better seismic station density, as well as better quality seismometers.

At a few California geothermal fields, there have been no earthquakes within the specified 3 km region under examination, and therefore it is impossible to determine M_c prior to when pumping began. For these cases, I expand the radial distance for which I include earthquakes, from 3 to 10 km and determine a new completeness threshold. Then, I analyze pre- and co-pumping

earthquakes within 3 km of active injection wells, using the newly obtained M_c. The fields for which this analysis was required include The Geysers, Susanville, and Wendel. The co-pumping M_c is only used when I look at earthquakes since pumping was initiated; otherwise I use the conservative (higher magnitude), pre-pumping M_c. For the results tables presented (Tables 3.1-3.3), I always apply the more conservative magnitude to both radii, if M_c values differ.

It is useful to contrast results for earthquakes within 3 and 10 km distances from wells; when observing data close to the wells, the impact of injection and production is often more pronounced than at greater distances (e.g. Martínez-Garzón et al. 2014**)**. If earthquakes have been induced, by focusing on earthquakes very close to wells, I am more likely to see spatial, temporal, and depth characteristics common to induced earthquakes (e.g. Shapiro et al. 2003). I present and compare monthly earthquake rate densities (monthly number of earthquakes per square km) at both 3 and 10 km radii from active injection wells, for each of the nine geothermal fields with ongoing energy production activities (Amedee and Litchfield are shut-in).

Results also include comparison of earthquake depths prior to and coincident with pumping. If earthquake hypocenters cluster around injection depths, rather than being more evenly distributed, this is evidence that earthquakes are induced. I assume that hypocenter depth distribution doesn't change with magnitude, which allows me to compare cumulative depth distributions at varying levels of completeness. By comparing the pre- and co-pumping time intervals (with the same distance and magnitude parameters), one can observe if and by how much hypocenter depths have changed with the introduction of energy production activities. To obtain pumping depths, I use DOGGR's Geosteam query tool and average injection depths for 6 randomly selected active wells. If a field has less than 6 wells, I average all active injection depths. Well information is confidential at some fields (Coso and East Mesa), so correlations

cannot be drawn between pumping depth and earthquake depth. Variations in pre- and co-pumping depths are still useful evidence for or against induced seismicity. Observations for each field are discussed below.

Brawley

Injection and production wells operated at Brawley from January 1982 until December 1985. Wells were shut-in until operation resumed in January 2009. This affords a unique glimpse into post injection seismicity, and how the same location responds when pumping recommences decades later. As I discuss below, since resumption of fluid injection and withdrawal in 2009, the earthquake rate has increased.

During the recorded earthquake catalog for Brawley, there are a few important high-seismicity times worth mentioning. The month with the most $M \geq M_c$ earthquakes (Figures 3.3A.i and 3.3A.ii) coincides with the M_w6.4 Imperial Valley earthquake in 1979. Although surface rupture was only recorded over about 30 km, aftershocks from the 1979 earthquake quake extended for more than 100km along the trace of the Imperial Fault and Brawley Seismic Zone (Johnson and Hutton 1982). This can be observed with the spike of 45 earthquakes in September 1979. Starting August 26, 2012, more than 600 events were recorded during an earthquake swarm in the vicinity of the Brawley Seismic Zone, of which 41 earthquakes were above the M2.9 completeness threshold (Hauksson et al. 2013). This swarm corresponds to a month with injected and produced volumes (1,811,457,000 kg each) within 10% of the maximum monthly pumping values at Brawley.

Brawley's unique pumping history allows for comparison of two different "before and after" time periods. I group this temporal sequence into four periods: P1 (passive, before first pumping

in 1982), A1 (active pumping, 1982-1985), P2 (passive, 1985-2009), and A2 (active pumping, 2009-the end of 2015). Within 3 km from active injection wells at and above the pre-pumping completeness threshold of 3.0, earthquake rate density (ERD; monthly unless otherwise specified) decreased from 0.0021 earthquakes/km^2/month (EQ/km^2/mo) during P1, to 0.0010 EQ/km2/mo during A1. During P2, ERDs declined further to 0.0007 EQ/km2/mo, and increased substantially to 0.0058 EQ/km2/mo during A2. Averaged together, A1 and A2 experienced an ERD of 0.0548, compared to 0.0021 in P1 (Table 3.1; In the table, the co-pumping ERD averages A1 and A2 together). I discuss this statistical significance of these values in section 3.4.1.3. I replicate results with the co-pumping completeness threshold of M1.5, and discuss rate differences at the lower M_c here. ERDs ranged from 0.0204 during A1 to 0.0134 during P2 up to 0.1086 EQ/km2/mo during A2. At both completeness levels (the smaller of which includes more earthquakes, but can not retroactively be applied to the pre-pumping period), a decline in earthquake rate density is observed when transitioning from A1 to P2. A considerable increase in ERD when pumping recommenced during the A2 time period.

I increase the radius to 10 km, at which I include earthquakes for analysis, and perform the same calculations as above. During P1 with M_c = 3.0, there were 0.0013 EQ/km2/mo. Throughout A1, there were 0.0006 EQ/km2/mo; a decrease to 0.0003 EQ/km2/mo during the P2 pumping hiatus; and an increase to 0.0015 EQ/km2/mo during A2. When considering earthquakes $M \geq M_c$1.5, there were 0.0122 EQ/km2/mo during A1, 0.0003 during P2, and 0.0311 throughout. Even at this greater distance, there is still a detectable signature in the changing rate density of earthquakes from times when pumping activities are active versus inactive.

It is worthwhile to directly evaluate co-pumping ERDs with consistent completeness thresholds at different radii. With both M_c = 1.5 and 3.0, ERD increases when considering earthquake

within a 3 km radius from active injection wells, compared to earthquakes ERDs at a 10 km radius. This increase is a direct measurement of increased seismicity rates coincident with pumping, near injection wells at geothermal fields.

The large majority of hypocenters at Brawley are in the upper 15 km of the crust. Randomly sampled injection well bottom depths extend to 1.3 km (and average about 1 km depth). Compared with other fields in the Imperial Valley (Heber and East Mesa), Brawley's dispersed hypocenter distribution is not unusual. Brawley does not exhibit the same shallow hypocenter clustering in the top few km of the crust as the Salton Sea Geothermal Field exhibits. It is worthwhile to take note of the distinctive depth distributions before and after pumping was initiated. Approximately 20% of earthquakes coincident with pumping occur above 5 km depth, whereas only about 5% of earthquakes prior to pumping fall at or above the same depth (Figure 3.5A).

Casa Diablo

July 1985 marked the beginning of injection and production at the Casa Diablo geothermal field. Already seismically active, the initiation of pumping led to ERD increases both close to and far from active injection wells (Figures 3.3Bi and 3.3Bii; Table 3.1). When comparing co-pumping ERDs within 3 and 10 km from wells at the co-pumping completeness threshold, there is a 320% higher rate of earthquakes close to the wells. That is almost twice as much as the 180% pre-pumping ERD difference. It is interesting to note that out of all 9 fields I examine in this section, Casa Diablo has the highest earthquake rate density within 3 km of active injection wells since pumping began (3.3B.iii).

At first glance, Casa Diablo's pre- and co-pumping hypocenter depth profiles look very similar; however, important differences exist (Figure 3.5B). Since pumping began, less than 1% of hypocenters occurred at depths greater than 7 km, compared to the 10% prior to pumping. Casa Diablo injection wells are located at about 2.25 km elevation, in the vicinity of Mammoth Mountain. Well-bottom depths average 650 m; these measurements are usually taken from a few meters above ground (either from the Kelly bushing or derrick floor). Injection depths at Casa Diablo, therefore, are typically around 1.6 km above sea level. Hypocenter depths are measured from sea level, hence the earthquakes that occur above zero-depth are still below the surface. Just fewer than 5% of co-pumping earthquakes are located between the highest elevation and sea level (a +2 km profile). Prior to pumping, less than 2% of earthquakes occurred above sea level, with no hypocenters shallower than 0.5 km above sea level. Since pumping began, hypocenters have occurred at depths more shallow than previously recorded. These new shallow earthquake depths correlate with injection depths (1.6 km above sea level).

Coso

Injection and production activities began at Coso in May 1985. When one scrutinizes the earthquake catalog prior to and during pumping, it is evident that earthquakes ($M \geq M_{c\text{-}pre}$) are occurring at more constant and elevated rates since pumping began (Figures 3.3C.i and 3.3C.ii). Prior to pumping, both near and far from injection wells, ERDs were constant (Table 3.1). This shows an even distribution of earthquakes in what was already a seismically active area. During pumping, earthquake rates increase both near and far from the wells (Figures 3.3C.iii and 3.3C.iv). If one examines even closer to the wells (1 km radius over which earthquakes are considered), ERD values increase from 0.0010 EQ/km2/mo within 3 km to 0.0014 within 1 km.

When examining the earthquakes since pumping began with the co-pumping completeness threshold, the rate density change is more dramatic: 0.0216 within 3 km distance to 0.0415 within 1 km.

Unfortunately, all well information at Coso (besides the state-mandated monthly injection and production volumes) is confidential. Without this information, it is inappropriate to draw specific conclusions between hypocenter depths since pumping began (known), and the depth at which pumping occurs (unknown). One can, however, compare populations of pre- and co-pumping hypocenters to see how pumping may have altered the depths at which earthquakes are occurring. At Coso, the vast majority (>95%) of earthquakes coincident with pumping have occurred in the uppermost 5 km of the crust (Figure 3.5C). Prior to pumping, a large proportion of Coso's earthquakes (82%) also occurred at depths equal to or shallower than 5 km.

East Mesa

Prior to pumping at East Mesa, there were only three earthquakes $M \geq M_c 3.3$ within 3 km of the wells (all occurred between 1939-1940). The two earthquakes in 1940 occurred a few days after the $M6.9$ Holtville earthquake, and may have been aftershocks or triggered by the mainshock, which was only about 10 km from the field (http://earthquake.usgs.gov/earthquakes/eventpage/ci3365279). There have been no earthquakes at or larger than $M_c 3.3$ since energy production activities began.

East Mesa experiences minimal variability in net fluid volume change (DOGGR 2015). There are also very few earthquakes at this field; there is currently an average of one earthquake ($M \geq 1.6$) every 167 years per km^2, within 3 km of East Mesa's injection wells. Following the start of pumping, there were no earthquakes ($M \geq 1.6$) within 3 km for more than four years; during

this time, injection and production volumes were less than 1 million kg per month. In October 1987, the month prior to the first earthquake, injection volumes jumped 38% to 1,888,923 kg injected. Perhaps in response to the earthquake, injection during December 1987 dropped to 434,124 kg. Since the pumping initiated in January 1983, there has been an average of 0.0005 monthly earthquakes per km^2, within 3 km of the 56 active injection wells. This rate density is 150% higher than when considering earthquakes within 10 km of the wells.

Just as with Coso, well-bottom depths at East Mesa are confidential, and do not shed light on if current hypocenter depths are influenced by pumping. Unfortunately, it appears that all pre-pumping earthquakes were assigned a default depth (for poorly constrained hypocenters), so comparisons cannot be made between pre- and co-pumping earthquake depths. The distribution of co-pumping hypocenters is not concentrated at shallow depths, which suggests most of the earthquakes at East Mesa are likely natural (Figure 3.5D).

The Geysers

Early in The Geysers history, the field only underwent production; injection did not begin until May 1969. For the first 9 years of The Geysers history, only yearly production volumes are available (DOGGR 2011). Monthly data are available starting in January 1969. During the early history of the field, the net difference between injection and production was at its highest (Figure 3.3Di-ii). Production volumes increased to their highest monthly total of 9,973,046,000 kilograms in July 1987. Monthly injection volumes exhibit periodic behavior, which has been correlated with local precipitation levels (e.g. Martínez-Garzón 2014).

After the initiation of production in 1960, the monthly rate of earthquakes above the completeness level within 3 km of active injection wells generally has increased over time (Figure 3.3D.iii). Over the decade leading up to the maximum production at the Geysers (in

1987), the total rate of $M \geq 1.1$ earthquakes climbed from an average of 32.3 per month in 1977 to 196.5 per month in 1987. Following peak production in 1987, field operators sought more of a net balance between produced and injected water, and reduced production while yearly injection volumes were held relatively constant. This reduction in production volume is coincident with an average of 192.1 earthquakes per month, from 1987 until 2003. In November 2003, the Santa Rosa Geysers Recharge Project (SRGRP) began, in an effort to bring additional water to replenish The Geysers steam field. Daily, the pipeline pumps 12.62 million gallons of tertiary treated wastewater from the nearby city of Santa Rosa to The Geysers, which contributes to the generation of approximately 100 additional megawatts of energy per day (City of Santa Rosa). In the 12+ years since the initiation of SRGRP at The Geysers, the average monthly rate of earthquakes has increased 39.1% from the previous 146 months, from 185.6 to 258.2 earthquakes per month. Many of The Geysers' highest monthly earthquake counts were preceded by months in which injection exceeded production, including May 2005, which saw 620 earthquakes greater than $M1.1$. Immediately following the introduction of SRGRP as a water source, a very consistent relationship emerged between cyclical peaks in injection and peaks in monthly earthquake counts (vertical dashed line in Figures 3.3Di-iv show SRGRP initiation date).

The Berkeley Seismic Network catalog began recording earthquakes in 1910, however the first $M \geq 3.0$ earthquake was not recorded within 3 km of a currently active injection well at The Geysers until after pumping began in February 1963 (Figure 3.3D.i). Nearby earthquakes (within 5-10 km of presently active injection wells) were recorded prior to pumping, but none within 3 km. This supports the observation that there was a lack of earthquakes in the immediate vicinity of the wells (at distances less than 3 km) prior to the onset of geothermal production. Since

earthquakes above the completeness level were recorded within 10 km of future active injection wells, I am confident that if there had been earthquakes with magnitudes higher than the completeness threshold, they would have been recorded.

Once pumping began, ERDs both near (≤3 km) and farther (≤10 km) from wells increased ($M \geq M_{c\text{-}pre}$), with a greater increase occurring close to wells (Figures 3.3D.iii-iv; Table 3.1). After pumping initiated, there is almost a 270% higher ERD for earthquakes with magnitudes greater than or equal to M_c=1.5 within 3 km of wells, as opposed to within a 10 km radius. Production rates increased at a slower rate during the time when $M \geq 3.0$ earthquakes began to be recorded with regularity in 1972 (possibly indicating completeness) until the end of 1978, than from 1979 until peak production in 1987. Earthquake occurrence averaged 0.4 per month from 1971-78, as opposed to the 2.5 times higher average of 1.4 $M \geq 3.0$ earthquakes per month from 1979-1987. Following peak production, from 1988 until the introduction of the SRGRP pipeline in 2003, there were 1.9 $M \geq 3.0$ earthquakes per month. From 2004 through the end of 2015, 1.4 $M \geq 3.0$ earthquakes per month were recorded. Apart from a rate change as production neared its peak in 1987, a steady increase in the rate of $M3$ and larger earthquakes has not been observed, unlike with $M \geq 1.1$ quakes. This may be an indication that close to the wells, $M \geq 3.0$ earthquakes are less sensitive to monthly variations in injection and production volumes than $M \geq 1.1$ quakes.

As there were no earthquakes $M \geq M_{c\text{-}pre}$ within 3 km of wells prior to pumping, it is impossible to contrast hypocenter depths before and after pumping. One can, however, make observations about hypocenter depths and injection depths since pumping began. For the wells I sample at The Geysers, injection depths average 3 km, but extend as deep as 3.6 km. Only 1% of earthquakes at The Geysers occurred deeper than 5 km (Figure 3.5E). About 90% of The Geysers earthquakes occur at or above 3.6 km.

Heber

There have been fewer earthquakes during the time of pumping than before it, at the pre-pumping completeness magnitude of 3.1 (Figures 3.3E.i-ii). During co-pumping years, there are more earthquakes per km^2 at distances of 10 km from all injection wells than at 3 km (Table 3.1). I compare earthquake depths before and during pumping operations at Heber (Figure 3.5F), and find that hypocenter depths are evenly distributed. This shows that earthquakes are not clustered around the wells (average injection depth of 1.7km), and is evidence that there are mostly natural earthquakes at this field.

Salton Sea

Prior to pumping at the Salton Sea, there was no difference in ERD close to or far from wells. However, within 3 km of active injection wells once pumping began, there was an order of magnitude increase in monthly earthquake rate density (at $M_{c\text{-}pre}$) (Table 3.1). This difference can be qualitatively visualized in Figure 3.3F.i; there is an obvious earthquake rate change after pumping begins. At a radius of 10 km, during pumping there has been a noticeable 150% increase in ERD over the previous 10 km-radius rate. During pumping (using pre-pumping completeness), a higher rate density than previously measured, can be observed close to the wells. When comparing earthquakes at the co-pumping completeness, there is again a higher ERD close to the wells. In both cases, the increase in ERD is a four-fold increase closer to the wells (Table 3.1).

One can observe a stark contrast in depths of earthquakes after pumping initiated, compared with those prior to human activity commenced at the field. Around 85% of hypocenters that are coincident with pumping occur within the uppermost 5 km of crust; over 20% are shallower than

2 km (Figure 3.5G). Before pumping began, only 20% of hypocenters occurred at or above 5 km depth. This change in where the majority of hypocenters are located correlates with the onset of pumping, even when ignoring early earthquake locations, for which 6 km depths were assigned. The five years prior to pumping show a scattering of depths, which is less common after 1982 (Figures 3.3F.i and ii). Sampled well-bottom depths extend to 2.4 km (averaging 2.05 km).

Brodsky and Lajoie (2013) find evidence for anthropogenic earthquakes at the Salton Sea Geothermal Field. They use an ETAS model to characterize correlations between injection, production, and net production (production minus injection). During the onset of pumping operations at the field, all three pumping parameters correlate well with earthquake occurrence. From 2006-2012 (the end of the study), net production relates more closely to seismicity. They also observe a several-month time lag between injection or production and earthquakes, but find a zero-month maximum correlation between net production and earthquakes.

Susanville

Prior to the initiation of pumping at the Susanville geothermal field, there were no earthquakes ($M \geq M_c$) recorded within 3 km of the future location of the single injection well (BDSN, NCSN). The first earthquake (M_c = 2.1, within 3 km of the well) was recorded occurred only a few months after the first period of injection. The area around the well is not very seismically active; there have only been two earthquakes (given the same magnitude and distance parameters) since production began in 1982.

When comparing earthquakes prior to pumping with those occurring during pumping activities, I apply a completeness threshold that includes earthquakes prior to when energy production

activities commenced. At Susanville, there have been no earthquakes within 3 km of wells, above the pre-pumping *M*2.9 completeness threshold for the duration of the earthquake catalog. Susanville's one active injection well has a well-bottom depth of 0.35 km. As there are only two earthquakes ($M \geq M_{c\text{-}co}$) coincident with pumping, one cannot draw any reasonable connections between the depth of the earthquakes and the well-bottom depth (Figure 3.5H).

Wendel

Since pumping began in June 1985, there has only been one earthquake larger than the *M*2.5 completeness threshold within 3 km of the single injection well. It is not well correlated with any changes in pumping parameters. Similar to Susanville, there were no earthquakes within 3 km of wells at Wendel from the start of the catalog through the end of 2015, above the pre-pumping magnitude of completeness threshold of *M*2.7.

Injection depths extend to 1.9 km in depth. As there has only been one earthquake in close proximity to the well (at a depth of 2.8 km), there is poor evidence for a relationship between injection depths and earthquakes at this site (Figure 3.5I).

3.4.1.3 Statistical significance

I perform two significance tests and herein describe each test, their respective null hypotheses, and assumptions.

I perform a binomial test, for which the null hypothesis is that the earthquakes occur at random times over the whole observation period. The binomial cumulative distribution formula is given by $F(N;n,p) = \sum_{n \leq N} \frac{n!}{N!(n-N)!} p^N (1-p)^{n-N}$, (3.2)

where N is the number of successes (earthquakes $M \geq M_{c\text{-}pre}$ during the pumping period), n is the number of trials (earthquakes $M \geq M_{c\text{-}pre}$ during the entire catalog), and p is the probability of success on an individual trial. For p, I use the fraction of time in the co-pumping interval, relative to catalog duration.

When the probability is high, the number of observed events in the co-pumping interval exceeds what would be expected at random, thus the null hypothesis would be rejected in favor of rates increased by pumping. Both close to and far from injection wells, the null hypothesis can be rejected with at least 95% confidence at the Casa Diablo, Coso, Geysers, and Salton Sea geothermal fields (Table 3.2). Binomial probability assumes that the earthquake events are independent of one another, so the results are not rigorous because aftershocks cluster in time with mainshocks (and I have not used a declustered catalog). Nevertheless, they do give an end-member indication of what could be considered significant.

By simulation, dependence between earthquakes is rendered irrelevant by randomizing the start of the time period during which earthquakes are considered. To achieve this randomization, one can assume that there is some earthquake record, independent of pumping. One just happens to count the pumping interval as being important, and asks, "is the pumping interval special?"

To test the null hypothesis that earthquakes are randomly distributed throughout the catalog, I take the entire extent of each field's earthquake catalog and compare the actual pumping interval to uniformly distributed intervals of the same length. I truncate the catalogs at 12/31/15 23:59:59. Pumping intervals range from approximately 30 years at Wendel to 56 years at The Geysers. I then divide the duration prior to pumping into 100 equal-length segments, e.g. $\Delta t = \frac{t_2 - t_1}{100}$ (Figure 3.6). Starting with t_1, I calculate the number of earthquakes until $t_1+(t_3-t_2)$. I then add Δt to the start and end dates 100 times, which culminates with the pumping interval. This results in

earthquake counts from 100 equal-length time windows with duration identical to that from when pumping commenced until the end of 2015 (Table 3.3). There is an *n*% chance that *N* earthquakes or more would occur during that time window, where *N* is the number of observed earthquakes above a specified completeness threshold during the time period with pumping. I calculate the probability of observing the same number or more of earthquakes as during the pumping period, given that the null hypothesis is true. I choose a confidence interval of 95%, which corresponds to 5% significance. If fewer than 5 time periods in 100 have equal or more numbers of earthquakes (above a completeness threshold) to the pumping period, I can reject the null hypothesis at 95% confidence. During this simulation, I have taken a uniform set of starting intervals, rather than drawing them uniformly from a fixed time interval. This simplifies calculations and allows for quick determination of an answer.

As seen in Table 3.3, I can reject the null hypothesis at The Geysers and Salton Sea geothermal fields, which is in agreement with previous work by Allis (1982), Brodsky and Lajoie (2013) and others. At each of these fields, there were less than 5/100 time windows with equal or more numbers of earthquakes to the pumping period. This demonstrates the uniqueness of the recent period of earthquakes, during which energy production has been occurring. At The Geysers and Salton Sea, it is statistically significant that earthquakes are more likely during times with ongoing production and injection.

3.4.1.4 Spatiotemporal methods discussions and concluding remarks

In the previous section, I compared monthly pumping parameters (monthly injection, production, and net volume difference) with monthly earthquake occurrence, and examine pre- and co-pumping hypocenter depth changes. There are some first order connections that can be made

using this method, though it is challenging to draw short-term connections between pumping and earthquakes at a monthly scale. Long-term trends are visible, however, and provide context for prevailing shifts in earthquake behavior.

It is clear that the net volume difference is an important factor in the Salton Sea, as seen in Brodsky and Lajoie (2013). However, the direction of the volume change that precedes seismicity is not consistent across all of the fields we examine; in some cases seismicity appears to follow a surplus in fluid volume, whereas in the Salton Sea and others, earthquakes appear to happen at times of great negative volume change. The time delay associated with pumping and earthquakes is very clearly a complex relationship.

Geothermal energy production has been in operation for at least 30 years at each California field. Prior seismic records are often sparse and are only complete to approximately magnitude 3. When comparing pre- and co-pumping earthquake histories, they must be compared at the same magnitude threshold. Assuming that induced earthquakes often occur at small magnitudes (e.g. Majer et al., 2007), earthquakes less then magnitude 3 contain important information not apparent in the catalog of larger earthquakes only. The magnitude of completeness decreases (to ~M1.5-2) when only examining earthquakes that have occurred since the onset of pumping. A lower completeness threshold permits observation of seismicity fluctuations over a broader range of magnitudes, perhaps allowing for more detailed relationships to appear between seismicity and changes in water injection and production.

The need for better resolved pumping data is illustrated at all geothermal fields. It is challenging to see detailed relationships between continuous seismicity and monthly, location-nonspecific data. Ideally, continuous injection and production data would be available for all wells at a geothermal field. If finer resolution pumping data (e.g. hourly, daily, or weekly) were publicly

available and denser networks of seismic stations were installed, correlations could be made between much lower magnitude events and a more detailed pumping history.

3.4.2 Criteria checklists

Davis and Frohlich (1993) asked 'if an earthquake has occurred, was it caused by injection?' The authors also investigated the potential for a future injection site to have damaging earthquakes. They examined four factors, which may contribute to earthquake activity: historical background seismicity, local geology, the regional state of stress, and injection practices. The authors examined the spatial and temporal correlations between injection and earthquakes.

Davis, Nyffenegger, and Frohlich (1995) published a modified set of criteria, which are applicable to regions where earthquakes and fluid withdrawal occur, but no injection takes place.

When examining California geothermal fields, I use Davis and Frohlich's (1993) checklist for all sites with both injection and production. Where only production occurs (Litchfield, Amedee), I employ the criteria of Davis, Nyffenegger, and Frohlich (1995).

Below, I introduce the criteria from Davis and Frohlich (1993) and Davis, Nyffenegger, and Frohlich (1995). A few criteria are selected and discussed in greater detail, and a summary of results is presented for the major geothermal fields in California.

3.4.2.1 Davis and Frohlich (1993) criteria, relevant to injection

Davis and Frohlich (1993) presented a series of criteria, to evaluate if a future injection site is likely to induce an earthquake. The authors phrased their conditions such that a "yes" response supports fluid injection as the cause of an earthquake, and a "no" answer implies that fluid

injection did not play a role in causing the earthquake sequence. In my analysis, I comply with the authors' methods of answering their questions, and reply with a 'yes,' 'yes?,' 'no?,' or 'no.' In many cases, a definitive response is unclear.

Question 1: Are these events the first known earthquakes of this character in the region?

Question 2: Is there a clear correlation between injection and seismicity?

Question 3a: Are epicenters near wells (within 5 km)?

Question 3b: Do some earthquakes occur at or near injection depths?

Question 3c: If not, are there known geologic structures that may channel flow to sites of earthquakes?

Question 4a: Are changes in fluid pressure sufficient to encourage seismic or aseismic failure at well bottoms?

Question 4b: Are changes in fluid pressure sufficient to encourage seismic or aseismic failure at hypocentral locations?

With five or more "yes" answers, the authors concluded that fluid injection induced the earthquake sequence in question.

3.4.2.2 Davis, Nyffenegger, and Frohlich (1995) criteria, relevant to extraction

Davis, Nyffenegger, and Frohlich (1995) presented criteria, based on Davis and Frohlich (1993), to determine if earthquakes were likely caused by fluid withdrawal. Again, the authors phrased their criteria such that a "yes" response supports fluid withdrawal as the cause of an earthquake, and "no" indicates that fluid withdrawal was not responsible for causing the earthquake sequence.

Question 1a: Are these events the first known earthquakes of this character in the region?

Question 1b: Did the events only begin after fluid withdrawal had commenced?

Question 1c: Is there a clear correlation between withdrawal and seismicity?

Question 2a: Are epicenters within 5 km of wells?

Question 2b: Do some earthquakes occur at production depths?

Question 2c: Do epicenters appear spatially related to the production region?

Question 3a: Did production cause a significant change in fluid pressures?

Question 3b: Did seismicity begin only after fluid pressures had dropped significantly?

Question 3c: Is the observed seismicity explainable in terms of current models relating to fault activity?

With seven or more "yes" answers, the authors concluded that fluid withdrawal induced the earthquake sequence in question.

3.4.2.3 Is there a clear correlation between injection/withdrawal and seismicity?

I plot the volume of injected and produced fluids, the difference between the two (injection – production), and monthly earthquake count over time (Figures 3.3A-I). This allows for direct comparison between pumping parameters and seismicity, over the same duration.

3.4.2.3a "Yes" examples: The Geysers and Brawley

The Geysers:

It appears that an improvement in the detection capabilities occurred at The Geysers in 1975 (Figure 3.3E). This conveniently allows observation of the increasing monthly earthquake counts leading to the peak in production during the late 1980s. The subsequent decline in monthly

production volumes corresponds with a relatively steady earthquake rate between the late 1980s and late 1990s. The earthquake rate increases again around the initiation of the Southeast Geysers Effluent Project (SEGEP) in 1997. Monthly earthquake rates peak following the introduction of new water sources from the Santa Rosa Geysers Recharge Project (SRGRP). Both SEGEP and SRGRP brought nearby water (from Clear Lake and Santa Rosa, respectively) to increase potential volume for injection at The Geysers. It is interesting to note that, since a few years after the addition of the SRGRP water source, the long-term monthly earthquake rate has a more modest increase in rate, excluding seasonal increases in earthquake rate corresponding to periods of high precipitation. Perhaps the reintroduction of large volumes of fluid into the field from SEGEP and SRGRP has shifted the behavior or mechanism for the earthquakes in the field. Out of all of the geothermal fields examined in this study, The Geysers experiences the greatest overall volumes of injection and production, as well as the highest total number of earthquakes.

Brawley:

An in-depth examination of well locations and changes in injection volumes and rates shows clear correlation between injection and seismicity (Figure 3.3A). The largest earthquake at Brawley was a *M*5.4 in 2012; it was immediately preceded by a month that, at the time, had the highest volumes of injection and production ever recorded at the field (approximately 1.9×10^6 kg). During most months at Brawley, approximately equal amounts of fluid are injected and withdrawn. This is not true in most other geothermal fields, and may contribute to the low monthly earthquake totals at Brawley.

Pumping ceased in 1985 and resumed in 2009 (previously defined as P2). This affords a unique glimpse into post-injection seismicity, and how the same location responds when pumping

resumes decades later. Seismicity rates were extremely low during 25 years period with no pumping. Since resumption of fluid injection and withdrawal in 2009 (A2), the earthquake rate has greatly increased from P2. As shown in section 3.4.1.2, the earthquake rate density decreases 52% from the first A1 to P2 (with M_c = 1.5, radius = 3 km). When activities resumed in 2009, ERD increases over 700%. As is observed at many other sites with induced seismicity, there was a time delay between the resumption of pumping and when earthquake rates increased (e.g. de Pater and Baisch 2011; Cypser and Davis 1994).

3.4.2.3b "No?" example: Wendel

Since the catalog began in 1910, only one earthquake ($M \geq M_{c\text{-}pre}$) occurred has within 10 km of Wendel (Figure 3.3I.ii). This earthquake occurred after pumping operations began. There is no obvious relationship between $M \geq 3$ earthquakes and pumping volume.

3.4.2.4 Do some earthquakes occur at or near injection depths?

Data for individuals wells are available using the Geosteam query tool on the DOGGR website (DOGGR 2011). All or some information about a well may be confidential, yet others may have years of scanned well logs and a bounty of other data. I randomly select up to six wells per field and find a range of injection depths; some fields only have one or two injection wells.

For the southern California catalogs used here, 90% of the vertical errors are less than 1.25 km, and 90% of the horizontal errors are less than 0.75 km (Hauksson et al. 2012). For the northern California data set, absolute locations have median errors of less than 0.30 km in horizontal and 0.88 km in vertical directions (Waldhauser and Schaff 2008).

3.4.2.4a "Yes" example: Geysers

Most earthquake hypocenters in The Geysers geothermal field occur at or shallower than 5 km depth, with some injection depths extending as deep as 3.6 km. An individual investigation of wells and surrounding seismicity shows a close correlation between injection depth and hypocenter locations (Figure 3.4).

3.4.2.4b "No?" example: East Mesa

All active injection well data are confidential, so I am not able to determine if earthquake hypocenters and injection depths are similar. However, based on injection depths at other Imperial Valley geothermal fields, it is likely that injection at East Mesa occurs at a minimum depth of 1-2.5 km. Two earthquake hypocenters are near this depth, while most occur at or deeper than 5 km (Figure 3.5D).

3.4.2.4c "Maybe" example: Coso

All active injection well data for the Coso Geothermal Field are confidential. However, Davatzes and Hickman (2006) show that well 34-9RD2, located at 36.035, -117.776 (DOGGR 2011), extends at least 3 km below ground level. Elevation at the wellhead is approximately 1.2 km, which means injection at 34-9RD2 occurs at a minimum depth of 1.8 km (U.S. Geological Survey 2015). Since 1986, when injection commenced at Coso, most seismicity has been located in the upper 5 km of the crust (Figure 3.5C). Hypocentral depths have been getting shallower since pumping began, perhaps indicating a strong link between earthquake and well locations. Most earthquakes for the last fifteen years have occurred within the top 2.5 km of the crust. Over

the last decade, very few earthquakes have been deeper than 2 km, which is the approximate depth (below sea level) of pumping I have been able to deduce from the little information released about these wells. Even though Coso's individual well records are confidential, as shown, it is likely that injection occurs at depths similar to the majority of hypocenters.

3.4.2.5 Analysis of Davis and Frohlich (1993) and Davis et al. (1995)

Using the criteria outlined by Davis and Frohlich (1993) and Davis et al. (1995), I investigate the hypothesis that earthquakes are being/have been induced in California's geothermal fields (see Tables 3.4 and 3.5). Most of the authors' questions require subjective answers, due to differences in data quality and completeness. However, their criteria offer a way to compare multiple injection projects to one another, and to contrast places known to induce earthquakes and those where it yet to be determined.

"Are these the first known EQs of this character in this region?" This is easier to answer for Central and Eastern US, where earthquakes occur less frequently (e.g. Ellsworth 2013). In seismically active areas, how far from a well can an earthquake be located and still be considered? California is home to geothermal fields within close proximity to one another; activity in one field may not be related to the other. Also, prior regional earthquakes do not inhibit future induced earthquakes; rather they simply denote a naturally high background seismicity rate. The importance of the criteria differs from one region to another, depending on how seismically active it is (and other factors). For example, the question about prior seismicity seems only to apply to places without a lot of previous naturally occurring earthquake activity. The relevance of each question may depend on location, and users of these criteria may wish to

consider seismicity, ongoing pumping (such as irrigation), and other local factors when investigating possibly induced earthquakes.

When examining a profile of an active or past seismic sequence, in both papers the authors only looked at earthquakes within 5 km of wells. However, when determining if injection may cause seismicity at a future location, they examined all faults and prior seismicity within 20 km of the proposed site. According to the authors, a well can induce earthquakes only up to a 5 km distance; however, active seismic areas within 20 km are cause for concern at proposed injection sites. In California, there are few places that do not have seismicity within a 20 km radius. This raises the important question of 'To what distance can you induce seismicity from injection activities?'

3.4.2.6 Recommendations and conclusions

It is clear that the monthly net volume difference is an important factor in the Salton Sea, as seen in Brodsky and Lajoie (2013). Further confusing the picture, the volume change that precedes seismicity is not consistent across all of the fields examined; in some cases seismicity follows a surplus in fluid volume (e.g. The Geysers), whereas in the Salton Sea and others, earthquakes also correspond with fluid deficits. This variability in response to fluids may imply different earthquake mechanisms from field to field; disparities in the time over which fluid can induce seismicity; and/or that earthquake behavior can change over time (e.g. Majer et al. 2007). What these variations prove is that the relationship between fluid injection and production in geothermal fields and seismicity is very complicated!

For both current and future geothermal field sites, it is critical to ask: 'Could injection (or production) potentially trigger seismicity on a nearby fault system?' Wesnousky (2006) presents

earthquake ruptures that jump from one fault to another at distances up to 5 km, but ignores what he calls "gaps," or areas between two ruptured faults with no mappable fault trace between the two. Black (2008) includes these "gaps" and finds additional instances where ruptures jumped distances up to 7 km. In the *M*7.8 2001 Kunlun, China earthquake, a 30 km gap with no mapped surface rupture bridged the distance between the surface traces of two ruptured faults (Fu et al. 2005). It is prudent to include all faults within at least 5 km of injection and production sites in any hazard analysis, and would be reasonable to include faults at even greater distances.

When evaluating Davis and Frohlich's (1993) criteria it is difficult to determine whether or not pressure changes could induce failure in a seismically active area. It is challenging to determine both fluid pressure and stress at earthquake hypocenters. Despite some difficult-to-address questions, the criteria checklists do, however, provide a metric for testing. The way the questions were designed, however, skew the results towards a "not induced" declaration for fields with a high natural background rate. When examining a population of potentially induced earthquakes in a previously seismically active location, it is important to consider alternative methods to Davis and Frohlich (1993) and Davis et al. (1995).

3.5 Maximum likelihood estimation of proportion of induced earthquakes

I explore two end-member hypotheses to explain earthquakes in California geothermal fields. My main hypothesis is that the rate of earthquakes is proportional to the rate of injection; if this were proved valid, one would observe more earthquakes during times with injection, although this isn't guaranteed. This will be referred to as the "injection" hypothesis. The null hypothesis is that the earthquake rate is constant and randomly distributed in time; I term this the "uniform" hypothesis. The resulting earthquake catalog would show no significant correlation between

injection and earthquake distribution. I present maximum likelihood fits to earthquake catalog and pumping data. Probabilities are based on a linear combination normalized injection data and normalized uniform earthquake distributions. Pumping volumes and earthquake numbers are yearly sums; the likelihood of this occurring is evaluated. The log-likelihood is summed over the duration of pumping; the proportionality of the two hypotheses that gave the highest value (maximum likelihood) represents the most likely combination.

3.5.1 Study locations

I continue to focus on California geothermal fields, due to availability of monthly pumping data. With this work, however, focus shifts to injection volume, as injection is widely recognized as a source of induced seismicity (e.g. McGarr 2014, Ellsworth 2013). Wendel and Susanville are excluded, as neither has experienced any earthquakes $M \geq M_{c\text{-}pre}$ since the catalog began.

3.5.2 Data selection

Earthquakes are selected from the beginning of the available earthquake catalog for area of each geothermal field through the end of 2015, and are included if epicenters lie within 3 km of active injection wells. Data presented are limited according to pre-injection magnitude of completeness ($M_{c\text{-}pre}$). Determining M_c, the lowest magnitude for which all earthquakes in a given space and time have been detected, is essential when calculating seismicity parameters such as the b-value of the Gutenberg-Richter relationship (Gutenberg and Richter 1944). M_c serves as a lower magnitude bound for many of the analyses I perform. The method I use to determine M_c has already been described in Section 2.2.2 and Figure 2.3.

3.5.3 Linear combination of two end-member hypotheses

For each geothermal field, I use the previously determined completeness thresholds for earthquakes within 3 km of active injection wells, during the injection period (see Table 3.1). I create a weighted distribution, with a combination of the two hypotheses ("uniform" and "injection") in 10% increments totaling 1.0. An optimal solution is determined for each field, with the maximum likelihood representing the ideal weighting of each hypothesis (see Figure 3.7A and B). For example, the best fit for Casa Diablo is 0.4*injection+0.6*uniform. Results for all fields are displayed in Figure 3.8. Brawley and The Geysers demonstrate a good fit for the injection-weighted model, with Coso and Heber fitting the uniform earthquake hypothesis. All other fields result in a mixed combination of the two hypotheses. For Brawley, only used the years during which pumping occurred were included in the analysis (1982-1985 and 2009-2015).

3.5.4 Temporal history of earthquakes and injection at California geothermal fields

Examining the earthquake response to injection volume can explain some of my results. For some sites (e.g. Coso), there is a poor correlation between injection and seismicity, which explains the low relative contribution of the injection-induced hypothesis (Figure 3.3C). At Coso, the tight clustering of earthquakes around wells, in a very small geographic area relative to the area sampled (3 km from all injection wells), may help explain the result of 0*injection+1.0*uniform (pers. comm. with Martin Schoenball, Dec. 16, 2015). An examination of all earthquakes within 1 km of injection wells at Coso does not shed more light on the situation, as the same result hold true. A time delay between injection and seismicity may also contribute to poor correlations between injection and earthquakes.

A strong correlation between injection and earthquakes supports the conclusion that a substantial portion of an earthquake population may be induced, such as the relationship that can be observed at Brawley and The Geysers (Figures 3.3A and D).

3.5.5 Conclusions

For multiple geothermal fields examined, the observed distributions of earthquakes are not explainable with random natural variations; induced earthquakes may help explain the difference between the two distributions. For geothermal fields with higher likelihoods for the "induced" hypothesis, my model predicts that injection-induced earthquakes significantly contribute to the overall population of earthquakes.

3.5.6 Discussion

There is a trade-off between examining a long-duration catalog and looking at the most consistent and complete data. When determining which data parameters to use, it is necessary to examine what is most important to the study: the number of earthquakes in the catalog versus confidence in the completeness threshold. I strive to have a learning period 1-2 times the length of the test period. This will hopefully help to balance completeness, number of earthquakes, and b-value.

Possible delays (beyond one month) between earthquake occurrence and injection have not been accounted for in this work. This is a simplified model of a more complex mechanism. In the future, I would suggest building production into the model, as well as accounting for time-delays. One could also compare the geothermal site to a nearby control region without pumping,

and calculate the impact of pumping on earthquakes between two geologically and tectonically similar areas.

Assumptions and shortcomings of this approach include: 1) production does not play a role in induced earthquakes. Brodsky and Lajoie (2013) demonstrate that Salton Sea seismicity correlates with production volumes; 2) there is a linear relationship between injection and earthquake. This is a simple model, and can be developed more in the future; 3) time delay is not factored into the relationship. It has been demonstrated that there is a delay between pumping activities and the resulting earthquakes (e.g. Keranen et al. 2013); 4) rock mechanics and hydraulic modeling are not considered; 5) I assume earthquakes are independent of one another. This is not an accurate portrayal of earthquake activity; and 6) clustering in the data (e.g. aftershocks) has not been corrected for.

3.6 Policy implications

If there were to be a moderate-large earthquake in any of these geothermal fields, especially for those located near major fault systems, crucial operational and public safety decisions will need to be made in the face of serious uncertainty. While the criteria discussed above are useful in ascertaining if a site may have caused an earthquake sequence, it by no means yields a definitive answer. These criteria may be more useful in areas not already seismically active, as demonstrated by many of the examples in the papers. Therefore, it is critical to create flexible policies to allow for decision making in times of uncertainty. It is important that policies can be enacted without a "smoking gun", and can be effective without a definitive signal that an earthquake was induced.

Partnerships are needed between government agencies, energy companies, geothermal operators, and communities that could be impacted by nearby earthquakes. An example of an effective preemptive communications system is the Seismic Monitoring Advisory Committee (SMAC). SMAC meets twice a year, and is a collaboration between Calpine (The majority operator at The Geysers), Lawrence Berkeley National Laboratory, the Northern California Power Agency, and the communities closest to the geothermal field.

Currently field operators are legally required to report monthly fluid volume totals to DOGGR (DOGGR 2015). Most other information can be kept confidential. If greater regulatory oversight were given to DOGGR, it could pave the way for more frequent and detailed communication between operators and the state about pumping and seismic activity within the field. I have sought out policies or plans that exist for California state agencies, in the event that a damaging earthquake occurs in close proximity to a geothermal field. There appear to be none.

The need for better resolution pumping data is illustrated at all geothermal fields, in particular at the Brawley and Salton Sea fields. It is challenging to see a signal in the seismicity when it is being compared to monthly data that are aggregated over an entire geothermal field.

3.7 Conclusions

Although many induced quakes are too small to be felt by humans (microquakes), it is important to characterize their relation to human activities. Working to better characterize these small magnitude events can help elucidate the physics and processes behind larger induced quakes. Understandably, there is a growing public concern over induced felt earthquakes. With the proximity of the San Andreas Fault and other large fault systems, it is important for relevant

personnel to have a protocol ready for how to proceed in the event of a moderate to large earthquake near a geothermal field.

For each field, I present a summary of the evidence for or against induced seismicity. I categorize whether the observations at each field make it a strong, poor, or moderate candidate for having induced earthquakes. I strive to objectively identify evidence for induced earthquakes at each geothermal field, and summarize these results in Table 3.6. Some subjectivity is unavoidable given the complexity of the physical process and the limitation of available data. For each of the three methods I present in this chapter, I rank the evidence presented on a scale of 0-3. I define 3 as strong or obvious evidence in favor of induced seismicity, 2 is moderate or less clear evidence, 1 is poor evidence, and 0 is no evidence in favor of induced seismicity, and includes evidence against earthquakes having been induced. My spatiotemporal and relative contribution studies are objective and repeatable, but the weighting between the three studies is somewhat subjective because the calculations depend on some imperfect assumptions. I have documented my decision-making process, so that others can use this information when trying to decide if earthquakes may be induced at a specific location.

When examining spatiotemporal correlations (Section 3.4.1), if there was evidence that earthquakes started up around the same time as pumping, a field received a "2" score. If there was evidence in excess of that (such as a long-term change in depth of earthquakes that correlates with injection depths), it scored a "3." Slight evidence received a "1."

When answering the questions in Davis and Frohlich's criteria checklists (Section 3.4.2), if a field had received five or more "Yes" answers, it would have scored a 3. Four "Yes" responses resulted in a score of 2, while three resulted in a score of 1. None of the California fields had fewer than three "Yes" results, but those would have received a 0.

Finally, I presented a simple new model (Sectioon 3.5), which resulted in a maximum likelihood of a combination of two end-member hypotheses (one representing earthquakes controlled by injection, and the other representing randomly occurring earthquakes). The results of this method are displayed in Figure 3.8. For fields with a 1.0 or 0.9 proportion of induced earthquakes (Brawley and The Geysers), they received a score of 3. For those with a mix of the two hypotheses (0.3-0.8), they were scored as a 2, while those likely to have zero injection-induced earthquakes scored a 0.

I sum the results in the final column. Fields scoring higher than a 7, Brawley, The Geysers, and Salton Sea, are considered to have strong evidence for induced seismicity. A score of 3-6 indicates moderate to strong evidence for induced seismicity. These fields include Casa Diablo, Coso, East Mesa, and Susanville. A score of 2 or fewer points demonstrates poor evidence for induced earthquakes, and is the result for Wendel and Heber.

Out of the three techniques discussed in this Chapter, only the criteria checklist method was applied to Litchfield and Amedee. Therefore, I did not include them in the table. Neither field demonstrates any evidence for induced earthquakes.

3.7.1 Fields with very strong evidence for induced seismicity

Brawley

Brawley's unique 25-year shut-in between two intervals with pumping allows seismicity changes to be observed after pumping stopped and resumed again at the same location. At both $M_{c\text{-}pre}$ and $M_{c\text{-}co}$ within 3 km, earthquake rate density decreases during the pumping hiatus, but upon recommencement of fluid injection and withdrawal in 2009, ERD increases over 700% (for both M_cs). When the radius is increased to 10 km, the rate density, from the hiatus to the most recent

pumping period, increases over two orders of magnitude (Table 3.1). There is an increase in co-pumping ERDs (at both M_cs), when decreasing the radius over which earthquakes are included from 10 to 3 km. This shows that earthquake rates are higher near injection wells at Brawley. Had aftershocks and/or triggered earthquakes in the Brawley field from the 1979 Imperial Valley earthquake not happened, there might have been a statistically significant difference between intervals with and without pumping.

Although earthquakes at Brawley do not cluster in the top few km of the crust as at the Salton Sea, a change in hypocenter depths did occur after the initiation of pumping. Before pumping began in 1982, 95% of earthquakes occurred deeper than 5 km. Since 1982, only 80% of earthquakes occur at or below 5 km depth (Figure 3.5A).

There is likely induced seismicity at the Brawley geothermal field, as evidenced by the change in earthquake rate density after the pumping hiatus. However, due to infrequent but productive earthquake sequences, it is difficult to see finely detailed connections between pumping and earthquakes. In the future, earthquake declustering (which removes non-independent earthquakes, such as aftershocks,) at Brawley might allow for more thorough detection of induced seismicity.

The Geysers

There are many observations that make me confident that The Geysers experiences induced seismicity. These include spatiotemporal correlations between earthquakes and pumping parameters and statistical significance. Prior to pumping at The Geysers, no earthquakes were recorded within 5 km of presently active injection wells. Earthquakes ($M \geq M_{c\text{-}pre}$) were recorded in close proximity to the 5 km cutoff, however. Therefore, had there been an earthquake prior to

1960 with magnitudes higher than the completeness threshold, it likely would have been recorded.

Once pumping began, earthquakes were recorded with regularity, and at very high rates. Starting in 1960, earthquake rate densities both near and far from wells increased ($M \geq M_{c\text{-}pre}$), with a larger increase close to wells (Table 3.1). As presented in section 3.4.1.2, earthquake rate densities increased with increasing production volumes through the production apex in the 1980s. When monthly volumes began to decrease after the 1987 production zenith, earthquake rates increased at a slower pace. There are also strong relationships between seasonal injection maxima and peaks in earthquake occurrence. This has been particularly evident since SRGRP was introduced in 1997.

Prior to 1960, there were no earthquakes within 3 km of wells; clearly there was no concentration of earthquakes near the surface. Since pumping commenced, approximately 90% of The Geysers earthquakes have occurred at or above injection depths. This is unique, especially when compared to other fields with a more constant-depth hypocenter distribution.

When determining if the current co-pumping time period is unique, I can say with >95% confidence that this number of earthquakes is significantly different than past equal-duration periods. Out of 100 windows with duration equal to the length of pumping at The Geysers, the period contemporaneous with pumping has experienced the largest number of earthquakes. There is only a 1% chance of this occurring.

Salton Sea

There is a stark contrast in pre- and co-pumping earthquake histories. An order of magnitude increase in monthly earthquake rate density (at $M_{c\text{-}pre}$) within 3 km of active injection wells

occurs after the initiation of pumping. At 10 km from each well, a 150% increase in ERD occurs over the previous rate density. There is a higher ERD (at $M_{c\text{-}co}$) within a 3 km radius, as compared a radius of 10 km.

Hypocenter depths also support that the Salton Sea geothermal field experiences induced earthquakes. Prior to pumping, 80% of quakes occurred deeper than 5 km, versus 15% during pumping. Over 20% of hypocenters are shallower than the average injection depth of 2 km.

Brodsky and Lajoie (2013) examine seismicity at the Salton Sea Geothermal Field. The authors used ETAS modeling to compare declustered seismicity with monthly injection and production volumes. They observed a correlation between seismicity and produced fluid volume. In my work with some of the Imperial Valley geothermal fields, I also see a correlation between produced volume and the triggering of large sequences of events. At the Salton Sea geothermal field, I also see a correlation between changes in net fluid volume and seismicity. Brodsky and Lajoie conclude that net volume difference is a key player; I concur with their results.

As with the Geysers, I can say with >95% confidence that the current time period with pumping is statistically significantly different from the other 99 equal-length time windows tested. Only one other time period has as many or more earthquakes as the pumping period. There is only a 2% chance of this occurring.

3.7.2 Fields with poor evidence for induced seismicity

East Mesa

There is little evidence for induced seismicity at East Mesa, besides the first co-pumping earthquake occurring after a rapid rise in monthly pumping volumes (38% injection and 44% production volume increases).

Heber

As summarized in section 3.4.1.2, earthquakes are more common at greater radial distances from Heber's injection wells (1.79 vs. 0.91 monthly earthquakes/km^2 at 10 km vs. 3 km, respectively). Similarly, a greater earthquake rate density occurred prior to pumping initiation, rather than after. Hypocenter depths since injection and production began do not cluster around pumping depth. All of these relationships support the idea that earthquakes at Heber are naturally occurring.

Susanville

This is an extremely low seismicity field. There is slight evidence for induced earthquakes. The first earthquake ($M \geq M_c$) to occur within 3 km occurred shortly after the first few months of injection. This may have been induced by injection or the contemporaneous increase in production. Although the raw numbers are small, there is a 50% increase in earthquake rate density as the earthquake observation region decreases from 10 to 3 km from the injection well. This alone is not convincing enough to assume that the two earthquakes within 3 km of the injection well, with $M \geq M_{c\text{-}co}$ have been induced.

Wendel

There is no obvious relationship between $M \geq 2.5$ earthquakes and pumping at this field.

3.7.3. Fields with moderate to strong evidence for induced seismicity

Casa Diablo

Since pumping began at Casa Diablo in July 1985, earthquake depths have been concentrated near the surface; over 95% of hypocenters have occurred at depths less than or equal to 6 km. 3%

of the earthquakes from the current period occur closer to the surface than any earthquake prior to pumping (Figure 3.5B). Injection at Casa Diablo occurs at depths near 0.6 km. The field was seismically active prior to pumping, but since July 1985, ERD has increased both close and far from wells (Table 3.1). The ERD ratio between 3 and 10 km (showing if earthquakes are more likely to occur close to wells), it is twice as high since pumping began than previously. Out of all fields examined, Casa Diablo has the highest earthquake rate density within 3 km of active injection wells since pumping began.

The most obvious relationship between earthquakes and pumping occurred in 1991. Over 600 earthquakes occurred immediately following the largest single increase in injection and production volumes throughout the entire pumping record (Figure 3.3B.iii). The decade of highest earthquake activity (1990-2000) coincides with and follows the modification in pumping where monthly volumes increased from an average of $5x10^5$ kg/month to $2x10^6$ kg/month.

For the binomial test, the pumping period at Casa Diablo is significantly different than prior to pumping. However, this test assumes event independence, which an unprocessed catalog does not have. Therefore, results are not precise, but yield a suggestion of what could be considered significant. For the moving window test, less than half of intervals have as many or greater earthquakes than the pumping period. For this number to be significant, only 5 or fewer intervals should qualify. There are pieces of evidence that suggest that induced earthquakes have likely occurred at Casa Diablo, but I do not think there is enough evidence to be certain.

Coso

When analyzing long-term changes at Coso, earthquakes have occurred at elevated rates since pumping began (Figure 3.3C.iii and 3.3C.iv). After pumping began, earthquake rate densities

increase both near and farther from wells (Table 3.1) When I produced results for within a 1 km of active injection wells, ERDs increased for both completeness thresholds. Besides monthly pumping volumes, specific Coso well details are confidential. However, comparisons between pre- and co-pumping hypocenters (radius = 3 km) show a 14% increase in earthquakes at or above 5 km since pumping started in May of 1986.

Coso seismicity is constantly active, with most months containing between zero and 20 earthquakes (within 10 km, $M_{c\text{-}co}$). The field also is regularly operating with 1 million kg of injected water less the volume of produced water. This constant net fluid deficit may contribute to the prevalence of earthquakes at Coso.

At both 10 and 3 km radii, Coso's co-pumping window is the closest to being significant, without actually having few enough moving windows that have equal to or greater than the number of earthquakes as Coso's pumping interval. Within 3 km, 89% of moving windows had fewer earthquakes than during the pumping interval; for a 10 km radius, 93% of windows had a smaller earthquake count.) This is substantial, although not statistically significant to 95% confidence.

Chapter 3 Figures

Figure 3.1

Locations of all California geothermal fields, in red. Figure from CA Department of Oil Gas and Geothermal Resources (DOGGR 2015).

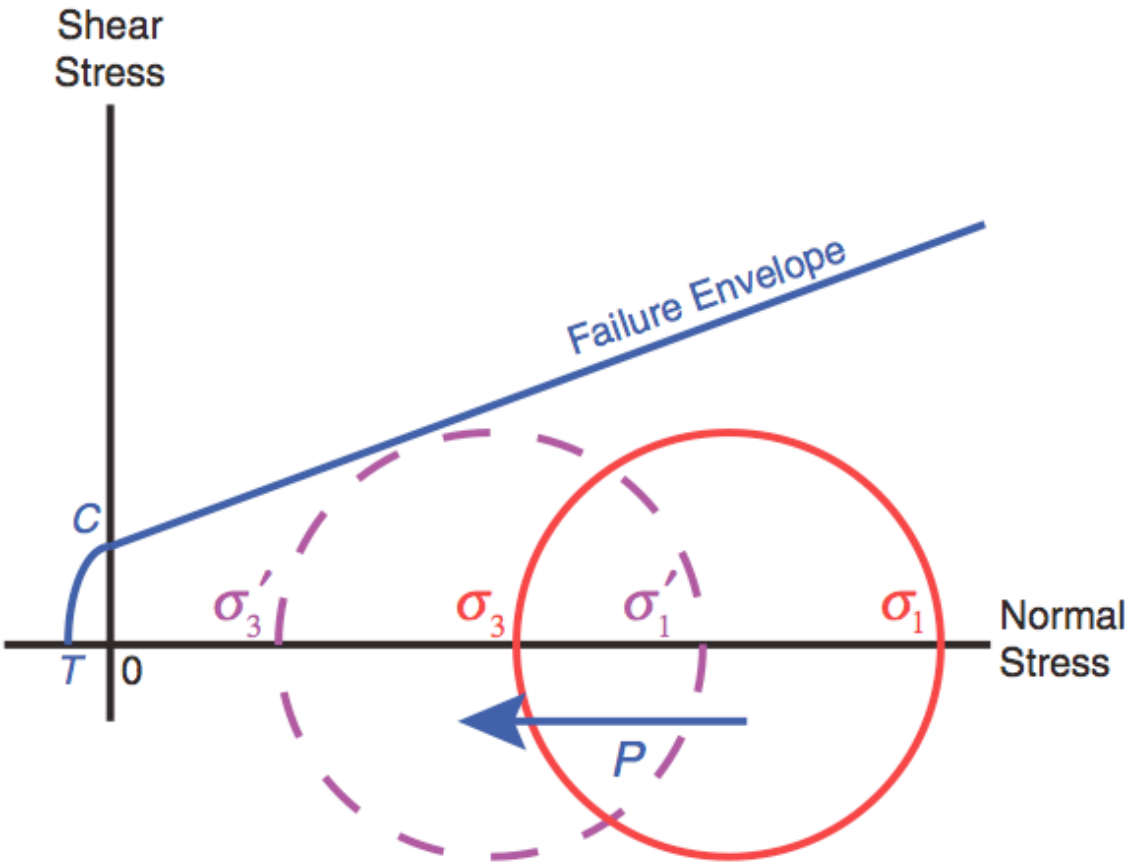

Figure 3.2

This Mohr-Coulomb diagram shows how an increase in fluid pressure can lower the effective normal stress (compressive when positive and tensile when negative), bringing a faulted rock closer to failure (figure from Rubinstein and Mahani 2015). σ_1 and σ_3 are the maximum and minimum normal stresses in a given location, respectively, and σ_1‘ and σ_3‘ are the reduced effective normal stresses after a fluid pressure increase (*P*). When stress conditions exceed a fault’s shear strength, slip may occur. The failure envelope (blue line) is the sum of the cohesion (*C*) and frictional resistance to slip on a fault.

3.3A.i

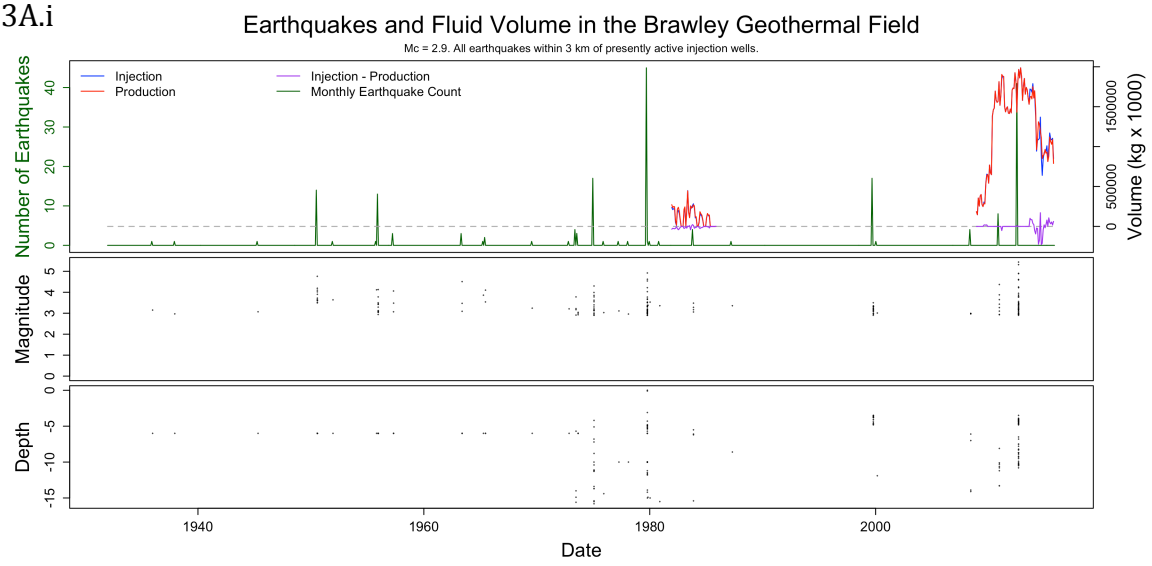
Earthquakes and Fluid Volume in the Brawley Geothermal Field
Mc = 2.9. All earthquakes within 3 km of presently active injection wells.
Injection
Production
Injection - Production
Monthly Earthquake Count
Number of Earthquakes
Volume (kg x 1000)
Magnitude
Depth
1940
1960
1980
2000
Date

3.3A.ii

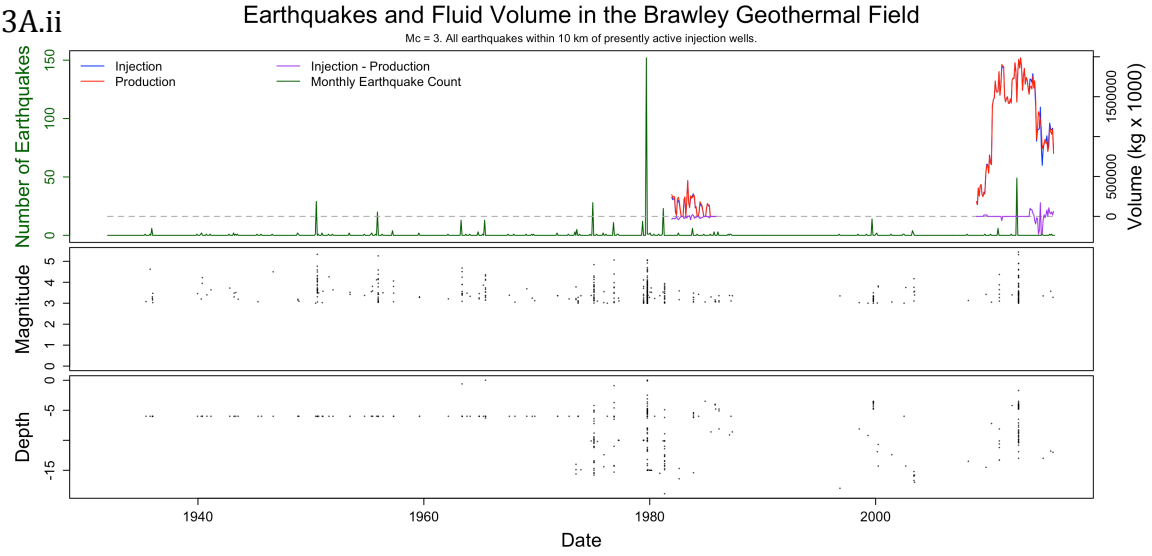
Earthquakes and Fluid Volume in the Brawley Geothermal Field
Mc = 3. All earthquakes within 10 km of presently active injection wells.
Injection
Production
Injection - Production
Monthly Earthquake Count
Number of Earthquakes
Volume (kg x 1000)
Magnitude
Depth
1940
1960
1980
2000
Date

3.3A.iii

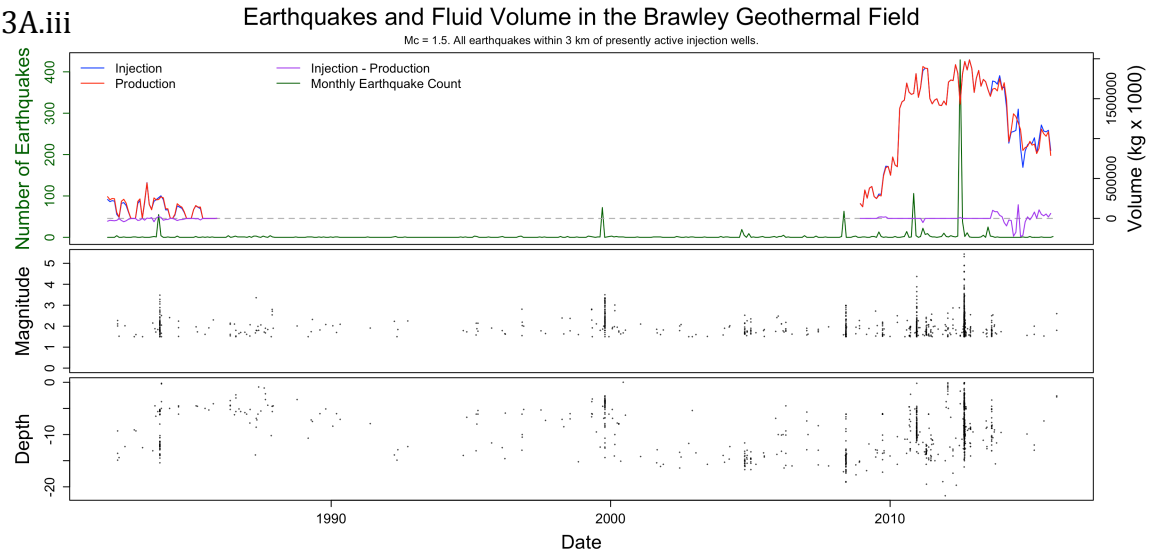

3.3A.iv

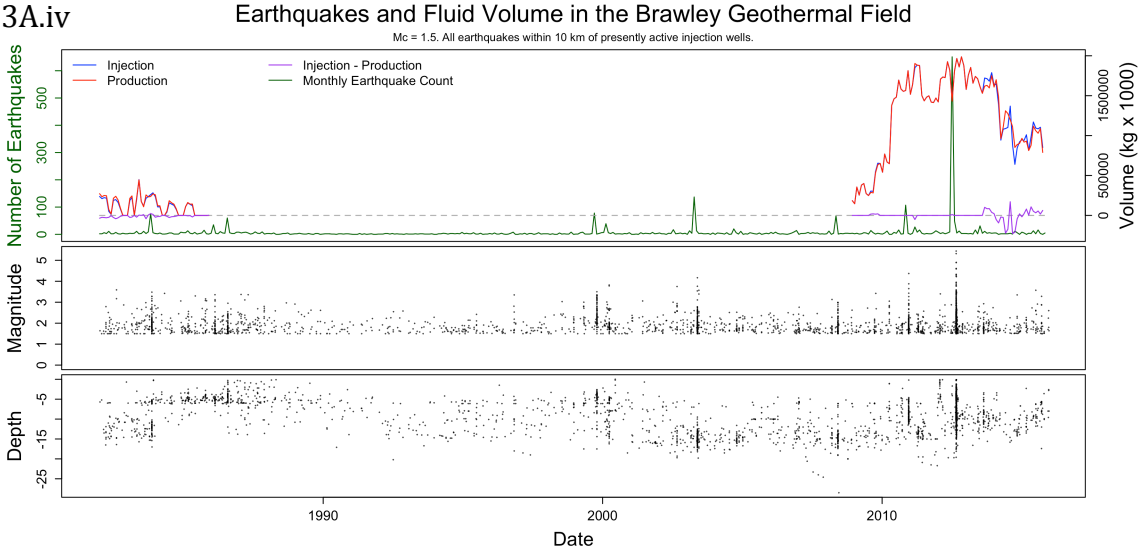

3.3B.i

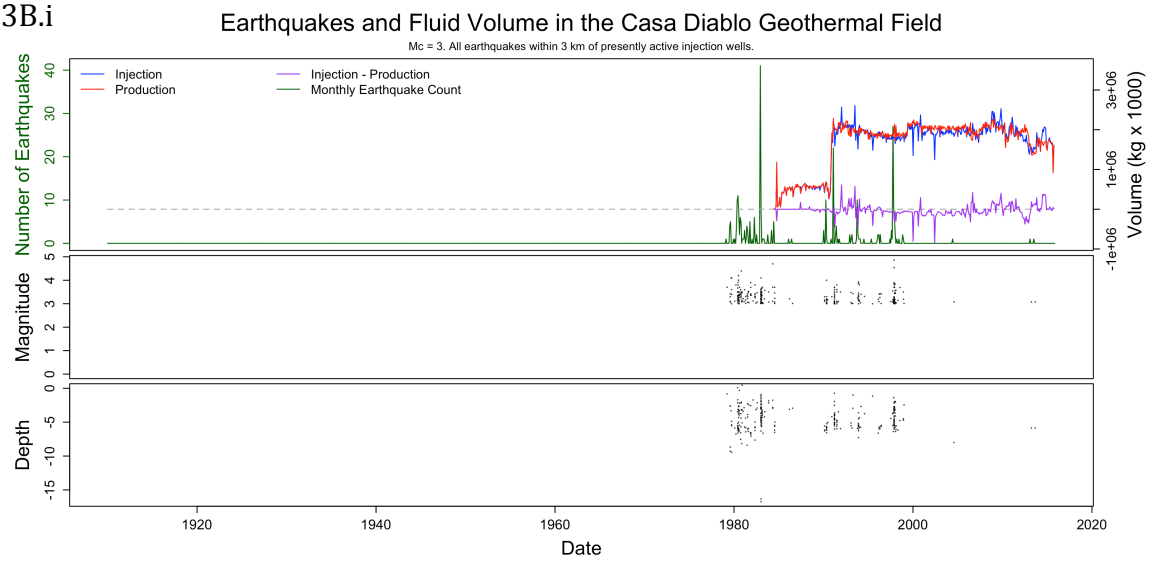
Earthquakes and Fluid Volume in the Casa Diablo Geothermal Field
Mc = 3. All earthquakes within 3 km of presently active injection wells.
Injection
Production
Injection - Production
Monthly Earthquake Count
Number of Earthquakes
Volume (kg x 1000)
Magnitude
Depth
Date

3.3B.ii

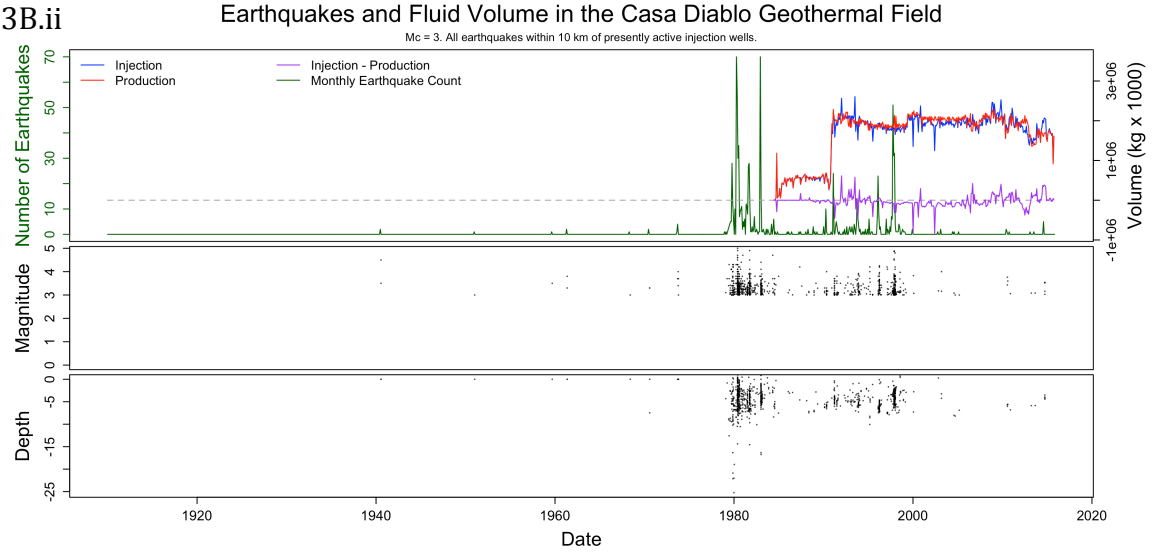
Earthquakes and Fluid Volume in the Casa Diablo Geothermal Field
Mc = 3. All earthquakes within 10 km of presently active injection wells.
Injection
Production
Injection - Production
Monthly Earthquake Count
Number of Earthquakes
Volume (kg x 1000)
Magnitude
Depth
Date

3.3B.iii

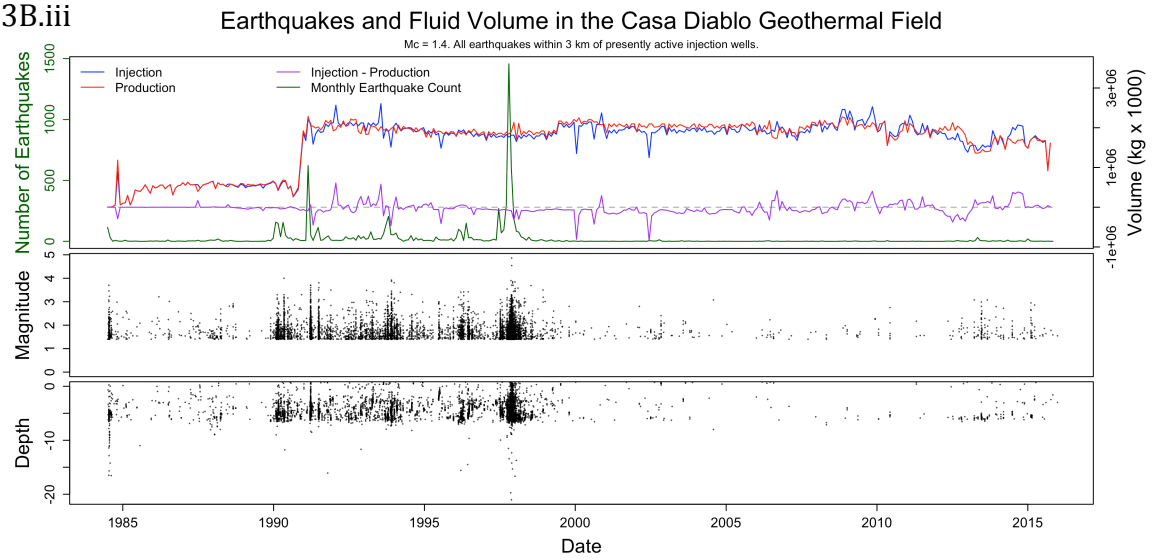

3.3B.iv

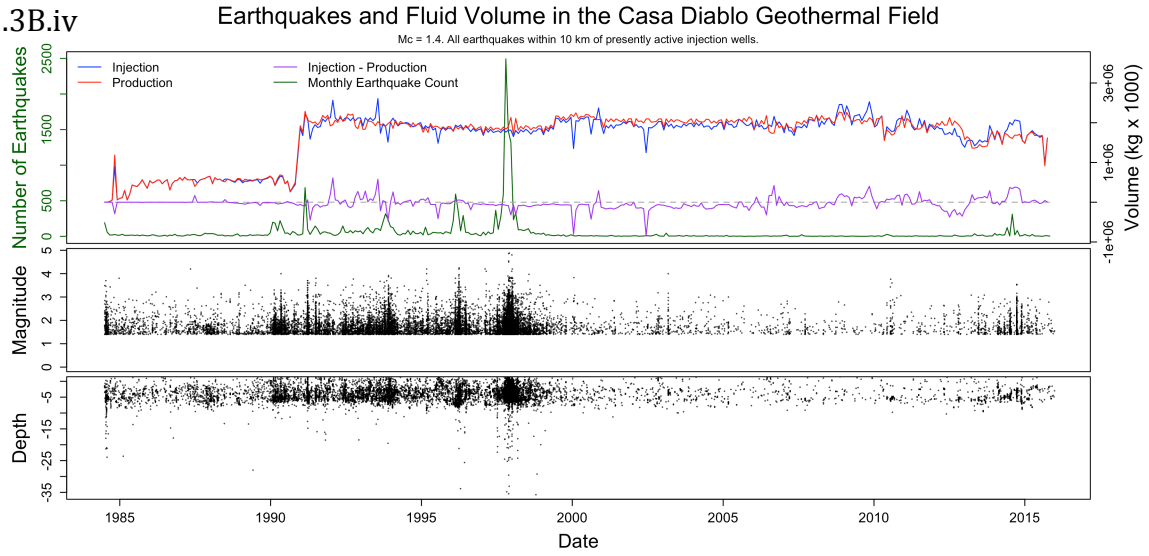

3.3C.i

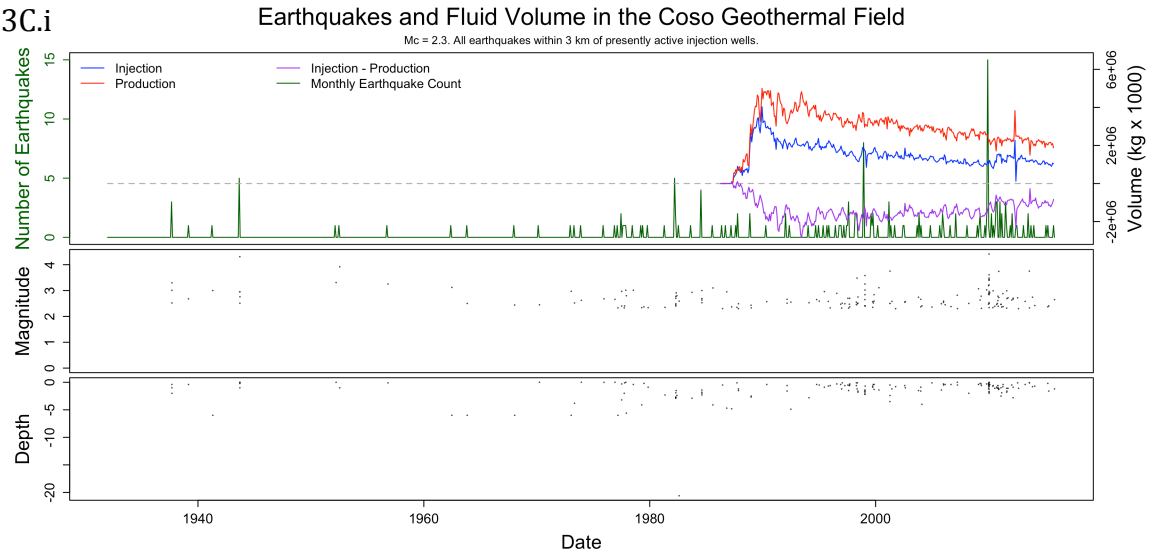
Earthquakes and Fluid Volume in the Coso Geothermal Field
Mc = 2.3. All earthquakes within 3 km of presently active injection wells.
Injection
Production
Injection - Production
Monthly Earthquake Count
Number of Earthquakes
Volume (kg x 1000)
Magnitude
Depth
Date
1940
1960
1980
2000

3.3C.ii

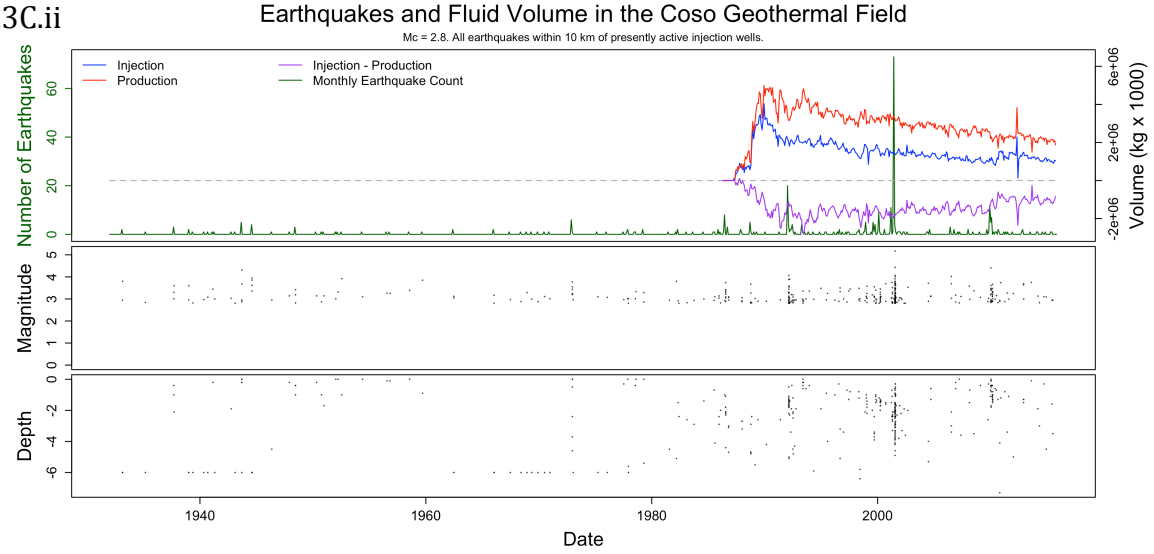
Earthquakes and Fluid Volume in the Coso Geothermal Field
Mc = 2.8. All earthquakes within 10 km of presently active injection wells.
Injection
Production
Injection - Production
Monthly Earthquake Count
Number of Earthquakes
Volume (kg x 1000)
Magnitude
Depth
Date
1940
1960
1980
2000

3.3C.iii

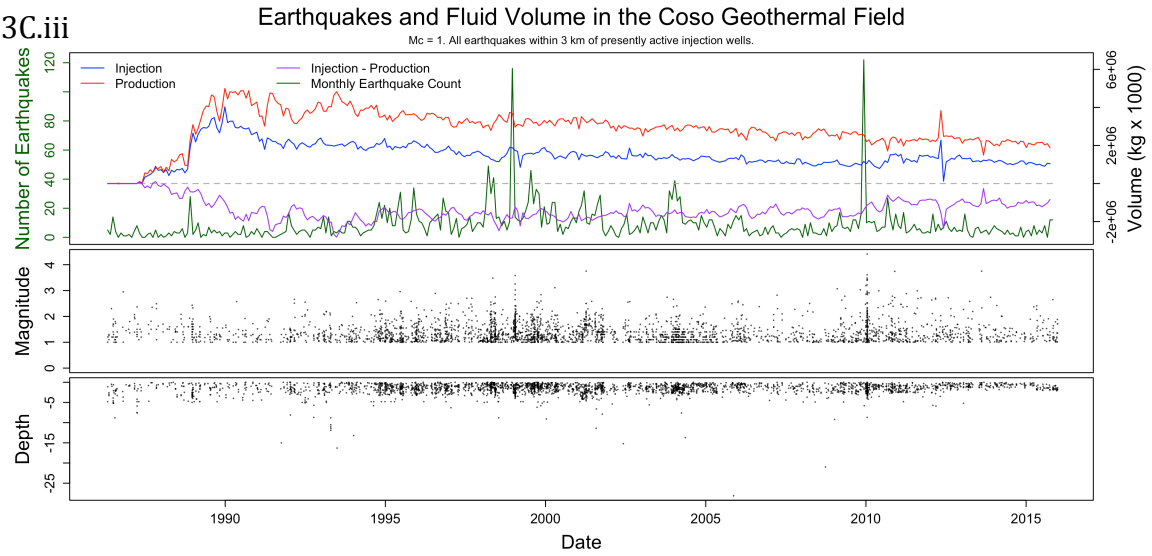

3.3C.iv

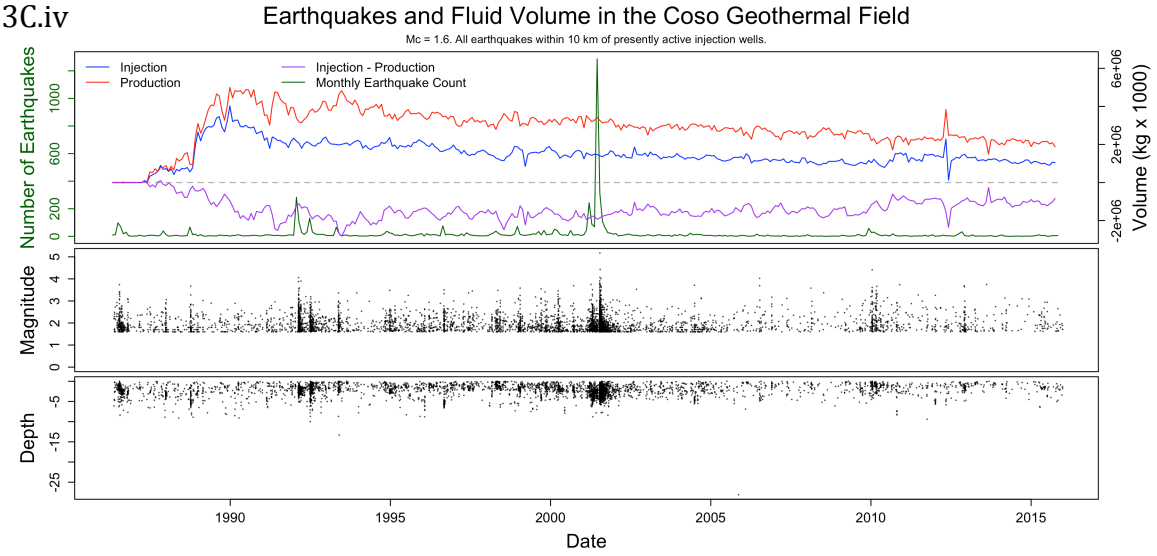

3.3D.i

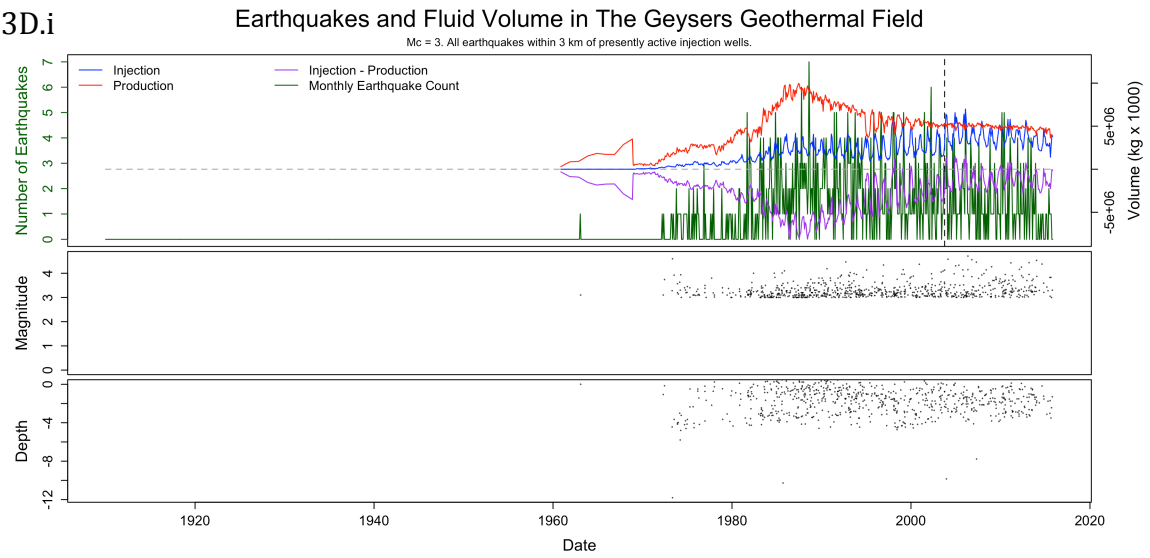
Earthquakes and Fluid Volume in The Geysers Geothermal Field
Mc = 3. All earthquakes within 3 km of presently active injection wells.
Injection
Production
Injection - Production
Monthly Earthquake Count
Number of Earthquakes
Volume (kg x 1000)
Magnitude
Depth
Date

3.3D.ii

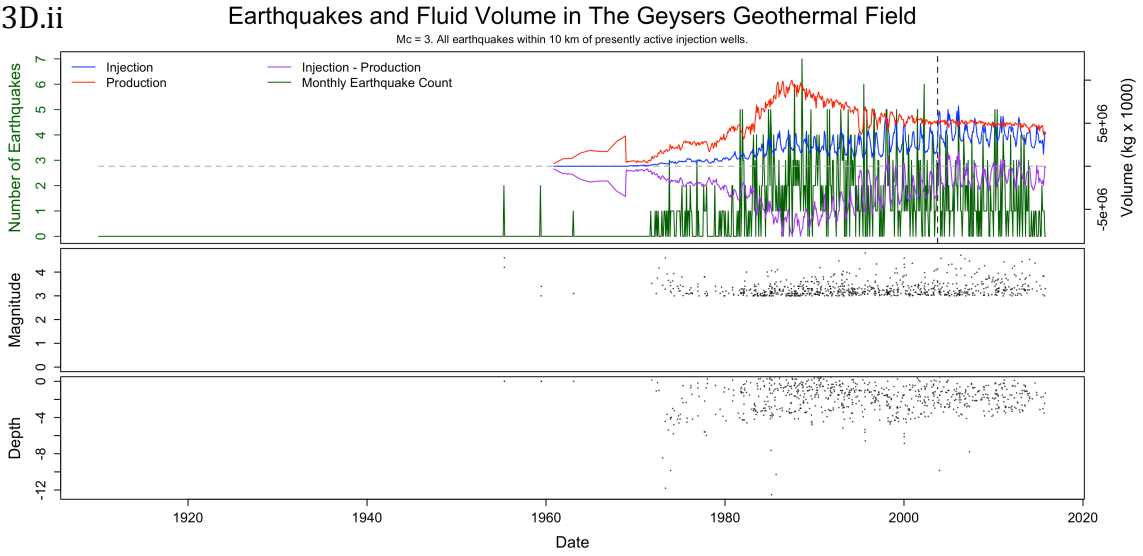
Earthquakes and Fluid Volume in The Geysers Geothermal Field
Mc = 3. All earthquakes within 10 km of presently active injection wells.
Injection
Production
Injection - Production
Monthly Earthquake Count
Number of Earthquakes
Volume (kg x 1000)
Magnitude
Depth
Date

3.3D.iii

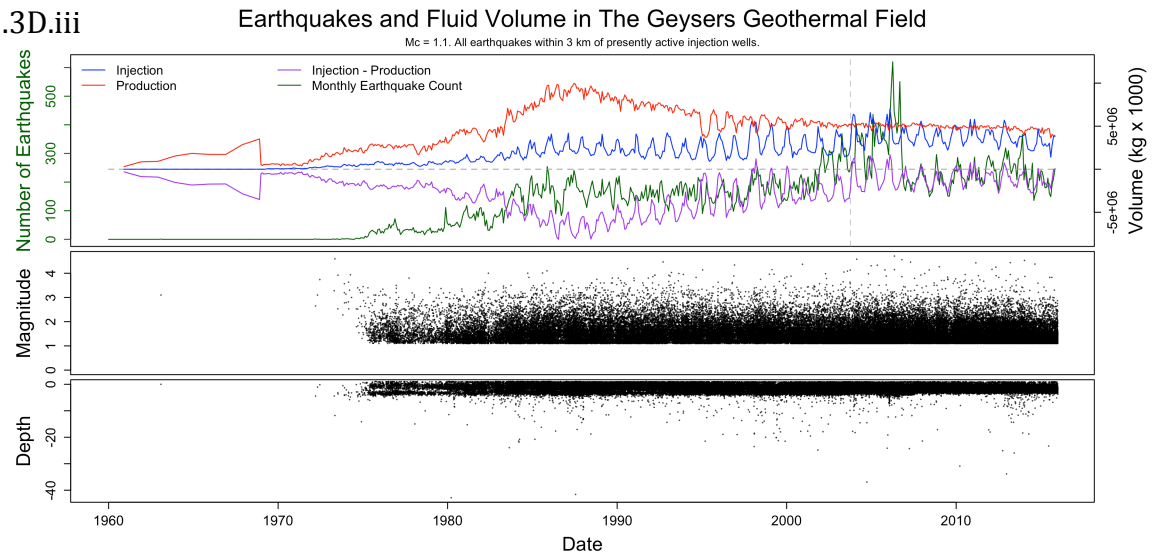

3.3D.iv

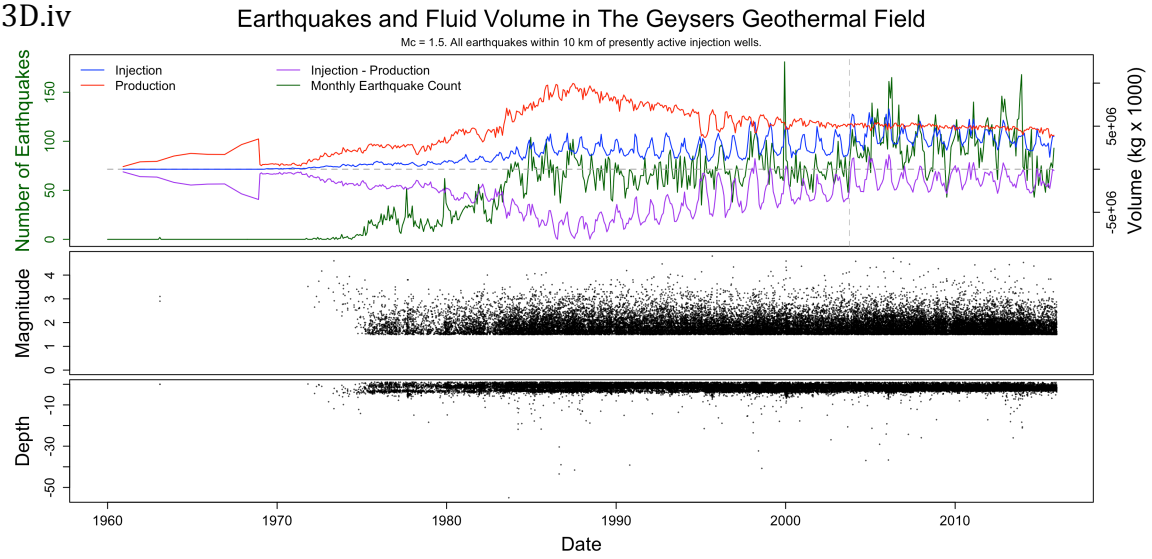

3.3E.i

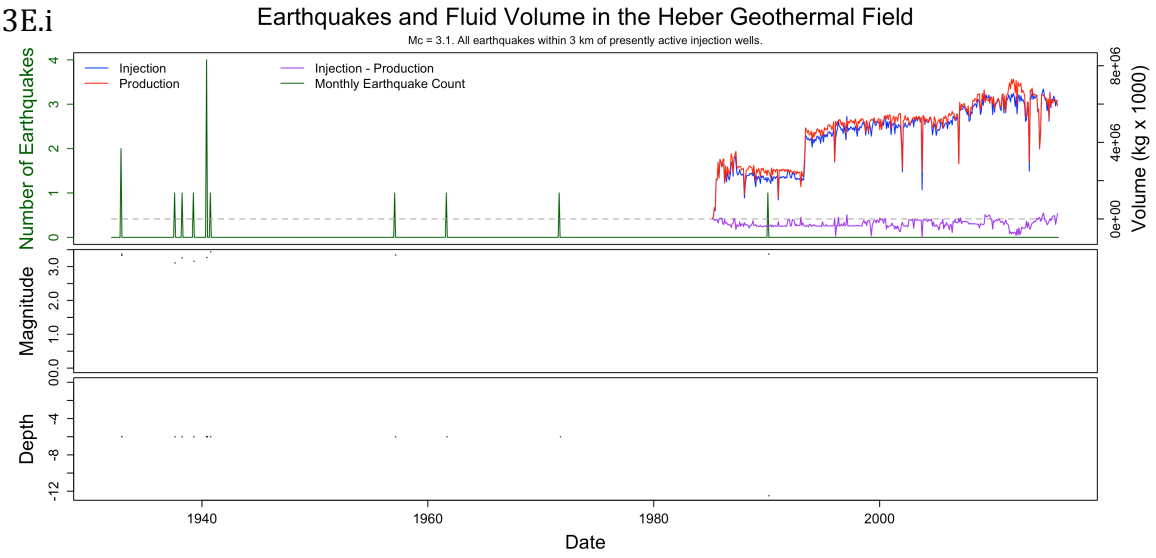
Earthquakes and Fluid Volume in the Heber Geothermal Field
Mc = 3.1. All earthquakes within 3 km of presently active injection wells.
Injection
Production
Injection - Production
Monthly Earthquake Count
Number of Earthquakes
Volume (kg x 1000)
Magnitude
Depth
Date
1940
1960
1980
2000

3.3E.ii

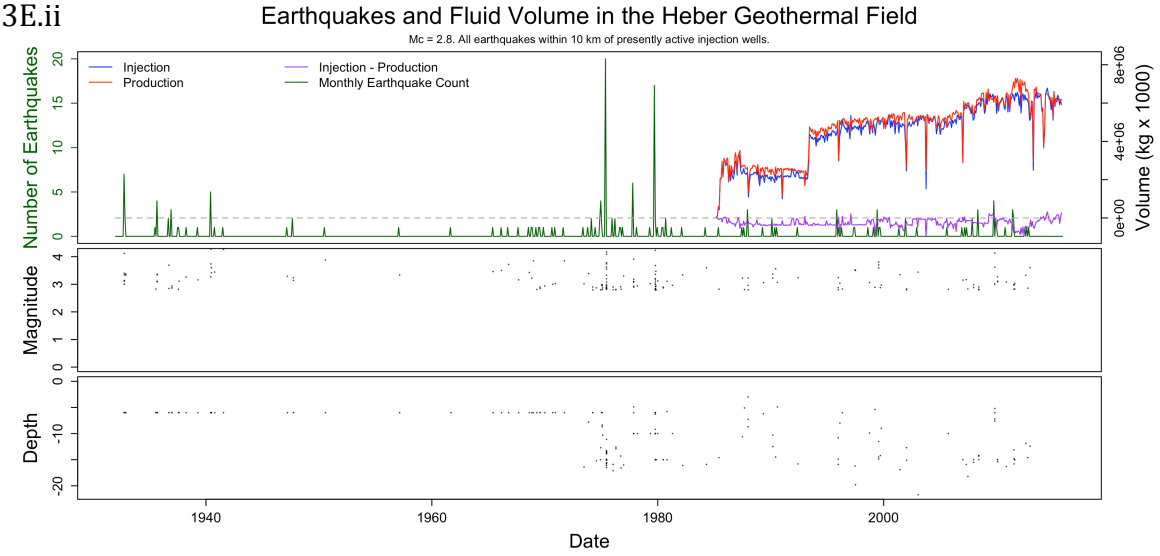
Earthquakes and Fluid Volume in the Heber Geothermal Field
Mc = 2.8. All earthquakes within 10 km of presently active injection wells.
Injection
Production
Injection - Production
Monthly Earthquake Count
Number of Earthquakes
Volume (kg x 1000)
Magnitude
Depth
Date
1940
1960
1980
2000

3.3E.iii

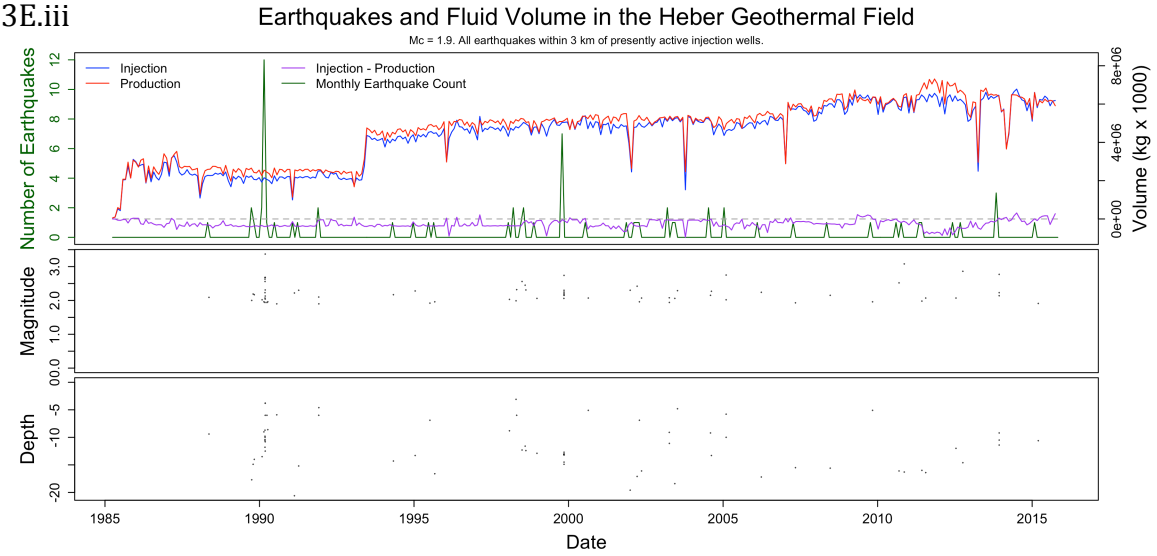

3.3E.iv

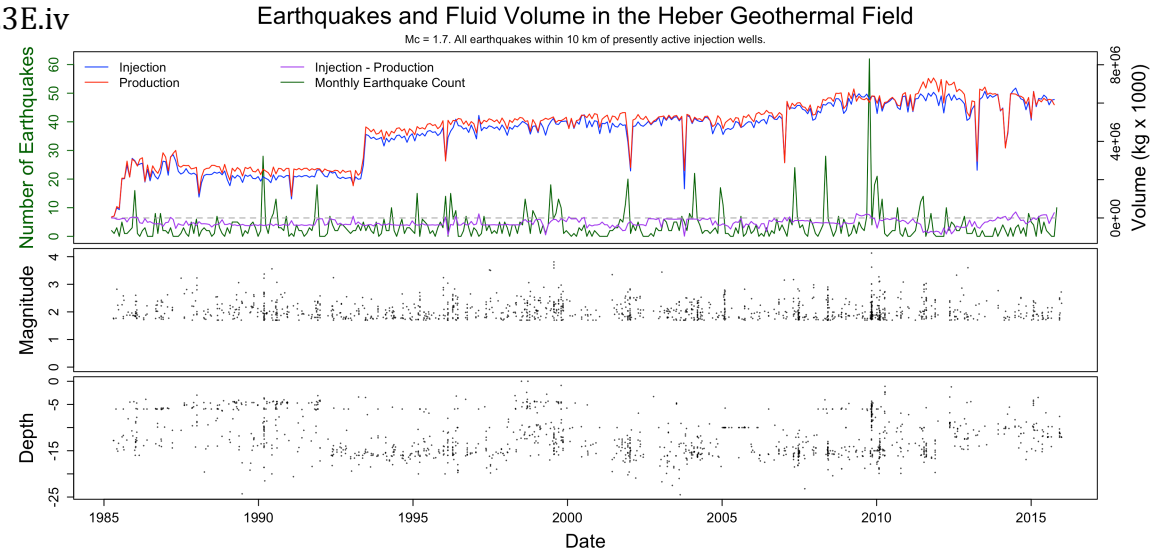

3.3F.i

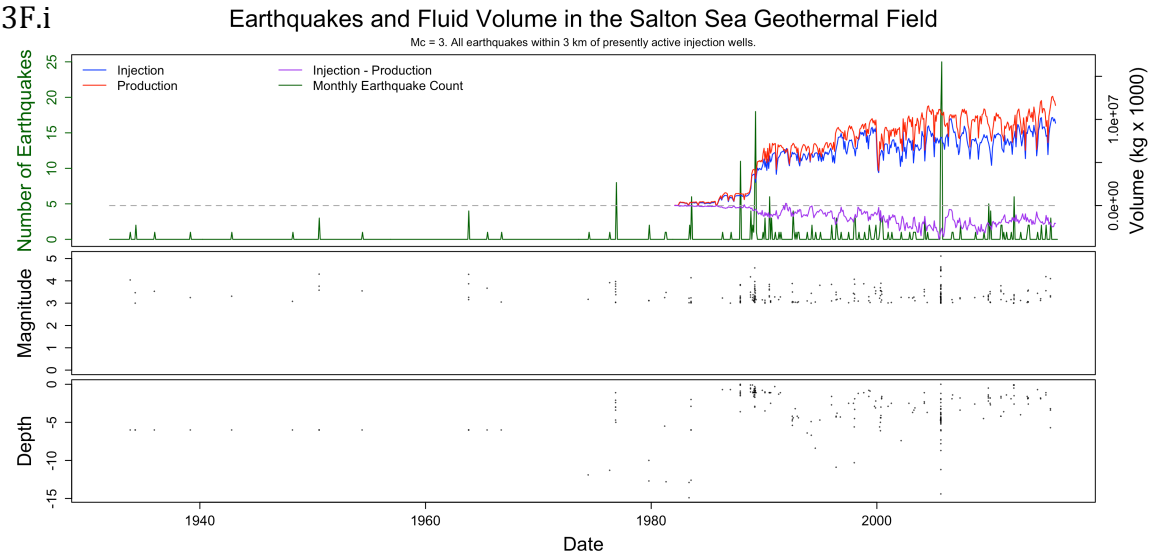
Earthquakes and Fluid Volume in the Salton Sea Geothermal Field
Mc = 3. All earthquakes within 3 km of presently active injection wells.
Injection
Production
Injection - Production
Monthly Earthquake Count
Number of Earthquakes
Volume (kg x 1000)
0.0e+00
1.0e+07
Magnitude
Depth
1940
1960
1980
2000
Date

3.3F.ii

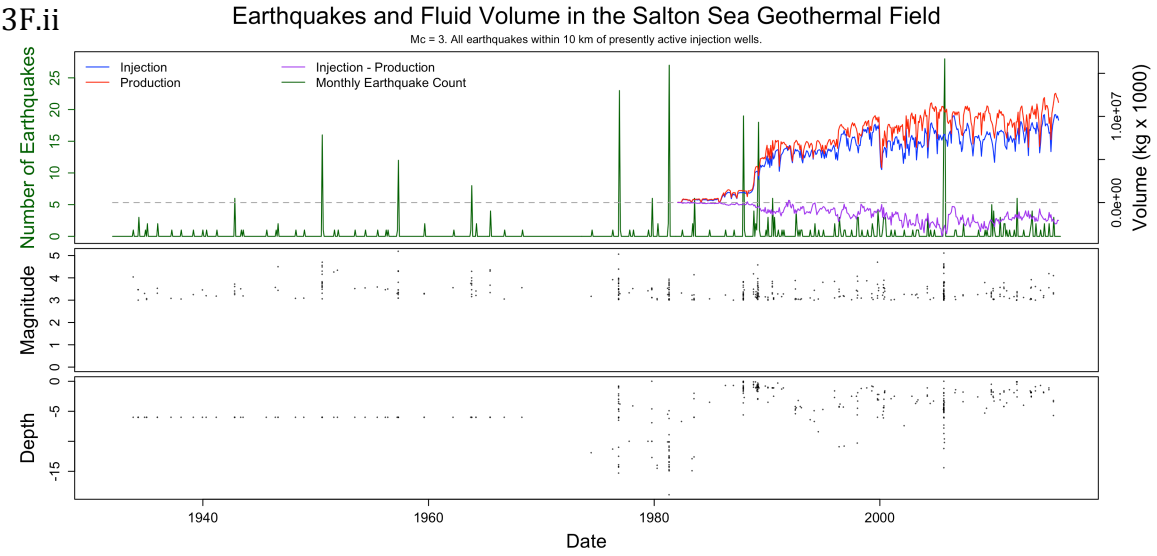
Earthquakes and Fluid Volume in the Salton Sea Geothermal Field
Mc = 3. All earthquakes within 10 km of presently active injection wells.
Injection
Production
Injection - Production
Monthly Earthquake Count
Number of Earthquakes
Volume (kg x 1000)
0.0e+00
1.0e+07
Magnitude
Depth
1940
1960
1980
2000
Date

3.3F.iii

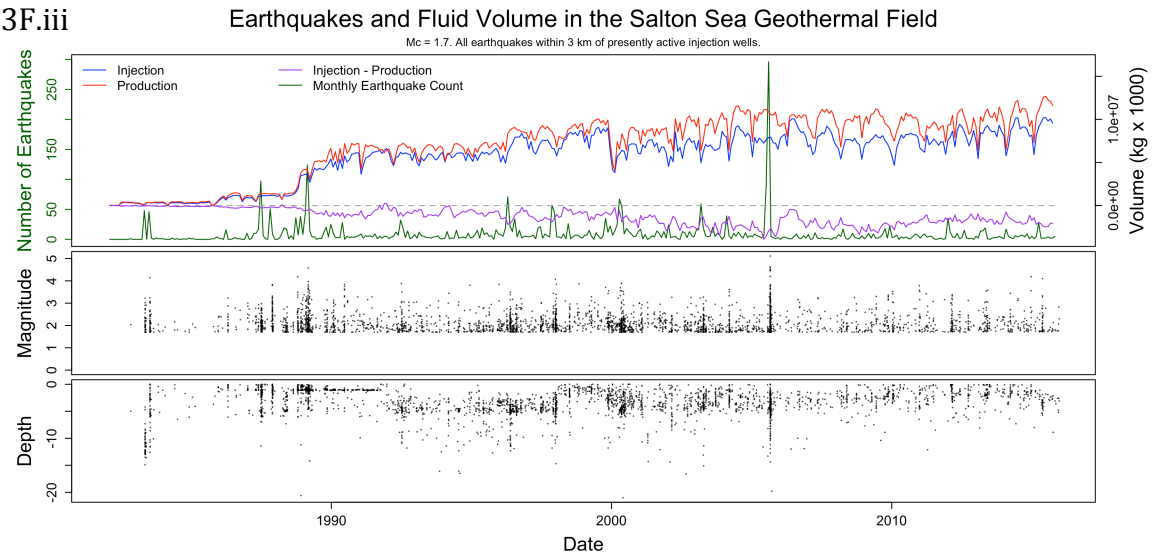

3.3F.iv

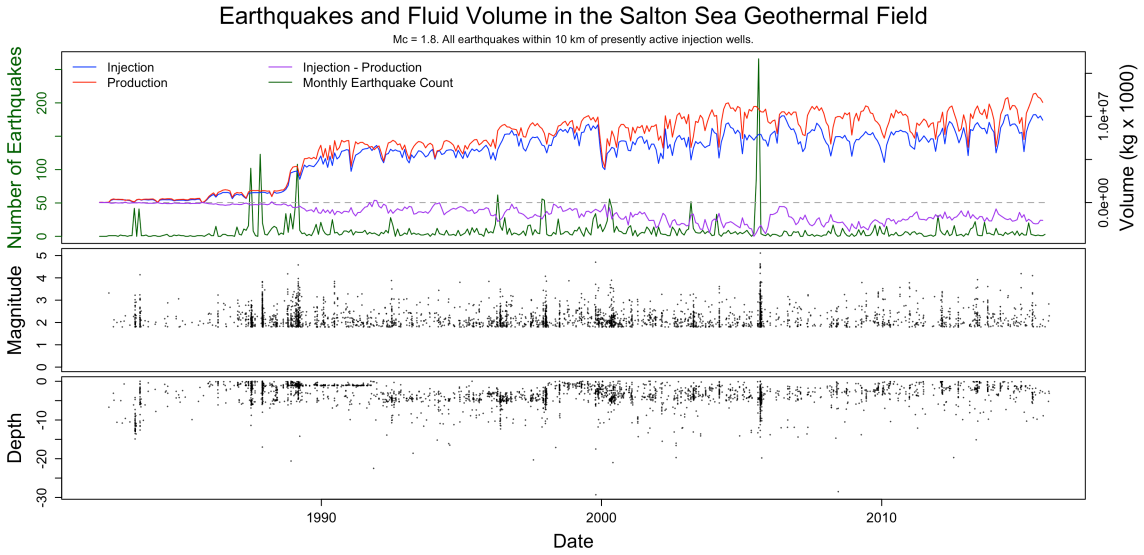

Figure 3.3 (A-F)

Time series showing number of monthly earthquakes (green data and corresponding axis); fluid injection, production and net (injection – production) volume over time; earthquake magnitudes; and hypocenter depths for a sample of California geothermal fields: A-Brawley; B-Casa Diablo; C-Coso; D-The Geysers; E-Heber; F-Salton Sea. I show four plots: **i. and ii.** These plots show data over the entire catalog duration (through 12/31/2015), using the pre-pumping completeness

threshold. **iii. and iv.** Data are displayed for the time period concurrent with pumping (through 12/31/2015), using the co-pumping completeness threshold. **i. and iii.** Earthquakes included in these plots are within 3 km of active injection wells. **ii. and iv.** Earthquakes included in these plots are within 10 km of active injection wells. When relationships are observed between monthly earthquake occurrences and pumping parameters, it may indicate a period where earthquakes were likely induced.

Northern California earthquakes were queried from the Brawley Seismic Network (BDSN, 2014; available 1910-2003; last accessed November 19, 2015) and Northern California Seismic Network catalogs (NCSN; available 1967-present; last accessed January 12, 2015). Southern California earthquakes are from the Southern California Earthquake Data Center (Hutton et al. 2010; SCEDC 2013). Earthquake data are cut-off after 12/31/2015 23:59:59. Pumping data are available through the California Department of Oil, Gas, and Geothermal Resources and were last accessed February 24, 2016 (DOGGR 2015).

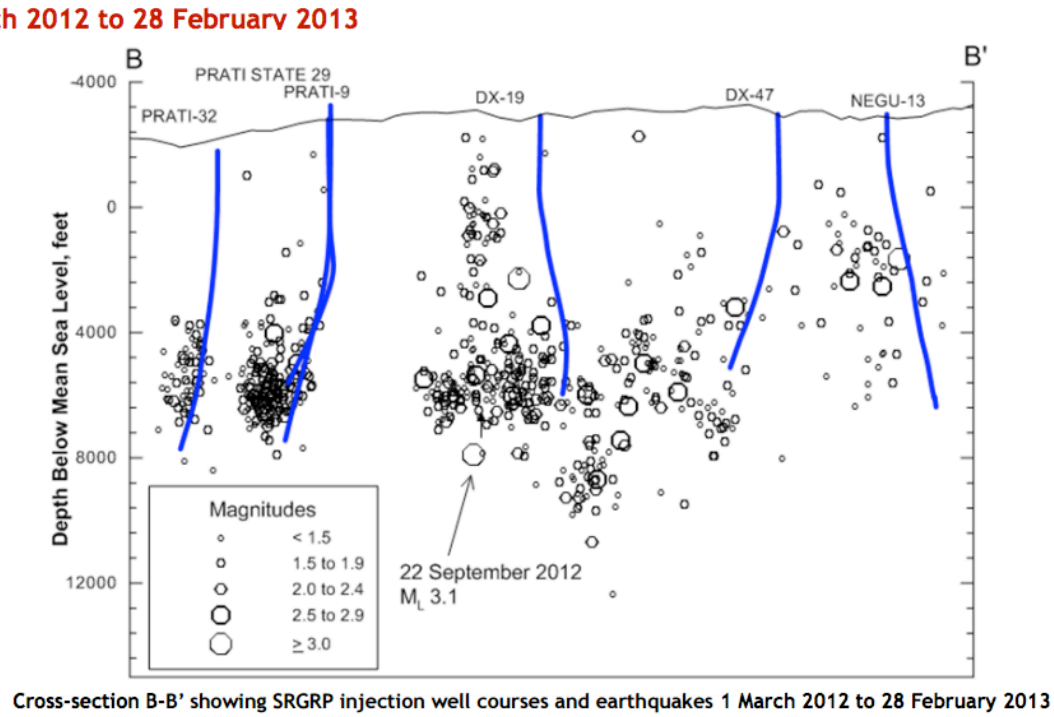

Figure 3.4

Cross-section showing six injection wells in the northwest corner of The Geysers geothermal reservoir and one year of proximal earthquakes (Hartline 2012). Seismicity is shown with dots scaled by magnitude, and clearly clusters near well-bottom depths. Printed with permission from Calpine.

3.5A

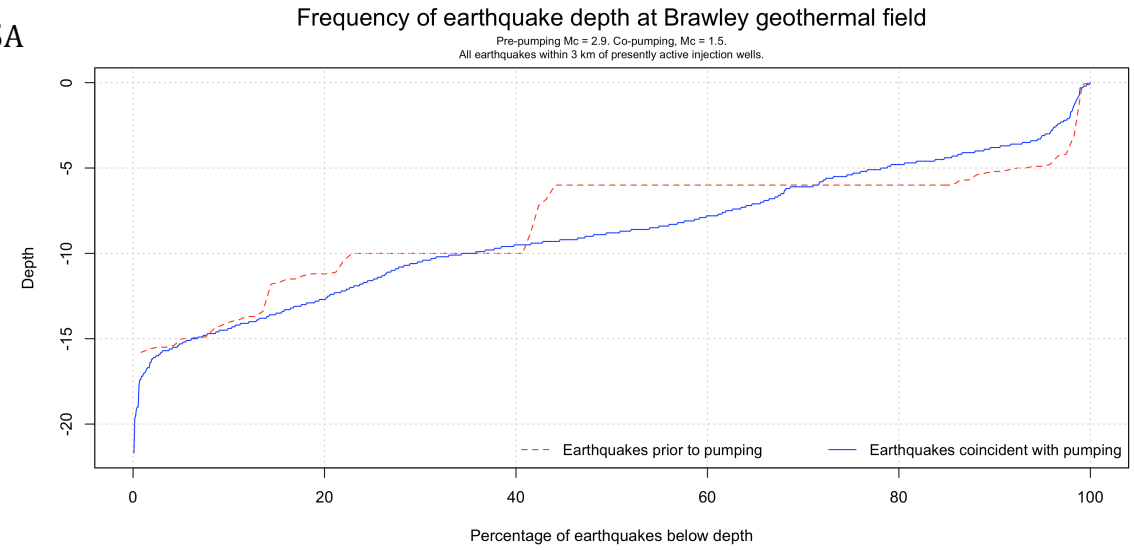
Frequency of earthquake depth at Brawley geothermal field
Pre-pumping Mc = 2.9. Co-pumping, Mc = 1.5.
All earthquakes within 3 km of presently active injection wells.
Depth
0
-5
-10
-15
-20
Earthquakes prior to pumping
Earthquakes coincident with pumping
0
20
40
60
80
100
Percentage of earthquakes below depth

3.5B

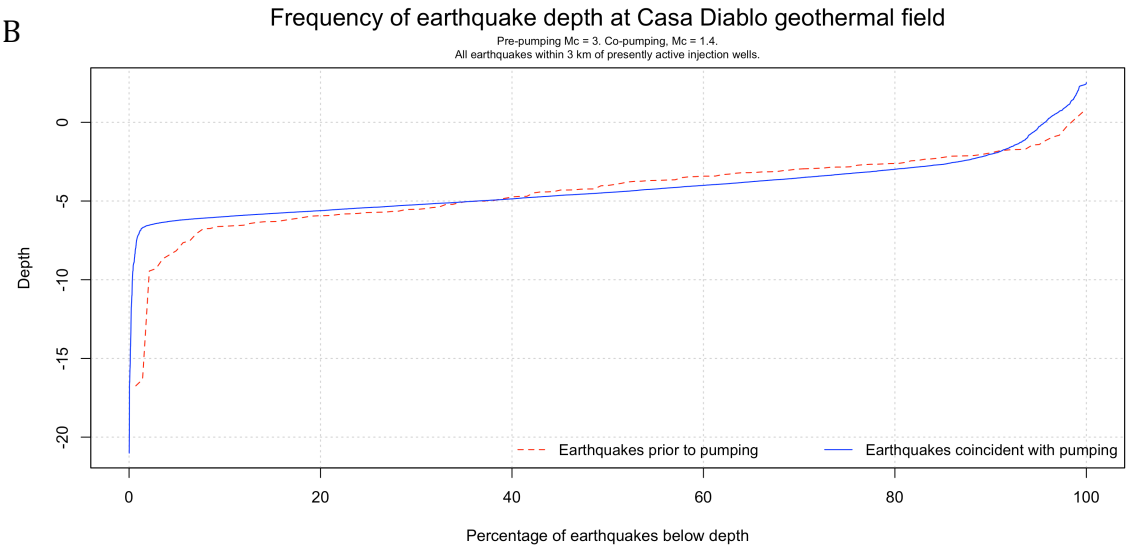
Frequency of earthquake depth at Casa Diablo geothermal field
Pre-pumping Mc = 3. Co-pumping, Mc = 1.4.
All earthquakes within 3 km of presently active injection wells.
Depth
0
-5
-10
-15
-20
Earthquakes prior to pumping
Earthquakes coincident with pumping
0
20
40
60
80
100
Percentage of earthquakes below depth

3.5C

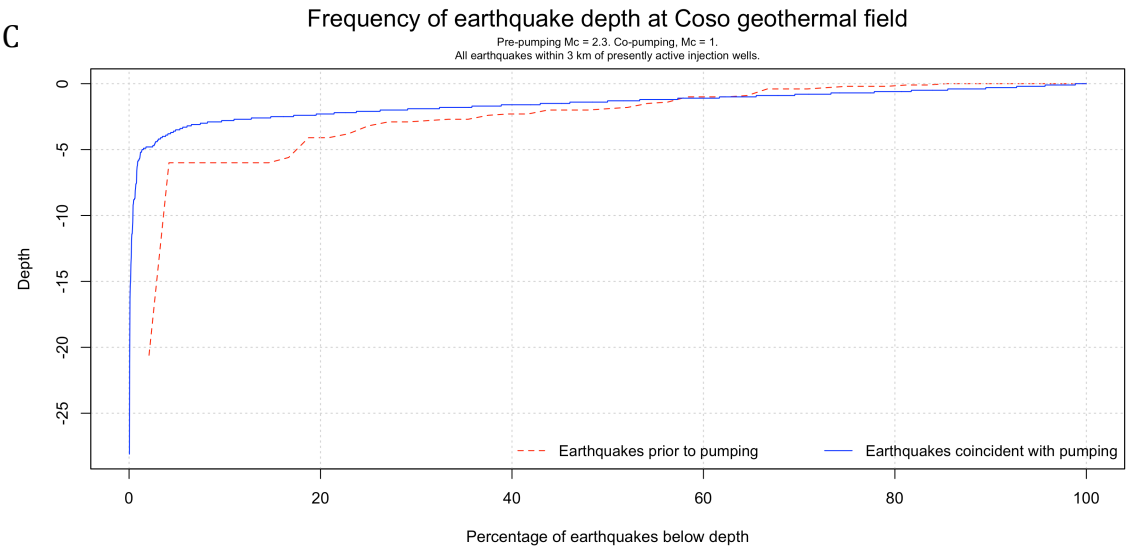
Frequency of earthquake depth at Coso geothermal field
Pre-pumping Mc = 2.3. Co-pumping, Mc = 1.
All earthquakes within 3 km of presently active injection wells.
Depth
0
-5
-10
-15
-20
-25
Earthquakes prior to pumping
Earthquakes coincident with pumping
0
20
40
60
80
100
Percentage of earthquakes below depth

3.5D

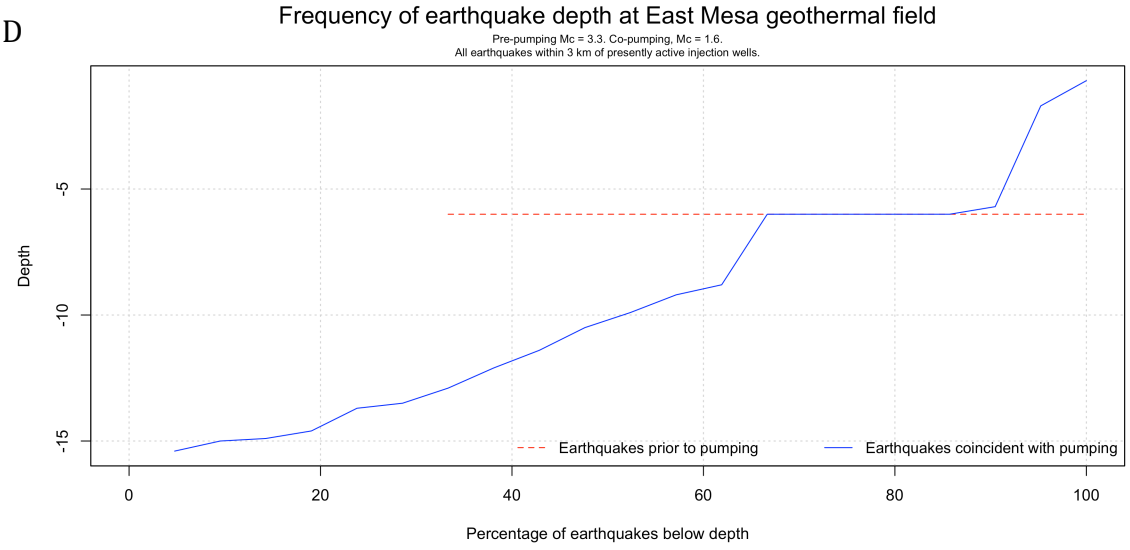
Frequency of earthquake depth at East Mesa geothermal field
Pre-pumping Mc = 3.3. Co-pumping, Mc = 1.6.
All earthquakes within 3 km of presently active injection wells.
Depth
-5
-10
-15
Earthquakes prior to pumping
Earthquakes coincident with pumping
0
20
40
60
80
100
Percentage of earthquakes below depth

3.5E

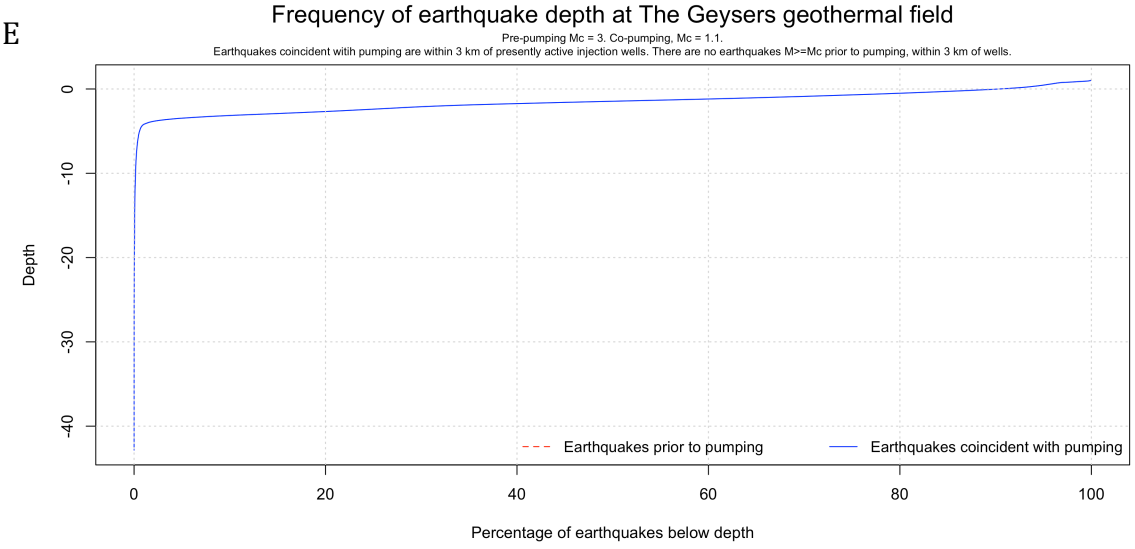
Frequency of earthquake depth at The Geysers geothermal field
Pre-pumping Mc = 3. Co-pumping, Mc = 1.1.
Earthquakes coincident witih pumping are within 3 km of presently active injection wells. There are no earthquakes M>=Mc prior to pumping, within 3 km of wells.
Depth
0
-10
-20
-30
-40
Earthquakes prior to pumping
Earthquakes coincident with pumping
0
20
40
60
80
100
Percentage of earthquakes below depth

3.5F

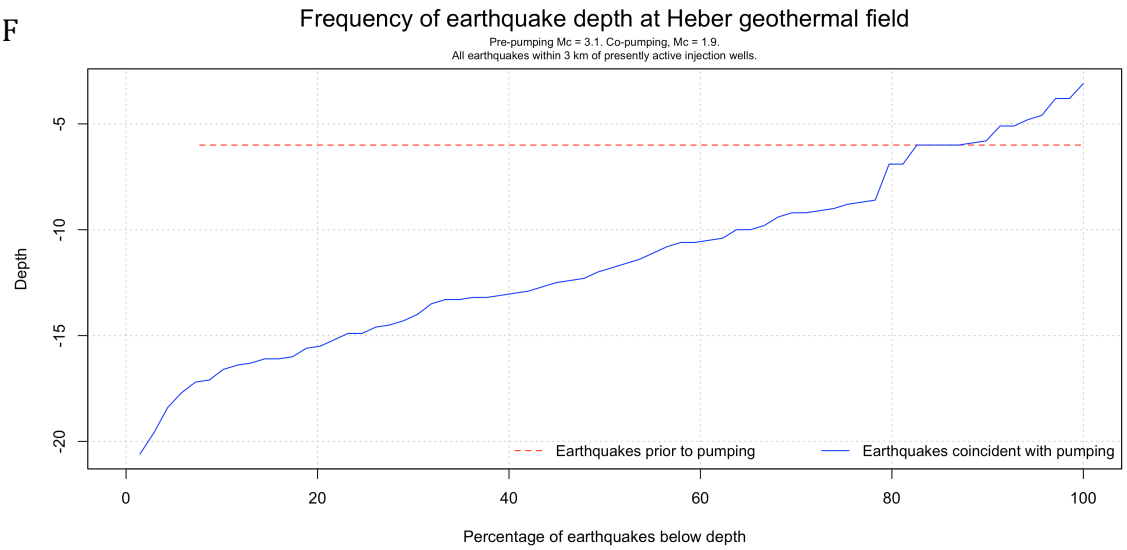
Frequency of earthquake depth at Heber geothermal field
Pre-pumping Mc = 3.1. Co-pumping, Mc = 1.9.
All earthquakes within 3 km of presently active injection wells.
Depth
-5
-10
-15
-20
Earthquakes prior to pumping
Earthquakes coincident with pumping
0
20
40
60
80
100
Percentage of earthquakes below depth

3.5G

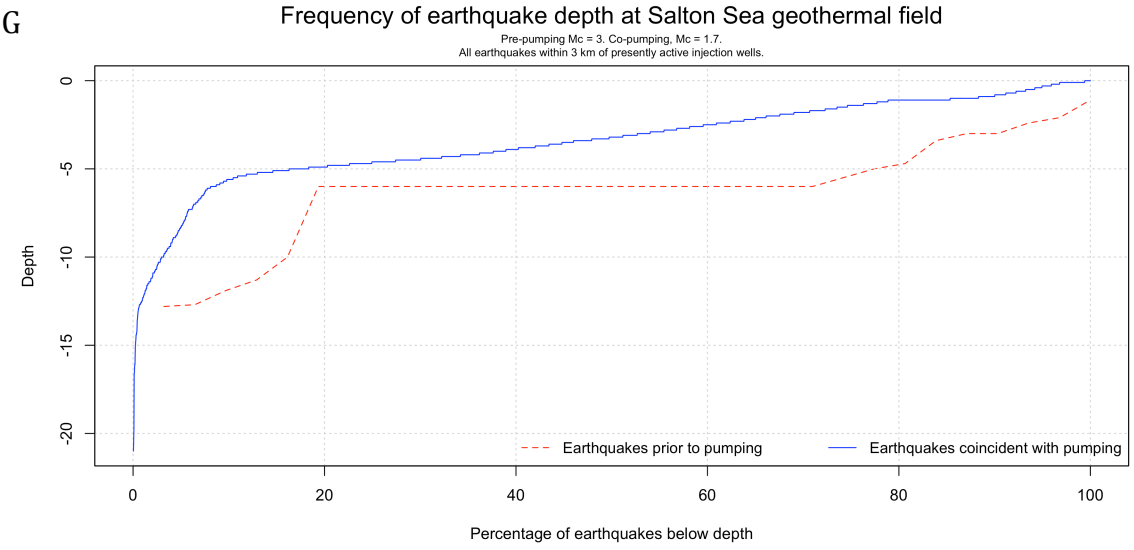
Frequency of earthquake depth at Salton Sea geothermal field
Pre-pumping Mc = 3. Co-pumping, Mc = 1.7.
All earthquakes within 3 km of presently active injection wells.
Depth
0
-5
-10
-15
-20
Earthquakes prior to pumping
Earthquakes coincident with pumping
0
20
40
60
80
100
Percentage of earthquakes below depth

3.5H

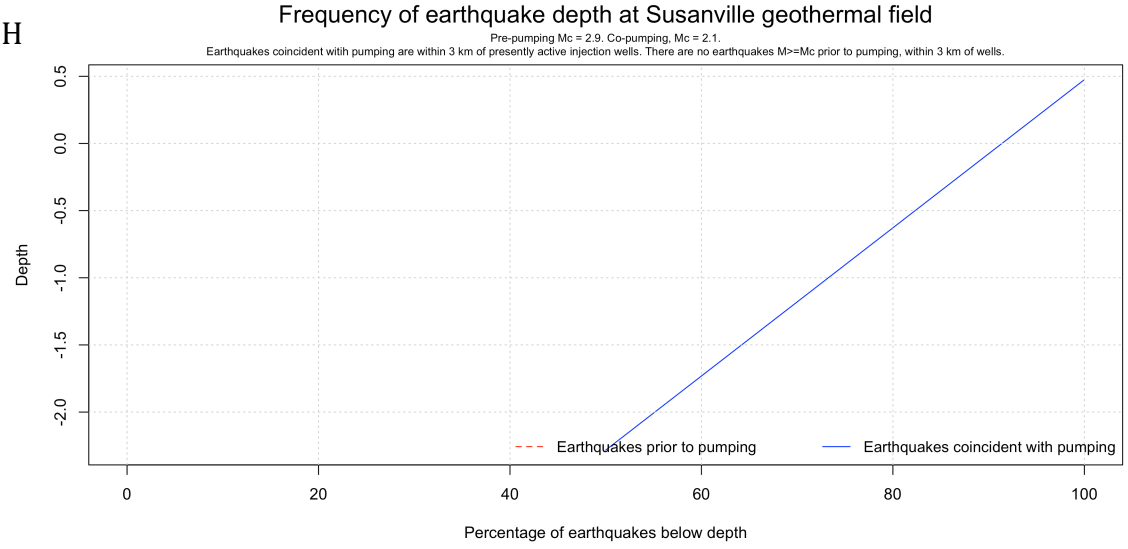
Frequency of earthquake depth at Susanville geothermal field
Pre-pumping Mc = 2.9. Co-pumping, Mc = 2.1.
Earthquakes coincident witih pumping are within 3 km of presently active injection wells. There are no earthquakes M>=Mc prior to pumping, within 3 km of wells.
Depth
0.5
0.0
-0.5
-1.0
-1.5
-2.0
Earthquakes prior to pumping
Earthquakes coincident with pumping
0
20
40
60
80
100
Percentage of earthquakes below depth

3.5I

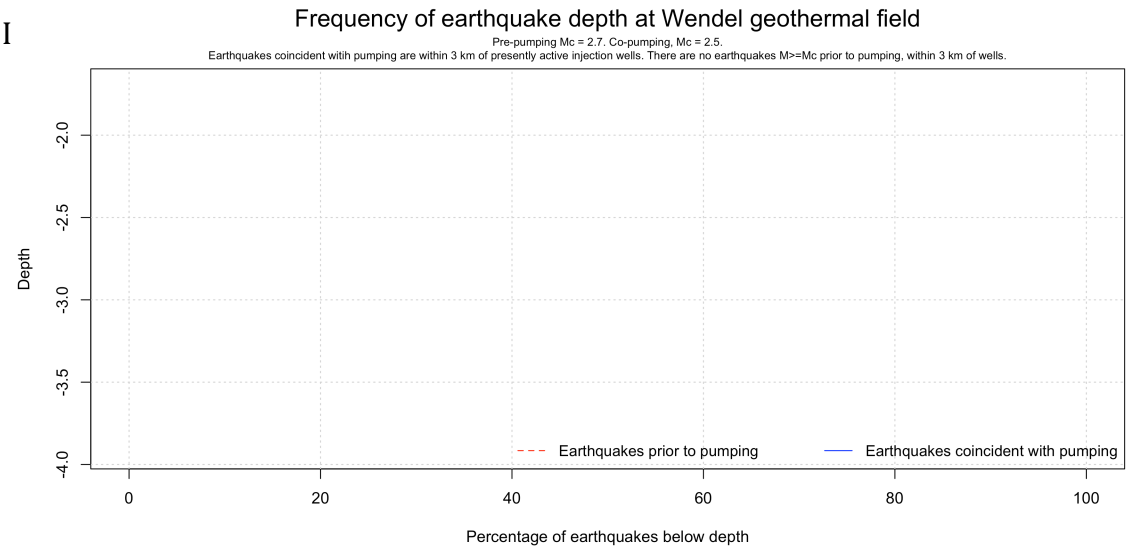

Figure 3.5 (A-I)

Cumulative comparison of pre-pumping hypocenter depths with hypocenter depths recorded after pumping began. When depths were not well bounded, the default depth assigned was usually 6 km. For this reason, many data series show an exceptionally large population of 6 km deep earthquakes.

There were no earthquakes greater than the completeness threshold prior to pumping at The Geysers, Susanville and Wendel geothermal fields. At Susanville, only two earthquakes occurred coincident with pumping (plotting at 50% and 100% on the x-axis). At Wendel, only one co-pumping earthquake occurred, and plots as a single point (hence, no lines are visible).

Field	*R*	*Prior to pumping*				*Coincident with pumping*					
		M≥M$_{c\text{-}pre}$				*M≥M$_{c\text{-}pre}$*		*M≥M$_{c\text{-}co}$*			
		ERD	*n*	*M_c*	*T_{pre}*	*ERD*	*n*	*ERD*	*n*	*M_c*	*T_{co}*
Brawley	3	0.0021	104	3.0	18263	0.0548	44	0.0645	827	1.5	4107
	10	0.0013	385			0.0011	75	0.0216	1518		
Casa Diablo	3	0.0053	142	3.0	27210	0.0122	138	0.6636	7498	1.4	11506
	10	0.0019	554			0.0030	364	0.1588	19091		
Coso	3	0.0003	20	2.8	19844	0.0010	33	0.0216	703	1.6	10837
	10	0.0003	80			0.0016	274	0.0347	6015		
East Mesa	3	0.0000	3	3.3	18628	0	0	0.0005	21	1.6	12053
	10	0.0001	19			0	0	0.0002	38		
The Geysers	3	0	0	3.0	18262	0.0054	749	0.2345	32697	1.5	20454
	10	0.0000	4			0.0015	776	0.0637	33657		
Heber	3	0.0003	13	3.1	19449	0	1	0.0025	69	1.9	11232
	10	0.0002	61			0.0001	22	0.0049	807		
Salton Sea	3	0.0004	31	3.0	18294	0.0042	210	0.0567	2806	1.8	12387
	10	0.0004	152			0.0010	238	0.0138	3286		
Susanville	3	0	0	2.9	26632	0	0	0.0002	2	2.1	12084
	10	0.0000	7			0.0000	2	0.0001	17		
Wendel	3	0	0	2.7	27545	0	0	0.0001	1	2.5	11171
	10	0.0000	1			0.0000	5	0.0001	9		

Table 3.1

Monthly number of earthquakes (n) per km^2 (earthquake rate density) at each geothermal field. R describes the maximum distance from each active injection well at which earthquakes are included in analysis. Using calculated completeness thresholds, I determine monthly earthquake rate densities (ERD) prior to and coincident with pumping. In order to directly compare periods before and during pumping, I include results for each time period using the pre-pumping M_c. To demonstrate the increased M_c since pumping began, I include the monthly earthquake rate

density of earthquakes with magnitudes above the co-pumping M_c. For context, durations of pre- and co-pumping periods are listed, in days (T_{pre} and T_{co}).

When a result is listed as "0" this indicates that there were no earthquakes above the completeness threshold recorded during this time period. Conversely, when an entry is "0.0000", there was at least one earthquake greater than M_c recorded during this time period, but not enough earthquakes to register above 0.0000 monthly earthquakes per km^2.

Field	*R*	T_{pre}	T_{co}	$M_{c\text{-}pre}$	*n*	*N*	*f(n)*	*f(t)*	*P*	*1-P*
Brawley	3	18263	4107	3.0	44	164	0.268	0.184	**0.995**	**0.005**
	10				75	496	0.151	0.184	0.025	0.975
Casa Diablo	3	27210	11506	3.0	138	280	0.493	0.297	**1.000**	**0.000**
	10				364	918	0.397	0.297	**1.000**	**0.000**
Coso	3	19844	10837	2.8	33	53	0.623	0.353	**1.000**	**0.000**
	10				274	354	0.774	0.353	**1.000**	**0.000**
East Mesa	3	18628	12053	3.3	0	3	0.000	0.393	N/A	N/A
	10				0	19	0.000	0.393	N/A	N/A
The Geysers	3	18262	20454	3.0	749	749	1.000	0.528	**1.000**	**0.000**
	10				776	780	0.995	0.528	**1.000**	**0.000**
Heber	3	19449	11232	3.1	1	14	0.071	0.366	0.002	0.998
	10				22	83	0.265	0.366	0.019	0.981
Salton Sea	3	18294	12387	3.0	210	241	0.871	0.404	**1.000**	**0.000**
	10				238	390	0.610	0.404	**1.000**	**0.000**
Susanville	3	26632	12084	2.9	0	0	N/A	0.312	N/A	N/A
	10				2	9	0.222	0.312	0.175	0.825
Wendel	3	27545	11171	2.7	0	0	N/A	0.289	N/A	N/A
	10				5	6	0.833	0.289	**0.991**	**0.009**

Table 3.2

For each field, the distance column registers the radius (R, in km) from active injection wells within which earthquakes are included in that row's totals, T_{pre} is the number of days prior to the first recorded pumping day, and T_{co} is the number of days contemporaneous with pumping. For Brawley, T_{co} is only the number of days during pumping periods (1982-1985 and 2009-12/31/2015), and not the shut-in/hiatus period from 1985-2009. n is the number of events that occurred in the co-pumping period ($M \geq M_{c\text{-}pre}$), N is the total number of events from the start of the catalog until the end of 2015 with $M \geq M_{c\text{-}pre}$), $f(n)$ is the fraction of events that occurred in the co-pumping interval (for comparison only, not used in the calculation), $f(t)$ is the fraction of time in the co-pumping interval (taken as the probability of success in a single trial, P is the

probability that fewer than the observed number would occur in the co-pumping interval (output of calculation), and *1-P* is the probability that the observed number or more would occur in the co-interval. If $P \geq 0.95$ (and $1\text{-}P \leq 0.5$), the null hypothesis can be rejected with 95% confidence; these values are highlighted with bold green text. *P* and *1-P* can not be calculated when no earthquakes above the completeness threshold were recorded during pumping.

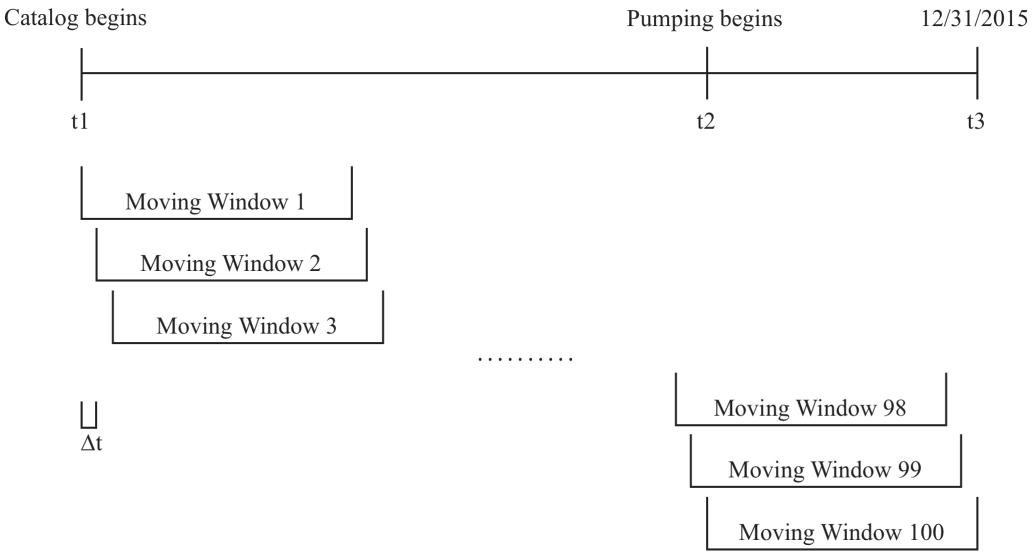

Figure 3.6

In order to evaluate the null hypothesis (h_0), I create 100 moving windows with durations equal to that of the pumping period. The 100th time period spans the length of energy production, from the start of pumping until 12/31/2015. For each moving window period, I compare the number of earthquakes ($M \geq M_{c\text{-}pre}$) to the observed quantity of events during the pumping interval.

Field	$M_{c\text{-}pre}$	*R*	*n*	*W*	*Reject h_0 with more than 95% confidence?*
Brawley	3.0	3	44	80	No
		10	75	27	No
Casa Diablo	3.0	3	138	43	No
		10	364	46	No
Coso	2.8	3	33	11	No
		10	274	7	No
East Mesa	3.3	3	0	100	No
		10	0	100	No
The Geysers	3.0	3	749	1	**Yes**
		10	776	1	**Yes**
Heber	3.1	3	1	100	No
		10	22	78	No
Salton Sea	3.0	3	210	2	**Yes**
		10	238	21	No
Susanville	2.9	3	0	100	No
		10	2	79	No
Wendel	2.7	3	0	100	No
		10	5	21	No

Table 3.3

If *W*, the number of time-windows (out of 100) with equal or more earthquakes to the co-pumping period, is less than or equal to 5/100 "successes," one can reject h_0 with at least 95% confidence (denoted a bold green "Yes"). *R* is the radius (in km) from active injection wells, within which I include earthquakes for analysis. *n* is the number of co-pumping earthquakes.

For Brawley, the moving window is composed of two fixed windows (representing the two periods of injection), separated by 24 years. Just as with the single moving window, I advance the fixed time windows by Δt for each of the 100 sample periods. Only earthquakes that occur during the pumping parts of the moving window (and not the 24 year hiatus,) are included in the earthquake count (*n*).

Geothermal Field	1	2	3a	3b	3c	4a	4b	*Total Number of Yes Responses*
Brawley	No	Yes	Yes	Yes	n/a	Yes	?	4
Casa Diablo	No	Yes	Yes	Yes	n/a	Yes	?	4
Coso	No	Yes	Yes	?	Yes	n/a	?	3
East Mesa	Yes?	Yes	Yes	?	No	n/a	?	3
The Geysers	No	Yes	Yes	Yes	n/a	Yes	?	4
Heber	No?	Yes	Yes	Yes	n/a	Yes	?	4
Salton Sea	No	Yes	Yes	Yes	n/a	Yes	?	4
Susanville	No?	Yes?	Yes	Yes	n/a	Yes	?	4
Wendel	Yes?	No?	Yes	Yes	n/a	Yes	?	4

Table 3.4

Results for wells with both injection and production. Columns 1-4b refer to criteria outlined in (Davis and Frohlich 1993), which are intended to resolve if an earthquake has been induced.

Geothermal Field	1a	1b	1c	2a	2b	2c	3a	3b	3c	Total Number of Yes Responses
Amedee	Yes?	Yes	Yes	Yes	Yes	No?	No	n/a	Yes?	6
Litchfield	No	Yes	Yes	Yes	Yes	No?	Yes	Yes	No?	6

Table 3.5

Results for production-only fields. Columns (1a-3c) refer to criteria outlined in (Davis, Nyffenegger, and Frohlich 1995), which are intended to resolve if an earthquake has been induced.

3.7A

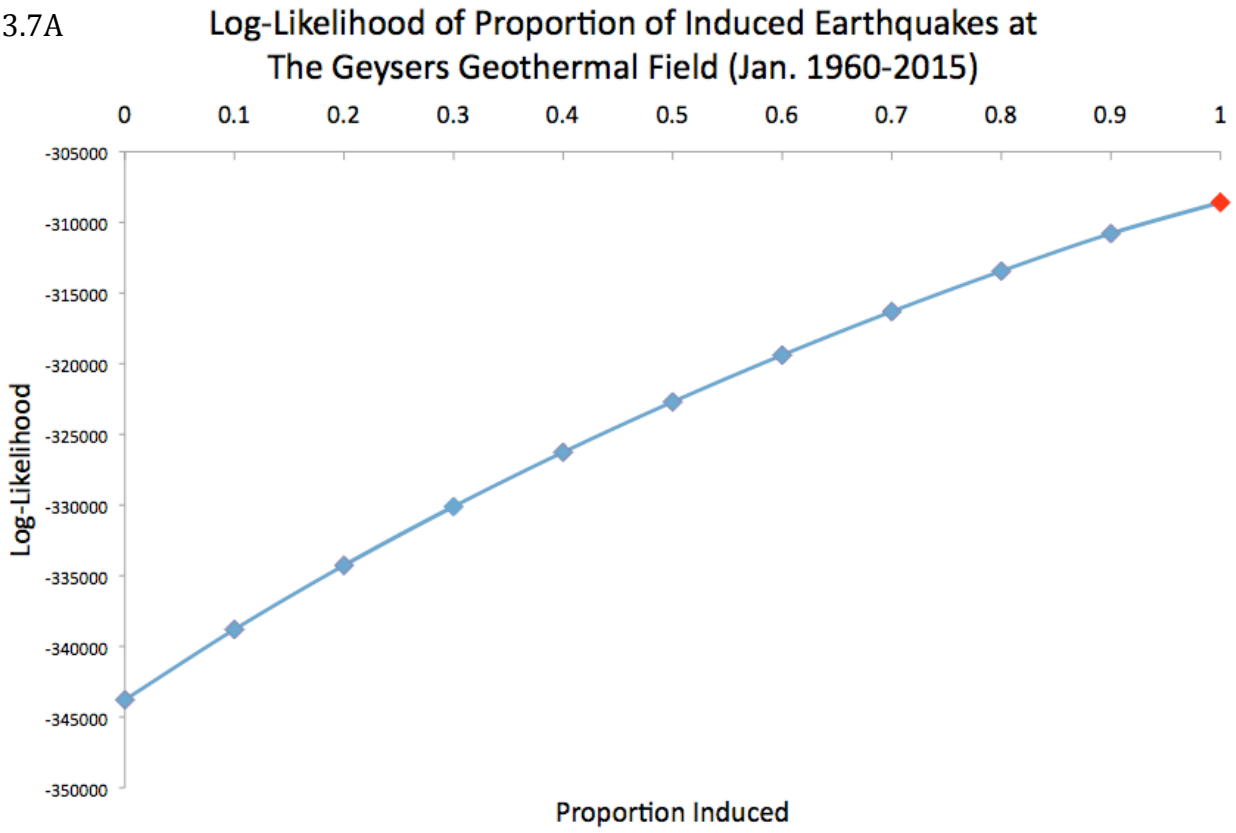
Log-Likelihood of Proportion of Induced Earthquakes at The Geysers Geothermal Field (Jan. 1960-2015)
0
0.1
0.2
0.3
0.4
0.5
0.6
0.7
0.8
0.9
1
-305000
-310000
-315000
-320000
-325000
-330000
-335000
-340000
-345000
-350000
Log-Likelihood
Proportion Induced

3.7B

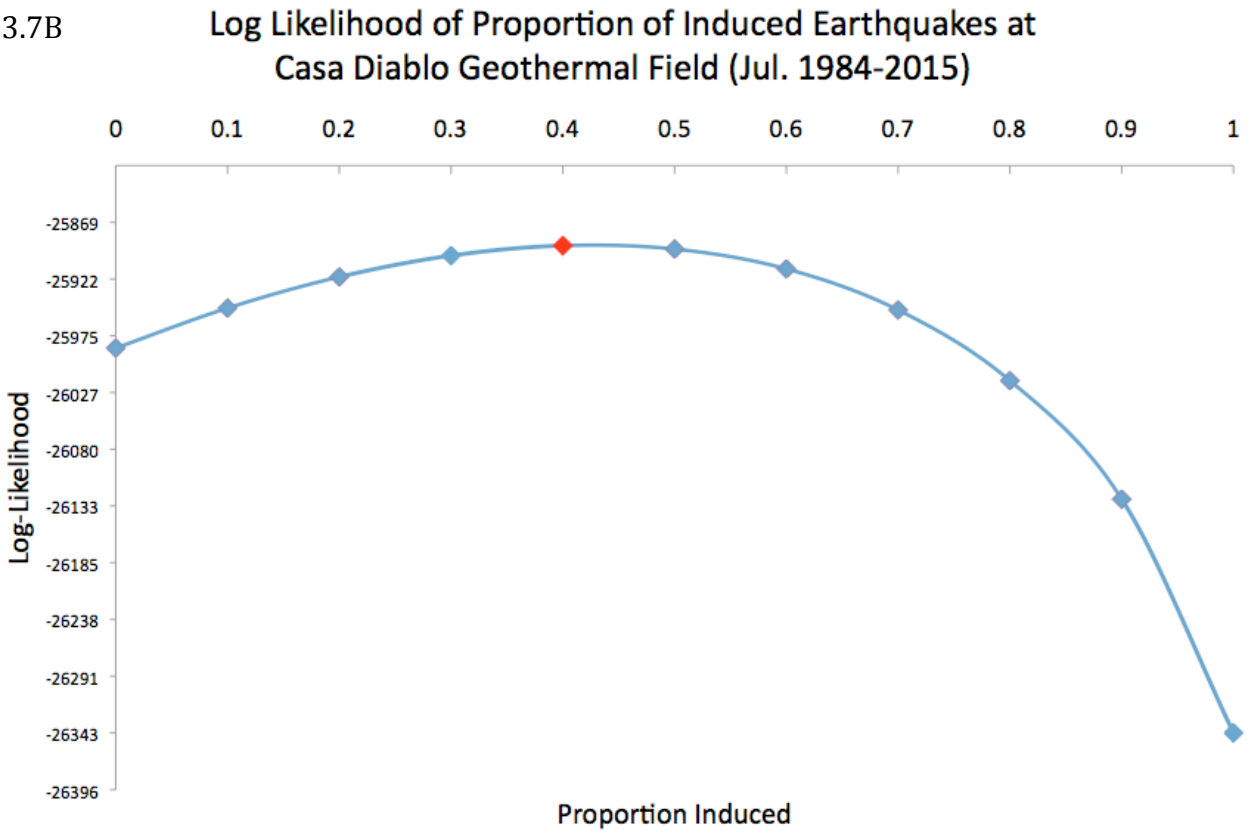

Figure 3.7 (A and B)

For A) The Geysers, the maximum likelihood combination of the two hypothesis that yield the observed earthquake catalog is best expressed by 1.0*injection and 0.0*uniform. For B) Casa Diablo, the best fit of the model is with 0.4*injection and 0.6*uniform. The optimal value for the "injection" hypothesis is indicated with a red diamond.

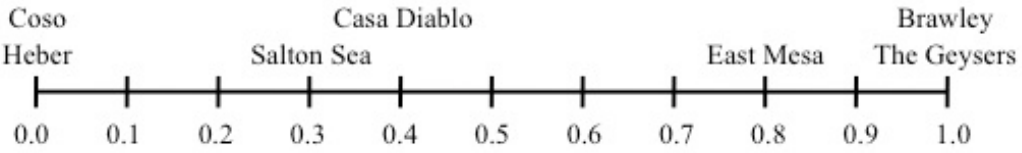

Figure 3.8

Results of the linear combination of the "injection" and "uniform" hypotheses. 0.0 indicates that earthquakes best fit the uniform hypothesis, while 1.0 indicates a strong correlation with the injection hypothesis. Numbers in between represent a mixed proportion of the two hypotheses. For example, the best fit to the linear model for Casa Diablo is 60% "uniform" and 40% "induced."

Field	Spatiotemporal correlation?	Criteria Checklist	Relative contribution	Total (/9)
Brawley	3	2	3	8
Casa Diablo	2	2	2	6
Coso	2	1	0	3
East Mesa	0	1	2	3
The Geysers	3	2	3	8
Heber	0	2	0	2
Salton Sea	3	2	2	7
Susanville	1	2	n/a	3
Wendel	0	2	n/a	2

Table 3.6

Analysis from Sections 3.4 and 3.5 is presented visually. Evidence is ranked on a scale from 0-3, with 3 being strong evidence, 2 is moderate evidence, 1 is weak evidence, and 0 is no evidence. Results are totaled in the last column. A score of 7 or higher denotes strong support for induced seismicity; 3-6 represents strong to moderate evidence; and 0-2 shows little to no indication of induced earthquakes.

3.8 References cited

Ake, J., K. Mahrer, D. O'Connell, and L. Block, 2005, Deep-injection and closely monitored induced seismicity at Paradox Valley, Bulletin of the Seismological Society of America, vol. 95, no. 2, p. 664-683.

Allen, D.R. and M.N. Mayuga, 1969, The mechanics of compaction and rebound, Wilmington oil field, Long Beach, California, U.S.A., in Land subsidence: International Association of the Science of Hydrology, UNESCO Publication 89, v. 2, p. 410-423.

Allis, R.G., 1982, Mechanism of induced seismicity at the Geysers Geothermal Reservoir, California. Geophys. Res. Lett. Vol. 9, p. 629–632.

Bardwell, G.E., 1966, Some statistical features of the relationship between Rocky Mountain Arsenal waste disposal and frequency of earth- quakes, Mountain Geologist, vol. 3, p. 37-42.

BDSN, 2014, Berkeley Digital Seismic Network. UC Berkeley Seismological Laboratory. Dataset. doi:10.7932/BDSN.

Black, N.M., 2008, Fault Length, Multi-Fault Rupture, and Earthquakes in California, Ph.D. Dissertation, 172 pp., University of California Los Angeles, Los Angeles.

Brodsky, E. and L. Lajoie, 2013, Anthropogenic Seismicity Rates and Operational Parameters at the Salton Sea Geothermal Field. Science, vol. 341, p. 543-546.

California Energy Commission, 2010, Geothermal Energy in California, CA.gov [Online], http://www.energy.ca.gov/geothermal/

City of Santa Rosa, Geysers Project: Stats and Facts, http://ci.santa-rosa.ca.us/departments/utilities/irwp/geysers/Pages/FactStat.aspx.

Cypser, D.A. and S.D. Davis, Liability for induced earthquakes. J. Envtl. L. & Litig., vol. 9, p. 551-589.

Davatzes, N.C. and S.H. Hickman, 2006, Stress and faulting in the Coso Geothermal Field: Update and recent results from the East Flank and Coso Wash: Proceedings, 31st Workshop on Geothermal Reservoir Engineering, Stanford University, Stanford California, January 30-February 1, 2006, SGP-TR-179, v. 31, 12 p.

Davis, S. and C. Frohlich, 1993, Did (or will) fluid injection cause earthquakes? – Criteria for a rational assessment. Seismological Research Letters, vol. 64, no. 3-4, July-December, 1993, p. 207-224.

Davis, S., P. Nyffenegger, and C. Frohlich, 1995, The 9 April 1993 Earthquake in South-Central Texas: Was It Induced by Fluid Withdrawal? Bulletin of the Seismological Society of America, vol. 85, no. 6, p. 1888-1895.

de Pater, C. J., and S. Baisch, 2011, Geomechanical study of Bowland Shale seismicity: Synthesis Report, Department of Energy and Climate Change, report 71.

DiPippo, R., 2012, *Geothermal Power Plants: Principles, Applications, Case Studies, and Environmental Impact*, *3rd ed*. Oxford: Butterworth-Heinemann.

(DOGGR) California Department of Oil, Gas, and Geothermal Resources, 2011, GeoSteam - Query Geothermal Well Records, Production and Injection Data. http://geosteam.conservation.ca.gov/WellSearch/GeoWellSearch.aspx, last accessed January 28, 2016.

(DOGGR) California Department of Oil, Gas, and Geothermal Resources, 2015, Oil, Gas & Geothermal – Maps, Production & Injection, www.conservation.ca.gov/dog/geothermal/manual/Pages/production.aspx, last accessed March 4, 2016.

Eberhart-Phillips, D. and D.H. Oppenheimer, 1984, Induced seismicity in The Geysers Geothermal Area, California, *Journal of Geophysical Research, vol.* 89, p. 1191–1207.

Elders W.A. and L.H. Cohen, 1983, The Salton Sea Geothermal Field, California, as a Near-Field Natural Analog of a Radioactive Waste Repository in Salt, Technical Report prepared for the Office of Nuclear Waste Isolation, BMI/ONWI-513, 163 p.

Evans, D. M., 1966, The Denver earthquakes and the Rocky Mountain Arsenal disposal well, The Mountain Geologist 3, 23-36.

Ellsworth, W.L., 2013, Injection-induced earthquakes, Science, vol. 341, is. 6142, p. 1225942 1-7.

Fialko, Y. and M. Simons, 2000, Deformation and seismicity in the Coso geothermal area, Inyo County, California: Observations and modeling using satellite radar interferometry, Journal of Geophysical Research, vol. 105, no. B9, p. 21781–21793.

Fu, B.H., Y. Awata, J.G. Du, Y. Ninomiya, and W.G. He, 2005, Complex geometry and segmentation of the surface rupture associated with the 14 November 2001 Great Kunlun earthquake, northern Tibet, China, Tectonophysics, vol. 407, p. 43-63.

Goldsmith, M., 1976, Geothermal Development and the Salton Sea, Environmental Quality Laboratory Memorandum No. 17, California Institute of Technology, http://authors.library.caltech.edu/25766/1/EQLmemo17.pdf.

Hartline, C. 2012, Calpine Corporation presentation to the Seismic Monitoring Advisory Committee Meeting (SMAC). http://www.geysers.com/media/Calpine%20May%2013,%202013%20SMAC.pdf, Geothermal Visitors Center Middletown, California, May 13.

Hauksson, E., W. Yang, and P.M. Shearer, 2012, Waveform Relocated Earthquake Catalog for Southern California (1981 to 2011). Bulletin of the Seismological Society of America, vol. 102, no. 5, p. 2239-2244.

Hauksson, E., J. Stock, R. Bilham, M. Boese, X. Chen, E.J. Fielding, J. Galetzka, K.W. Hudnut, K. Hutton, L.M. Jones, H. Kanamori, P.M. Shearer, J. Steidl, J. Treiman, S. Wei, and W. Yang, 2013, Report on the August 2012 Brawley Earthquake Swarm in Imperial Valley, Southern California, Seismological Research Letters, vol. 84, no. 2, p. 177-189.

Healy, J.H., W.W. Rubey, and D.T. Griggs, 1968, The Denver earthquakes. Science, vol. 161, no. 3848, p. 1301-1310.

Howard, J.H. and D. Towse, 1977, History of exploitation at Salton Sea Geothermal Field, California, Am. Assoc. Pet. Geol. Bull., vol. 61, no. 5.

Hubbert, M.K., and W.W. Rubey, 1969, Role of Fluid Pressure in Mechanics of Overthrust Faulting, Bulletin of the Seismological Society of America, vol. 70, p. 115–166.

Hutton, K., J. Woessner, and E. Hauksson, 2010, Earthquake Monitoring in Southern California for Seventy-Seven Years (1932–2008). Bulletin of the Seismological Society of America, vol. 100, no. 2, p. 423–446.

Johnson, C.E., and L.K. Hutton, 1982, Aftershocks and preearthquake seismicity, in The Imperial Valley, California, earthquake of October 15, 1979, C. E. Johnson, C. Rojahn, and R. V. Sharp (Editors), U.S. Geol. Surv. Profess. Pap. 1254, p. 59–76.

Kaven, J.O., S.H. Hickman, and N.C. Davatzes, 2011, Micro-seismicity, fault structure, and hydraulic compartmentalization within the Coso geothermal field, California, Proceedings of the Thirty-Sixth Workshop on Geothermal Reservoir Engineering, Stanford University, Jan 31-Feb 21.

Keranen, K.M., H.M. Savage, G.A. Abers, and E.S. Cochran, 2013, Potentially induced earthquakes in Oklahoma, USA: Links between wastewater injection and the 2011 M_w 5.7 earthquake sequence, Geology, doi: 10.1130/G34045.1.

Keranen, K.M, M. Weingarten, G.A. Abers, B.A. Bekins, and S. Ge, 2014, Sharp increase in central Oklahoma seismicity since 2008 induced by massive wastewater injection, Science, vol. 345, issue 6195, p. 448-451.

Kisslinger, C., 1976, A review of theories of mechanisms of induced seismicity, Engineering Geology, vol. 10, no. 2, p. 85–98.

Koenig, J., 1991, History of development at The Geysers geothermal field, California, Geothermal Resources Council, Monograph on The Geysers Geothermal Field, Special Report no. 17.

Kwiatek, G., P. Martínez-Garzón, G. Dresen, M. Bohnhoff, H. Sone, and C. Hartline, 2015, Effects of long-term fluid injection on induced seismicity parameters and maximum magnitude in northwestern part of The Geysers geothermal field, J. Geophys. Res. Solid Earth, vol. 120, doi:10.1002/2015JB012362.

Lajoie, L.J., 2012, Seismic response to fluid injection and production in two Salton Trough geothermal fields, southern California. UC Santa Cruz: Earth Science. Masters Thesis. Retrieved from: http://escholarship.org/uc/item/7gr8x35f.

Llenos, A.L. and A.J. Michael, 2013, Modeling Earthquake Rate Changes in Oklahoma and Arkansas: Possible Signatures of Induced Seismicity. Bulletin of the Seismological Society of America, vol. 103, no. 5, p. 2850–2861.

Lund, J.H., 2004, 100 Years of Geothermal Power Production, GHC Bulletin, p. 11-19, http://www.geothermalcommunities.eu/assets/elearning/7.11.art2.pdf.

Majer, E.L., R. Baria, M. Stark, S. Oates, J. Bommer, B. Smith, and H. Asanuma, 2007, Induced seismicity associated with Enhanced Geothermal Systems, Geothermics, vol. 36, p. 185–222.

Martínez-Garzón, P., G. Kwiatek, H. Sone, M. Bohnhoff, G. Dresen, and C. Hartline, 2014, Spatiotemporal changes, faulting regimes, and source parameters of induced seismicity: A case study from The Geysers geothermal field. Journal of Geophysical Research, vol. 119, no. 11, p. 8378-8396, doi: 10.1002/2014JB011385.

McGarr, A., D. Simpson, and L. Seeber, 2002, Case histories of induced and triggered seismicity, *International Handbook of Earthquake and Engineering Seismology*, Part A, W.H.K. Lee et al., eds., Academic Press, 647-661.

National Research Council, 2012, Induced seismicity potential in energy technologies, http://www.nap.edu/catalog/13355/induced-seismicity-potential-in-energy-technologies.

Northern California Seismic Network (NCSN) earthquake catalog, Northern California Earthquake Data Center, http://ncedc.org/ncedc/catalog-search.html; last accessed January 12, 2015.

Ogata, Y., 1988, Statistical Models for Earthquake Occurrences and Residual Analysis for Point Processes, Journal of the American Statistical Association, vol. 83, no. 401, p. 9-27.

Peppin, W.A. and C.G. Bufe, 1980, Induced versus natural earthquakes: search for a seismic discriminant. Bulletin of the Seismological Society of America, vol. 70, no. 1, p. 269-281.

Rubinstein, J.L. and A. B. Mahani, 2015, Myths and Facts on Wastewater Injection, Hydraulic Fracturing, Enhanced Oil Recovery, and Induced Seismicity, Seismological Research Letters, vol. 86, no. 4, 8pp.

Rutqvist, J., P. F. Dobson, J. Garcia, C. Hartline, P. Jeanne, C. M. Oldenburg, D. W. Vasco, and M. Walters, 2013, The Northwest Geysers EGS Demonstration Project, California: Pre-stimulation modeling and interpretation of the stimulation, Mathematical Geosciences, vol. 47, p. 3–29, doi:10.1007/s11004-013-9493-y. (Published online 2013. Re-published in 2015 special issue.)

SCEDC, 2013: Southern California Earthquake Center. Caltech. Dataset. http://service.scedc.caltech.edu/eq-catalogs/date_mag_loc.php, doi:10.7909/C3WD3xH1.

U.S. Geological Survey, 2015, *Cactus Peak quadrangle, California* [map]. 1:24,000. 7.5 Minute Series.

Waldhauser, F. and W.L. Ellsworth, 2000, A double-difference earthquake location algorithm: Method and application to the northern Hayward fault, California, Bulletin of the Seismological Society of America, vol. 90, no. 6, p. 1353–1368.

Waldhauser, F. and D.P. Schaff, 2008, Large-scale relocation of two decades of Northern California seismicity using cross-correlation and double-difference methods, J. Geophys. Res., vol. 113, p. B08311.

Wang, Q., D.D. Jackson, and J. Zhuang, 2010, Are Spontaneous earthquakes stationary in California?, Journal of Geophysical Research, vol. 115, B08310, doi:10.1029/2009JB007031.

Wesnousky, S. G., 2006, Predicting the endpoints of earthquake ruptures, Nature 444, no. 16, p. 358–360.

Zoback, M., 2010, Reservoir Mechanics, Cambridge University Press, New York, ISBN-978-0-521-77069-9.

4 Science-based decision making in a high-risk energy production environment

4.1 Introduction and motivation

Scientific risk management decisions, well-communicated to stakeholders, support effective mitigation. These decisions can take various forms, including curating energy production operation strategies, determining appropriate mitigation practices for potentially induced earthquakes, or engaging with the community. Mitigation approaches are varied, and may involve trying to limit magnitude or shaking produced by an earthquake, effectively communicating risk of potential earthquakes with local communities, tactically pumping far from populated areas, and legislating against risky practices.

When starting a new project that may induce earthquakes, performing a cost-benefit analysis (CBA) would be valuable, especially one that considers the worst-case scenario (Mignan et al. 2015). The cost, although hard to generalize, is important to illustrate. How can science contribute to an earthquake CBA? Timely and accurate scientific information can help determine costs and benefits of alternative decisions. I do not perform a CBA here, but I equip the reader with a scientific toolkit needed to reduce uncertainty and make informed decisions. When discussing costs, I am referring to the term in abstract; monetary investment or losses are not the only way to define a cost. Important "costs" can vary by community.

First, the hazard must be characterized—what is the probability of an event occurring? Helpful information includes a probability estimate of the frequency of earthquakes of different sizes, and the costs of different magnitude earthquakes. The probability of an adverse induced event may be influenced by various factors including fluid volume, geology of the perturbed

formation(s), proximity to faults, and operational standards. Population exposure dictates whether or not an earthquake is considered unacceptable, so it is wise to consider factors relating to human response. How fragile are local structures? How sensitive and/or risk averse to earthquakes is the local population? Are there large nearby faults? Is there a past history of damaging earthquakes, which have been ingrained in the shared community memory? What is excessive risk (to both operators and the community)? Is the community invested in the project (e.g. job production; economic boon; only source of power)? What are the costs of stopping (e.g. drilling costs), and are they outweighed by the benefit of energy production? Has the potential of a larger magnitude earthquake post-shut in been considered (e.g. Barth et al. 2011)? All of these are important to evaluate before beginning an energy production method that could produce earthquakes.

It is important to examine consequence of likely and worst-case earthquakes. As discussed in Section 4.4.2, there are consequences that can occur when the realm of possible outcomes from a disaster are not considered. Is there an impact on safety or public health? Could any critical facilities be disturbed (anything from nuclear facilities and lifelines to schools or hospitals)? What is the potential environmental impact? What will the effect be on the public? What are the financial impacts of various consequences? It would be useful to develop a risk matrix for potential induced seismicity (Figure 4.1), which determines the risk, given inputs of probability (the hazard) and the consequence (Nygaard et al. 2013).

Once risk has been evaluated, a risk mitigation strategy can be developed, tailored to the needs identified by the hazard and risk analysis. As described above, science is essential for informed decision-making. Herein, I review current and past mitigation strategies as well as existing protocol. Often, mitigation strategies try to manage risk (hazard times consequences) against an

agreed upon “acceptable” value (e.g. McGarr et al. 2015). I discuss “acceptable” and “unacceptable” earthquakes in a probabilistic framework for The Geysers geothermal field and share the responses of nearby communities to smaller and larger magnitude earthquakes. I use the USGS’s “Did You Feel It?” data to gauge the rate and acceptability of earthquakes to the local population. Throughout this chapter, I discuss mitigation strategies, including legislation designed to reduce induced earthquake hazards, and present a framework for science-based decision-making.

4.2 Summary of induced seismicity mitigation practices

A spectrum of actions can be taken if anthropogenic actions are suspected of causing earthquakes. The only way to ensure a long-term reduction in future earthquakes is to stop the perturbing action (termination). An oft-adopted approach is to alter operations (one form of mitigation). If production continues unabated, operators can use different methods to deal with any consequences that may result from pumping (proactive and reactive remediation). At the other end of the spectrum, operators can take a chance that results will be positive and no actions will have been necessary (purposeful inaction).

Mitigation, or action(s) taken to reduce the severity or impact of something, can take multiple forms. In the case of induced earthquakes, direct mitigation involves actively trying to change the earthquake hazard. This can be achieved through alteration of pumping procedures, or legislation to force behavioral changes in operation. Indirect mitigation involves changing the outcome of the hazard. For example, community outreach has the potential to increase tolerance to shaking. The hazard itself doesn’t change, but the reaction to it does.

Novel approaches are possible to alleviate potential harm from induced quakes because, unlike standard seismic risk mitigation, the earthquake hazard can be changed and risk can, perhaps, be better managed (e.g. Mignan et al. 2015, McGarr et al. 2015, and Zoback 2012). Newly developed practices are beginning to include more than one tactic, such as increased monitoring, a system to limit or stop operations if pre-determined thresholds are exceeded, and consistent community engagement (e.g. DECC 2015). This is a positive development, as relying on one method can be a risky decision, until a high-degree of confidence in controlling the hazard has been established (Bommer et al. 2015). A series of large reports have been released in recent years, all of which discuss emergent seismic behavior at energy production sites. Each chronicles aspects of induced seismicity mechanisms, case examples, and suggested best practices, through the lens of the Environmental Protection Agency (EPA), National Research Council (NRC), and Department of Energy (DOE) (EPA 2014, NRC 2012, and Majer et al. 2012). Below, I highlight a few mitigation techniques currently in use in the U.S. and around the world.

4.2.1 Traffic Light Protocol

In the last decade, the Traffic Light Protocol (TLP) has become a widely adapted system of monitoring seismicity with preset thresholds denoting acceptable levels of measurable physical conditions (Bommer et al. 2006). If these metrics are exceeded, pre-defined actions are taken to reduce earthquake activity. There are multiple cases where the maximum threshold was breached and pumping activities were halted, such as earthquakes in Youngstown, Ohio and Basel, Switzerland (Kim 2013; Deichmann and Giardini 2009). Traffic light protocols have been designed with both magnitude-based limits (e.g. Green et al. 2012) and thresholds based on ground shaking (e.g. Bommer et al. 2006). Among other applications, TLP implementation has

been suggested for all enhanced geothermal projects (EGS seek to increase permeability of a shallow target formation, in order to more easily extract energy from an underground heat source), as well as for wastewater disposal (Majer et al. 2012; Zoback 2012).

Typically, levels are set as follows: green means to proceed with normal operations; yellow indicates a need to exercise caution and possibly reduce injection and/or production rates; red usually means to stop all operations that could further perturb pore pressures. In order for a TLP to succeed, reliable, well-defined, and quickly measurable criteria for when a threshold is breached are essential. In order to de-escalate back to lower level, similar metrics are needed. All of this requires a seismic monitoring network; the more stations, the better the coverage is, and the lower the detectable magnitude.

TLP performance has been mixed. This is due to many occurrences where the largest earthquakes occurred after wells were shut-in (e.g. Häring et al. 2008; Majer et al. 2007). It is unrealistic to know if an earthquake would have happened if pumping continued, but was instead forestalled by terminating operations. TLP are evolving; Mignan and others (2015) have proposed an advanced risk-based traffic light system, rather than endeavoring to control hazard.

When implementing a TLP, individual projects will need to adjust criteria to fit the local needs. Is perceptible shaking acceptable or not? Are there any nearby population or structures that can be damaged in an earthquake? Rather than designing a TLP around magnitude (which does not vary by location), ground motion measures, such as peak ground velocity (PGV) or peak ground acceleration, describe site-specific shaking. Before beginning a project that may induce seismicity, it is essential to set up the proper monitoring network, and to clearly outline what shaking will result in responsive actions. Below, I present two case examples which detail TLP implementation.

4.2.1.1 Berlín, El Salvador

The development of a hot fractured rock geothermal project in Berlín, El Salvador led to the first explicitly and formally documented implementation of a TLP (Bommer et al. 2006). Prior work had alluded to similar management of earthquakes, but had not formally defined the technique (e.g. Healy et al. 1968). A fragile building stock (with many structures constructed out of masonry or adobe) in an already seismically active area, led Bommer and co-authors to develop a monitoring plan with the intent to limit ground shaking from the Berlín geothermal project. Traffic light levels were enacted to limit damage and felt events, with thresholds determined using median PGV and expert opinions (see Figure 4.2). Ultimately, seismicity rates were much lower than expected, and throughout the project, the green-light level was never exceeded (Bommer et al. 2006).

4.2.1.2 Bowland Shale, UK

In 2011, de Pater and Baisch suggested a TLP for future injection in the Bowland Shale, an impermeable gas play in the UK; this was prompted by larger than expected M2.3 and 1.5 earthquakes during stimulation. The authors decided a conservative approach was necessary, due to a lack of seismic building codes for residential dwellings and conservative UK blasting standards. According to German ground motion standards, the minimum magnitude where damage could occur is M2.6 (de Pater and Baisch 2011). The authors suggested that it was reasonable to assume a maximum post-injection magnitude increase of $M \leq 0.9$, and therefore established M1.7 as the red light threshold. The authors' suggested traffic light protocol is illustrated in Figure 4.3.

In December 2015, the UK government developed a primer on regulations and best practices for future onshore shale gas and oil exploitation (DECC 2015). As of early March 2016, despite exploratory efforts, there were no commercial shale-gas wells in Europe (Inman 2016). The DECC report included adaptation of a new TLP with red light levels set at *M*0.5 (Figure 4.4). The report also indicated the rationale for such a low maximum allowable earthquake: "Traffic light monitoring systems are affected by natural delays within geological systems such as the slow movement of fluids through faults, so it is important that the trigger levels are low enough to detect the smaller induced seismic events that may be an indication of or precursor to a larger induced seismic event later" (DECC 2015).

4.2.2 Community outreach

It has been shown that lack of communication about short-term projects that induce shaking yields unfavorable reactions (e.g. ISO 1989). Public outreach and operational transparency may decrease this adverse response (e.g. Bommer et al. 2006). The proximity of population centers to potentially induced earthquakes will impact public feedback (Bommer et al. 2015). The same is true if local inhabitants are already accustomed to periodic natural seismicity.

One example of effective community outreach is the Seismic Monitoring Advisory Committee (SMAC) at The Geysers. SMAC is a collaborative effort between energy production operators, USGS, Lawrence Berkeley National Laboratory, and other institutions to keep the public informed about seismic activity at The Geysers. Public meetings are held twice yearly, and presentations are available online (http://www.geysers.com/smac.aspx) for further transparency. Calpine, the main geothermal operator at The Geysers, holds community meetings in both nearby towns more than once a year. They also manage a phone line where concerned citizens

can call in damage complaints or concerns about felt earthquakes (e.g. Hartline 2014). SMAC serves as a successful public-private venture to continue operations while minimizing concern and keeping the public informed.

4.2.3 Tactical well locations

Increasing the distance between pumping operations and nearby communities is a simple and effective method to reduce seismic risk; induced seismicity is often focused near perturbing source (e.g. Bommer et al. 2015, McGarr et al. 2015). Calpine deliberately located EGS test wells (Prati-9, 31, and 32) far from the two towns closest to The Geysers, Anderson Springs and Cobb (Figure 4.5; Hartline 2013). When injection began at Prati 32, a microseismicity cloud formed almost immediately (Figure 4.6; Hartline 2013). Thus, maximizing the separation between the EGS test wells and nearby towns minimized the impact of these higher-injection-rate wells.

4.2.4 Reactionary legislation and procedural changes

It is important to develop a hazard mitigation plan prior to the onset of potential earthquake inducing activities. The increased efficacy of hazard reduction activities taken during initial stages of injection projects has long been recognized: “The possibility of controlling seismic hazard diminishes as the pore pressure effects migrate away from the injection interval and become less amenable to control from the wellhead” (Healy et al. 1968). Mitigation legislation (as discussed in section 4.3) has often been the result of an unacceptable or problematic

earthquake, which resulted in public outcry, negative media attention, and/or exceedence of a predetermined threshold.

Despite an unnatural earthquake rate increase in Oklahoma since 2009 (e.g. Ellsworth 2013), the Director of the Oklahoma Oil and Gas Conservation Division (OGCD) Tim Baker said in March 2016, that recent legislation is a "proactive move to get ahead of the earthquake activity" (OCC 2016a). The Oklahoma Geological Survey had previously observed magnitude 3 or larger earthquakes at the rate of 1.5 per year within the state. The rate jumped to 2 per week in 2013 and 2.5 per day in 2015 (OGS 2015). In the face of scientific consensus about the abnormal earthquake rate increase in the central and eastern U.S., many states have enacted legislation or developed advisories and recommendations aimed at controlling new and objectionable seismicity (e.g. NRC 2012, Weingarten et al. 2015, McGarr et al. 2015).

4.3 Recent legislation and actions related to induced seismicity

The Safe Drinking Water Act (SDWA) of 1974 is the main federal directive regulating underground injection activities. It does not directly tackle seismicity for most types of underground injection; rather, the SDWA permits individual states to enforce the Underground Injection Control (UIC) program with the aim of preventing contamination or endangerment of drinking water sources (The Safe Drinking Water Act of 1974, P.L. 93-523). UIC regulations require fault information surrounding proposed wells, however this is aimed at isolating the injected fluid from the drinking water supply and not the possibility of inducing earthquakes (NRC 2012). States can appeal to the EPA to gain "primacy," or primary enforcement responsibility, to internally execute and govern UIC statutes (http://water.epa.gov/type/groundwater/uic/Primacy.cfm). If granted primacy, states are given sovereignty to regulate

injection activities, inspect wells, approve permits, and can distribute these roles to one or multiple agencies (NRC 2012).

Many states, agencies, and organizations have proposed procedural guidelines and/or best practices to mitigate the hazard and risk associated with earthquakes that may be related to energy production. New regulatory developments include expanded permitting (which often requires additional geologic information), seismic monitoring, more stringent operational constraints, and even some moratoria have been enacted for areas of known seismic risk. Samplings of these protocols, particularly in the Central and Eastern U.S., include, but are not limited to Arkansas, California, Colorado, Illinois, Kansas, Ohio, Oklahoma, and Texas, all of which have been granted primacy (see Figure 4.7). Finley (2015) has proposed that federal regulations be introduced to provide consistent governance for underground pumping related to energy production. She argues that adaptation of such regulations would allow for continued expansion of the U.S. energy production industry without future increased induced seismicity risk. As fault lines do not conform to state borderlines, it makes sense to treat regulation with a more national approach.

4.3.1 Arkansas

In 2009, wastewater (a byproduct of the hydraulic fracturing process) began to be injected into eight disposal wells in North-Central Arkansas. This has been followed by an acceleration from two earthquakes in 2008 (prior to injection) to 157 in 2011, with 98% of recent earthquakes occurring with 6 km of a disposal well (within the study area of Horton 2012). The Arkansas Oil and Gas Commission (AOGC), the state's oil and gas regulatory agency, began investigating earthquakes that initiated about 3.5 months after the start of wastewater injection. The state also

has a separate Oil and Gas Commission ("Commission"), whose members are appointed by the governor. The Commission enacted a 2010 moratorium on drilling of new wastewater disposal wells surrounding areas with newly heightened seismic activity (EPA 2014). Operators of seven existing wells were required to report pressures and injection rates hourly, for six months; all other wastewater disposal wells were required to submit volumes and pressures daily (AOGC Rule H).

In mid-August 2010, disposal began at a new well (drilled prior to the moratorium), providing an opportunity to instrument new injection in an already seismically active location. In late September of the same year, a swarm of earthquakes began which led to nearly 1,000 events $M \leq 4.7$ over the next 6 months, and lit up a previously unmapped fault (Horton 2012). Unmapped faults exist everywhere, and careful seismicity mapping will uncover many of them. An unmapped fault is not resistant to induced earthquakes.

In March 2011, the AOGC issued an emergency shutdown order for two disposal wells. The rate and magnitude of earthquakes in the Guy-Greenbrier earthquake swarm declined over the next three months (Horton 2012). In July 2011, the Commission declared a permanent moratorium area around the Guy-Greenbrier Fault, in which no new disposal wells may be drilled (EPA 2014). This led to four wells being permanently shut-in (some voluntarily, others by AOGC mandate); in the six months after, only six earthquakes occurred on the Guy-Greenbrier Fault (Horton 2012). In his 2012 paper, Horton notes that a "close spatial and temporal correlation supports the hypothesis that the recent increase in earthquake activity is caused by fluid injection at the waste disposal wells."

4.3.2 California

Governor Jerry Brown signed Senate Bill 4 (SB 4) into law in 2013, which gave the directive to establish a regulatory program for oil and gas well stimulation treatments (such as hydraulic fracturing or acid treatments) (Mills and Morrissey 2015). The resulting regulations went into effect on July 1, 2015; the main components are summarized here. DOGGR has been tasked with preparing an Environmental Impact Report (available at: http://www.conservation.ca.gov/dog/Pages/SB4_Final_EIR_TOC.aspx) and creating a website to enable more transparency regarding well stimulations (Mills and Morrissey). Operators are required to comply with public disclosure and neighbor notification mandates. Explicit instructions are given for what data must be collected prior to and during stimulation treatments, and there are new limits placed on what information may be concealed as a "trade secret" (SB 4 2013). The bill does not impose new regulations on geothermal monitoring or operations.

4.3.3 Colorado

Following the August 2011 M5.3 in the Raton basin, Colorado (Rubinstein et al. 2014), the Colorado Oil and Gas Conservation Commission (COGCC) developed procedures requiring the Colorado Geologic Survey (CGS) to review all permits requesting injection into any geologic unit that may cause earthquakes (NRC 2012). The new policy also requires that well operators adhere to injection volume, rate, and pressure limits (COGCC 2011). CGS and COGCC jointly review and evaluate seismicity at proposed well sites (NRC 2012). The COGCC released a statement in January 2011, which said, "if historical seismicity has been identified in the vicinity of a proposed Class II UIC well, COGCC requires an operator to define the seismicity potential and the proximity to faults through geologic and geophysical data prior to any permit approval"

(COGCC 2011). Although written prior to the COGCC guidelines, Cypser (1996) provides guidance on the potential for liability over induced seismicity in the state.

4.3.4 Illinois

In June 2013, new state regulations were passed in which the Illinois Department of Natural Resources gained greater regulatory oversight for injection activities (Hydraulic Fracturing Regulatory Act). The state has also adopted a traffic light system, "allowing for low levels of seismicity while including additional monitoring and mitigation requirements when seismic events are of sufficient intensity to result in a concern for public health and safety" (Vinson and Elkins 2013). When an increase is merited in Illinois' TLP level, it could result either in injection reductions or cessation of activities.

4.3.5 Kansas

Kansas Governor Sam Brownback established a State Task Force on Induced Seismicity in response to a 2013 seismicity increase, primarily observed in three counties (Folger and Tieman 2014). The task force report led to increased seismic monitoring around the state, in an effort to be able to record earthquakes greater than $M1.5$. If a $M \geq 2$ earthquake occurs, the state's new response plan will be initiated; injection histories at all disposal wells within 10 km of the earthquake will be scrutinized (Kansas Seismic Action Plan 2014).

From 1981-2010, Kansas experienced 31 earthquakes. In 2014, they had 127 (greater than magnitude 2), which elicited action from the Kansas Corporation Commission (KCC 2015). In a March 19, 2015 order, the KCC ordered saltwater disposal rate reductions in areas with increased

seismic activity, citing a contemporaneous increase in the number of earthquakes and injection wells. Rather than targeting specific wells, the Commission noted, "individual earthquakes cannot be linked to individual injection wells" (KCC 2015).

4.3.6 Ohio

After the Dec 31, 2011 M4.0 Youngstown earthquake, multiple wells were shut-in and new well permitting was suspended (Tomastik 2013). The earthquake sequence caused the state to examine its permitting process, and in March 2012, the Ohio Division of Natural Resources (ODNR) developed a series of regulatory changes to their deep injection well program. Requirements included avoiding locating wells near known faults, reducing the depth of wells drilled into basement rock, continuous pressure monitoring, seismic monitoring planning, and installation of automated shut-off valves for if fluid pressures exceed a maximum set by ODNR (ODNR 2012). Permitting was resumed in November 2012 (Tomastik 2013). In 2012, Governor Kasich issued an Executive Order (2012-09K), requiring seismic monitoring plans, and forbidding drilling into basement (Ohio Oil and Gas Laws). The Division of Oil and Gas Resources Management is required to monitor seismicity before injection begins, for up to six months. Once injection commences, if there has been no evidence of concerning seismic events, seismic stations are relocated to a new injection site (Tomastik 2013).

4.3.7 Oklahoma

Oklahoma has seen a surge in earthquake occurrence since 2008; between 2008 and 2013, the state experienced 45% of all earthquakes $M \geq 3$ in the central and eastern U.S. (Keranen et al.

2014). A magnitude 5.7 earthquake near Prague, OK was likely caused by wastewater injection (Keranen et al. 2013). The state's change in earthquake rate is statistically significant, signaling that the drastic rate increase has not occurred naturally (Llenos and Michael 2013).

After seismicity rates increased (again) in 2013, the Oklahoma Corporation Commission (OCC) initiated a traffic light permitting system for Class II disposal wells (Folger and Tiemann 2014). This includes issuing temporary "yellow light" permits, which require more frequent disclosure of operational parameters and well integrity tests, and mandates a seismicity review. Using the National Research Council (2012) recommendations as a foundation, permitting and operational guidelines are constantly being updated as new information becomes available (Folger and Tiemann 2014, Zoback 2012, OCC 2016b).

Since April 2015, the state has taken 16 "actions related to seismicity," including publishing newly developed plans in response to new earthquake activity, creating maps showing areas of interest, and issuing new directives (OCC Website). In March 2015, the OCC released new mandates for well operators injecting into the Arbuckle formation (within specific "Areas of Interest", or AOIs), demanding that wells not be in contact or communication with basement rock (see Figure 4.8). If wells were shown to violate this, operators were instructed to plug wells back so they met the requirements (OCC 2015; the directive applied to 347 of 900 Arbuckle disposal wells). Most recently, a March 7, 2016 media advisory was issued; this press release announced further injection reductions into the Arbuckle Formation, as well as an expansion of the "yellow light" AOIs (OCC 2016a). In the same press release, OGCD Director Tim Baker announced a plan to reduce central Oklahoma wastewater disposal volumes by 40% from the 2014 total, citing that "the research and data has grown to provide the basis needed to both expand into a regional approach for volume reduction and increase the size of the AOI."

The state is also home to one of very few cases of induced seismicity litigation. During the Prague earthquake, a woman was injured from a falling chimney during the earthquake; she sued 26 companies, but her case was dismissed by the district court. The Oklahoma Supreme Court reversed the decision, since the suit only sought to recover damages (Finley 2015). According to Finley (2015), this case laid the foundation for similar legal action to be taken regarding induced seismicity impacts.

4.3.8 Texas

In November 2014, the Texas Railroad Commission (RRC) amended state's oil and gas protocols, issuing new guidelines for wastewater disposal permits, monitoring, and reporting. Requirements included that disposal well permit applicants must provide historical earthquake record within 100 square miles of proposed well site; well permits may be revoked or modified if injection is likely related to or found to have caused induced seismicity; and RRC staff may more frequently demand injected volumes and pressures (Texas Administrative Code 2014). These new regulations created a framework likely to reduce the number of induced earthquakes in Texas (Finley 2015).

4.4 Cautionary accounts of energy production challenges

When making decisions, one generally only knows the outcome of their choice, given the specific instances of the situation. It is beneficial to observe other outcomes, to see a range of possibilities, with different site-specific parameters. The examples below illustrate problems that may arise at different types of energy production sites. These can be used to guide future

planning, so that problematic and sometimes preventable challenges, like those described below, may be avoided.

4.4.1 Swiss geothermal projects

The Deep Heat Mining Project was a short-lived EGS venture in Basel, Switzerland (Häring et al. 2008). Stimulations were carried out from December 2-8, 2006, and resulted in more than 10,500 seismic events recorded during the injection phase (Deichmann and Giardini 2009). The morning of December 8th, a M_L2.6 earthquake occurred, which exceeded a previously determined allowable magnitude threshold (Häring et al. 2008). Later that day a M_L3.4 earthquake led to the well being opened in order to allow water to flow out and to reduce pressures (Deichmann and Giardini 2009). The EGS project was put on hold, after a negative public response to the earthquakes and resulting damage (Diechmann and Giardini 2009). In 2009, an independent study led to the project's abandonment, citing unexpected and societally unacceptable seismicity increases during and after stimulation at the EGS project, causing loss of investment, and led to litigation over damage compensation (Giardini 2009, Baisch et al. 2009, Ellsworth 2013). In 1356, the town was home to one of the strongest historic earthquakes in that part of Europe, which may have led to such a strong community response (Deichmann and Giardini 2009).

A geothermal project was developed in St. Gallen, Switzerland, with widespread community support (Moeck et al. 2015). Production began in 2013, and led to a M_L3.5; after a short hiatus, testing revealed a previously unknown methane gas reservoir below the well (Kraft et al. 2013, Moeck et al. 2015). Although a traffic light system was in use, the unexpected challenge posed by the gas reservoir forced operators to continue pressurizing the well instead of stopping operations, as laid out by the TLP (Kraft et al. 2013). The project was shut down due to low flow

rate of brine, unexpected high volumes natural gas, high costs, and future risk of induced earthquakes (Moeck et al. 2015). According to Moeck and others (2015), there is a chance of re-gearing the project for gas production, although this still hasn't happened years later. Despite community support, operational surprises and complications led to the shut down of St. Gallen's geothermal project (Stauffacher et al 2015).

4.4.2 Fukushima Daiichi nuclear power plant, Japan

The massive Tohoku earthquake and tsunami in March, 2011 caused equipment failures and inability to cool the reactor at the Fukushima Daiichi Nuclear Power Plant in Japan. This resulted in three nuclear meltdowns and release of radioactive material. If the nuclear plant had been located at higher elevation, the seawall had been constructed with conservative tsunami height estimate, or backup generators had been watertight or located elsewhere, the largest nuclear disaster since Chernobyl may have been prevented (Lipscey et al. 2013). Many of the problems leading to the meltdown existed prior to the tsunami, and could have been corrected, had they been modeled or planned for.

4.4.3 Aliso Canyon, CA methane leak

On October 23, 2015, a blowout occurred at a natural gas well connected to the Aliso Canyon underground storage facility, which is attributed to failure of 40-year-old pipe (Carson and Kreilis 2016). At its peak, the leak effectively doubled methane emission rates of the entire Los Angeles Basin (Conley et al. 2016). This led to extensive negative media coverage (e.g. http://www.latimes.com/science/la-me-porter-ranch-greenhouse-20160124-story.html and

http://www.nytimes.com/2016/04/03/magazine/the-invisible-catastrophe.html). Once the leak was discovered, efforts were quickly made to plug well. The initial plan didn't work, so a more time-consuming, technically difficult operation was implemented. This event drives home the need for proactive prevention, such as more frequent well inspections, so that reactionary responses are unnecessary (Carson and Kreilis 2016). According to Carson and Kreilis (2016), it also "exposes the possibility of inadequate oversight of approximately 400 underground natural gas storage facilities in the U.S., most of which are regulated by states."

4.5 Shaking tolerance study: The Geysers

When giving a presentation or writing, the presenter/author ought to craft their message with the intended audience in mind. The same applies to developing projects that may induce earthquakes; evaluation of a population's response to shaking may alter a project's implementation. This was clearly demonstrated in the public reaction to unexpected shaking in Basel, as described previously. Using The Geysers Geothermal Field as an example, I suggest a simple way to understand community reaction to induced shaking.

Calpine, the principal operator at The Geysers, operates an answering machine where concerned residents can call in to voice complaints or notify operators that they felt shaking from an earthquake. Calls have been received for earthquakes as small as *M*2.02, and a *M*4.44 quake on March 14, 2013 received 16 calls (Hartline 2014; Hartline 2013). This is a simple approach to show empathy to a community about felt earthquakes. It also is a way to gauge if earthquakes are being felt, the frequency of felt events, and what the intensity of shaking is nearby.

Another helpful resource is the USGS's *Did You Feel It?* (DYFI) system (http://earthquake.usgs.gov/data/dyfi/). Users can report an earthquake they felt and/or search

archives to see shaking from past earthquakes. From December 2000 to April 13, 2016, 405 felt events in the vicinity of The Geysers were reported to the DYFI system, averaging one felt earthquake every two weeks (Figure 4.9).

In summary, it is evident that the nearby communities do not display unrest at quakes smaller than *M*2; above that, people notice; an unacceptable magnitude (where people call for the project to be shut down) has not yet been observed, despite multiple *M*4.5 earthquakes. Similar monitoring of community responses to small earthquakes could be helpful when setting up a TLP for a new energy production project.

4.6 Scientific and communication-driven decision making framework

"Conclusive proof of induced seismicity is difficult to demonstrate but is not a prerequisite for taking early prudent action to address the possibility of induced seismicity" (EPA 2014). In Chapters 2 and 3, I have set up a foundation that may be used to quantitatively assess if any of an earthquake population may be induced. Understanding if earthquakes are induced allows for scrutiny of the efficacy of mitigation efforts.

Before beginning operations, it is important to quantitatively establish earthquake rate density. As many earthquakes associated with pumping activities occur at low magnitudes, having a robust seismic network with low magnitude detection thresholds is critical. Having seismic stations in place before potentially induced earthquakes start, will allow direct comparison of earthquake catalogs at low completeness thresholds. If earthquakes occur after pumping operations begin, a seismic network will help operators to evaluate what is going on and what they may do about it. Unlike naturally occurring seismicity, the unique option to mitigate earthquake hazard exists for induced earthquakes. The process I have outlined in Chapter 3, to

understand if a population of earthquakes is likely induced or natural, may be used to assess effectiveness of operational changes. One may look for correlations between earthquake occurrence and pumping, and inspect for earthquake rate density changes around wells after pumping has begun. It is also important to quantify what happens to the number of earthquakes and magnitude distribution (G-R a- and b-values).

The framework presented below includes actions that can be taken to make scientific information available that may help inform decisions about operational continuity and acceptable risk, even if the cause of the earthquakes is unknown. As I will discuss in Section 4.7, uncertainty can be reduced using detailed data, and more knowledgeable decisions can be made.

4.6.1 Monitoring

As illustrated by data limitations in Chapter 3, frequently sampled pumping data need to be widely accessible (McGarr 2015). More regulations are beginning to require more frequent volume and pressure data collection and dissemination, as well as newly mandated seismic monitoring plans (as discussed previously). This increase in data availability could allow for better correlations to be drawn between pumping and earthquake occurrence, as well as real-time hazard assessments (Wiemer et al. 2007).

Earthquake magnitude and location uncertainties depend on network density and detection threshold. Lowering the completeness threshold, which would better illuminates the range of earthquake activity, is dependent on network capabilities. To assist in this effort, stations can be placed in close proximity to energy production operations, many seismometers can be deployed to enhance network density, and stations ought to be put in quiet locations to reduce impacts of noise and lower detection thresholds (Baturan et al. 2016). Magnitude scales must be calibrated

between local and regional networks, such as USGS's Advanced National Seismic System (ANSS) or EarthScope's Transportable Array (http://www.quake.geo.berkeley.edu/anss/catalog-search.html, Meltzer et al. 1999). Magnitude discrepancies between magnitude scales could impact traffic light protocols (among other consequences). It is also important to minimize location uncertainties, especially in light of regulations that are based on the magnitudes of earthquakes near wells.

4.6.2 Pre-emptive modeling

Frequent sampling of high-quality, detailed data is necessary before, during and after pumping, to establish baseline data and to continue monitoring impacts of pumping. A non-exhaustive list of scientifically relevant information is presented: proximity to faults, depth to basement, strength of crust, state of stress, pore pressure, permeability, porosity, rheology, and tectonics. Obtaining as much of these data as possible, prior to the onset of pumping, will only serve to better assess potential for induced seismicity, inform decision-making, and advance scientific understanding of the development of the project (Majer et al. 2012).

Similar to some of California's geothermal fields, future energy production sites, located in seismically active regions, may include both tectonic and induced earthquakes. Based on pre-pumping earthquake rates, and rates after pumping has commenced, one can estimate future earthquake rate and magnitudes (based on a simple G-R relationship). If the pumping rate were to increase, a new expected rate could be assessed.

Science-based scenarios, developed from real-world data and constrained by realistic parameters, can be effective tools in managing the risk associated with seismicity from energy production. When developing the scenario science, there are advantages to involve magnitude-frequency

distributions (MFDs) that are based on both real and synthetic catalogs. Observed MFDs describe current and past earthquake behavior. Hypothetical MFDs could portend changes in earthquake rate if pumping rates were altered.

The development and use of realistic, science-based scenarios has been shown to guide critical infrastructure mitigation, inform public policy, and promote community action. For example, the ShakeOut Scenario (Jones et al. 2008) led to the development of the policy-focused Resilience by Design report commissioned by Mayor Eric Garcetti, and produced by a City of Los Angeles task force (2014). The ShakeOut and other scenarios have been effective tools in getting science into the decision-making process. As quoted in Resilience by Design, President Dwight D. Eisenhower knew the importance of planning for an emergency, "Plans are worthless, but planning is everything. There is a very great distinction because when you are planning for an emergency you must start with this one thing: the very definition of 'emergency' is that it is unexpected, therefore it is not going to happen the way you are planning." Resilience by Design utilizes the science in the ShakeOut Scenario to address critical seismic vulnerabilities. This report has led to new laws in Los Angeles, including mandatory retrofit of soft-first story and non-ductile reinforced concrete buildings (http://www.lamayor.org/resilience-design-building-stronger-los-angeles).

4.6.3 Community buy-in

I have already discussed two bookend examples of community relations: public acceptance of +M4 shaking near The Geysers, and the community-driven shutdown of the EGS project in Basel. This stark difference highlights the need for public buy-in from the initial stages of the project (Stauffacher et al. 2015). One way to do this is for industry, the scientific community,

and the local residents to collectively decide acceptable risk (Giardini 2009). Operators can involve the public in the decision-making process and may also create local jobs, fostering heightened community investment in the project.

As noted by Giardini (2009), "The public reacts with a vengeance if it perceives that a known problem has been hidden." Operators can curry public support by communicating with the local stakeholders and by promoting industry-society transparency (Bommer et al. 2015). A well-designed endeavor will have an education campaign (accessible to all socio-economic groups and those of varying scientific literacy,) that includes risk estimates (although this may be difficult to communicate). It is advantageous to describe the project's benefits to the community. A discussion of theoretical costs should not be circumvented, as people are more tolerant of shaking if they are warned that it's possible (Bommer et al. 2015). Avoiding surprises is likely for the best.

4.6.4 Short-term local earthquake hazard probability maps and/or forecasts

As demonstrated by the changing frequency and magnitude of earthquakes in the central and eastern U.S. over the last 7 years (Ellsworth 2013), it is important to characterize short-term hazard variability (Petersen et al. 2016). If seismicity changes, hazard models may be updated rapidly; new data collection reduces epistemic, or knowledge-based, uncertainties (Bommer et al. 2015). Aleatory, or random, uncertainty cannot be reduced with acquisition of more data. Revised risk estimates can quantify the impact of mitigation efforts, and may facilitate more informed decisions and future mitigation practices.

It is useful to relate probability to magnitude, in the context of induced seismicity mitigation. If there is a 95% chance of a M5 or larger earthquake in the next 5 years, perhaps that could trigger

a red light. If there was a 70% chance, that could prompt yellow light actions. These are just example thresholds, and a cost-benefit analysis could help set appropriate probability tolerances. In principle, the cost to continue operations (given the probability of exceeding a specific earthquake magnitude) could be weighed against the costs of stopping. I suggest this as a way that science may facilitate hazard evaluation.

In Chapter 2, I discuss the probability of experiencing no earthquakes of a given size (equation 2.5). An energy production operator may be more interested in knowing the probability of one or more earthquake of a given size occurring. A magnitude of concern (M) must be identified, as well as a time frame (T) over which the operator is interested. The magnitude rate (λ) can be determined from the Gutenberg-Richter magnitude-frequency distribution, and the probability of an earthquake of magnitude M occurring can be determined by using the equation for one or more occurrences of an event, given a Poisson process:

$$P(n \geq 1 | \lambda, T) = 1 - e^{-\lambda T} \tag{4.1}$$

(Evans et al. 1993).

This method of defining a time period and magnitude of concern, with earthquake rate determined from a G-R distribution, can be a valuable planning tool. Just as magnitude is used as a criterion for a TLP, a framework can be set, which more realistically and quantifiably describes the likelihood of encountering that critical threshold. A critical threshold (for either a given magnitude or ground motion) only addresses a specific scenario. Another approach to a cost-benefit analysis is to use a cost function as a function of magnitude, and integrate that cost function over the whole magnitude range. Small earthquake are more frequent but less costly, while large ones have the opposite character.

4.6.5 Consider elements beyond reducing the hazard, tailored to community's risk tolerance and need

A well-established risk model allows for tailoring of mitigation practices (Bommer et al. 2015). Mitigation is not one-size-fits-all! Some local and national economies rely strongly on natural gas, oil, or geothermal energy production, but occasional damage from small earthquakes is of concern. This is the case in The Netherlands, where involved parties (i.e. gas exploitation companies, government agencies, and scientific researchers) undertook collaborative planning to come up with a long-term method to reduce uncertainties and establish monitoring priorities (van Eck et al. 2006). This balanced approach led to the adoption of a mutually acceptable exploitation and mitigation strategy. Part of the agreed upon risk mitigation strategy is to strengthen local structures—most earthquake-related damage had been limited to non-structural masonry cracks—and provide compensation for economic losses due to ground shaking (Ellsworth et al. 2015).

4.6.6 Effective risk communication

Induced earthquakes are happening in traditionally seismically active locations, as well as places that have previously been seismically quiescent. Homes in the Central and Eastern US are more commonly built to withstand tornadoes and hurricanes, not earthquakes. In these places, buildings are often designed to be very rigid to withstand high winds. In "earthquake country," buildings are designed to flex and bend. On the U.S. West Coast, school children are taught to "drop, cover, and hold on" in earthquake drills, while their Midwest counterparts learn what to do in the event of a tornado warning. The newly released USGS National Seismic Hazard Map

report indicates that 7.9 million people live in the vicinity of induced earthquakes in the central and eastern US (see Figure 4.7; Petersen et al. 2016). This population presents a unique need; they are exposed to a high level of earthquake shaking hazard, yet likely have little to no training about what to do or how to prepare.

Michelle Wood (2014) introduced the concept of "communicating actionable risk," which shifts communication techniques from emphasizing risk to communicating suggested responses to the risk. She also reports that people are more likely to take action if preparedness communications are delivered by community members, rather than from governmental or nongovernmental organization representatives. Operators may consider, as an act of community engagement and civic responsibility, sponsoring or implementing public education campaigns.

Public education campaigns are most effective when communicated by peer role models, adopt social-network based strategies, and use repeated messaging across multiple dissemination channels (Wood 2014). One successful example of this has been the Great ShakeOut earthquake drill (with millions of yearly participants), which has cultivated a culture of talking about earthquake safety and preparedness with friends, family, and classmates (Wood and Glik 2013). Operators may wish to communicate with local media agencies and community organizations to discuss potential risks and rewards of the project. In Basel, Switzerland, a barrage of negative media stories occurred after earthquakes occurred which were associated with geothermal projects (Stauffacher et al. 2015).

Not all communities have equal access to information. Borque (2015) found that both home ownership and higher income increase preparedness; renters are less likely than homeowners to stockpile preparedness supplies or to know how to properly act during an earthquake. Efforts need to be made to communicate risk with different socio-economic groups, across variable

scientific literacy levels, and through multiple media (such as digital, print, and verbal communications). Consistent, understandable public messaging is a key component successfully propagating information (Wood 2014).

The way information is conveyed to users must be carefully considered. Probabilistic and uncertainty data can be hard to explain and understand. Without consideration of end-user backgrounds' and prior knowledge, results may easily be misunderstood or not even used. Simple terminology differences (i.e. 25%; 1 in 4; .25; or 25 in 100) can impact understanding and efficacy of communications (Thompson et al. 2015). Careful thought ought be given to what is conveyed, how it is presented, and who the audience will be. Clear visuals help multi-lingual communities or those with low science-literacy understand the risk and suggested preparedness actions. Social media may help disseminate information to a broad audience.

4.7 Uncertainty in decision making

To better comprehend the uncertainties associated with making decisions when earthquakes may or may not be induced, I present an analogy using blackjack. When you play a game of blackjack, cards are often dealt face down, and the only cards you see are the two in your hand. Let's assume those cards are akin to an observed earthquake catalog, while the whole deck represents an earthquake population (of which you are seeing a small portion). The more you know about what is in the deck, the more effectively you can bet and assess your odds of winning. Counting cards or seeing the other players' hands tells a player more information about what may come out of the deck next, or what the dealer may have. These are both ways of reducing epistemic uncertainty, or gaining knowledge about possible outcomes. Even if you

know everything about the deck of cards, you still do not know what card will come out next; this is the aleatory uncertainty.

In Chapter 2, I present an approach to quantify future probability of earthquakes at or above a given magnitude. In Chapter 3, I discuss how if a population of earthquakes is influenced by pumping, the Gutenberg-Richter a- and b-values may change. The sensitivity of the a-value to pumping rate (as described in Chapter 3) can be used to make "broom" diagrams, like Figure 2.7A. Broom diagrams illustrate the range of likely scenarios, given specific a- and b-values. Evaluating probabilities of potential earthquake scenarios, and characterizing changing circumstances (such as by evaluating increases or decreases in earthquake rate density), is similar to counting cards. By reducing epistemic (knowledge-based) uncertainties and assessing the situation, better-informed decisions are possible. Ways to minimize epistemic uncertainties associated with the tools I discuss include increasing the a-value and more accurately constraining the b-value. To achieve this, one needs a bigger catalog. Time can solve this problem, but lowering the completeness threshold can also be of assistance. This dissertation presents a powerful device in assessing the uncertainty associated with possibly induced earthquakes, and demonstrates how science is able to aid in the decision-making process by revealing some of the possible hands in the deck.

4.8 Discussion

Imagine that you oversee a small energy production operation, situated within 10 km of a major fault system. Prior to pumping, there was little to no seismicity, and after it commenced, only earthquakes less than *M*2.0 have been recorded. One day, a *M*5.5 earthquake occurs near one of your wells. What information would you require before deciding to stop or continue operations?

First, you would probably want to know more about the situation. Is your decision as simple as adhering to a previously determined acceptable magnitude limit? Or would you also consider proximity to other faults, change in local stress conditions, past earthquake history, etc.? What about stress conditions in the underground reservoir, or if injection or production was spatially and/or temporally correlated with the earthquake? I present this as a hypothetical situation, but it is based in reality. In the Imperial Valley, CA, four geothermal fields are located less than 20 km from major faults and within 12 km of magnitude 6.2 earthquakes in the last 30 years (see Figure 4.10). The Brawley geothermal field experienced an earthquake swarm with two *M*5.3+ earthquakes in 2012; the swarm has been indirectly attributed to injection activities (Wei et al. 2015).

Additional scientific data availability allows for improved modeling and analysis. Increased monitoring capabilities will make for better baseline data and model accuracy (as discussed in Section 4.6). This information may be of help in reducing uncertainties before making a decision about future operations. Hazard characterization (and if or how it fluctuates) will be helpful in planning for future scenarios.

Although some legal cases have surfaced around the country, if earthquake rates and magnitudes continue near the same trajectory, more cases are likely. Cypser and Davis (1994), in a discussion of induced seismicity liability, state the following: "Seismicity induced by one source might accelerate failure of support originating from another source, leaving both of the parties at fault proportionally liable to the injured parties."

Mitigation trial and error is being done in real time, and is faster than the publication system or legislative cycles. Perhaps a federally unified approach is appropriate, as suggested by Finley (2015), with minimum requirements including increased monitoring, basic modeling and hazard

quantification, community outreach, and risk communication. Science can be used as a tool to help mitigate potentially induced seismicity, and as an aide in the decision-making process during uncertain times.

Development of controlled experiments can help increase our understanding of the physics of induced seismicity. For example, geothermal field operators could preemptively evaluate the efficacy of operational strategies specific to their field, should a strong earthquake occur nearby. Two potential techniques are 1) suspending all operations and shutting-in all wells; or 2) rapidly reducing pore pressure in the reservoir by producing without injecting (which, admittedly creates a wastewater surplus). Operators could experiment with these or other methods before a crisis, in order to determine which approach would be more effective in their particular geothermal field. Interested geophysicists could partner with operators and learn from this experiment, too. By doing these tests at each geothermal field, one may potentially be able to learn more about specific site response, and shed light on the question of why some locations have induced earthquakes while others do not. This also presents a practical way to evaluate the maximum likelihood test described in Section 3.5. If earthquakes are 100% natural, one should be able to alter operational parameters with no significant changes to the earthquakes. If earthquakes are 100% induced, one should expect a strong seismic response to pumping changes.

4.9 Conclusions

Induced earthquake hazard is unique compared to natural earthquake hazard, because it can be mitigated. I evaluate and summarize various mitigation strategies, from traffic light systems and integrated community outreach, to directed and strategic pumping, or reactionary legislation and community-driven procedural changes. There has been a clear, temporal earthquake rate change

in many US states, especially Oklahoma (Goebel 2015). I review U.S. legislation governing induced earthquake mitigation in seven states with heightened recent earthquake activity. From this assessment, I conclude that implementing mitigation strategies quickly is essential; as outlined above, this supports similar conclusions over the last 45+ years (e.g. Healy et al. 1968, EPA 2014). In some cases, states, like Texas, have been able to effectively reduce earthquake rates (EPA 2014). In states where streamlined efforts took years to enact, like Oklahoma, earthquakes are still problematic and occurring at a high rate.

When deciding on a mitigation strategy, there is no single rubric that can be applied to all situations. One can consider multiple mitigation approaches, and tailor them to a community's needs and expectations. Other than never starting any perturbing actions, there is no universal remedy for induced seismicity (Bommer et al. 2015). A multi-faceted approach to mitigate emergent risk, rather relying on any one technique, may be more effective.

The Department of Energy (2012), Environmental Protection Agency (2014), and National Research Council (2012) reports on induced seismicity characterization and mitigation each recommend increased data collection and dissemination. In recent years, new procedures and pieces of legislation have been developed to mitigate the increase in energy-related induced earthquakes, many of which require seismic monitoring plans and more frequent sampling of fluid volumes and pressures. This new wealth of information, if shared openly and analyzed, could lead to uncertainty reduction in many areas. This may lead to a better understanding of variations in fluid volumes, pressures, and operational aspects, and how earthquakes are related to these parameters. There is also the potential to better constrain fault locations, rupture mechanisms, and local stresses. Reduced earthquake location errors could lead to a better understanding of fluid migration through microseismicity monitoring, leading to more detailed

reservoir dynamics models. Analysis of more detailed data may help identify if faults act as barriers or conduits to flow, and if this changes with fault age; how structures respond to shaking; and if there are physical differences between induced and tectonic earthquakes.

I outline ingredients of a science-based risk management framework, in which data are used to assess and evaluate evolving and uncertain situations. Conducting any energy-production related activities in a populated area carries its own challenges; this work presents options for how to mitigate potential induced hazards, as well as strategies for effective risk communication. Some of the most basic components of an effective energy production plan include monitoring and modeling to observe trends, establishing baseline data, and evaluating effectiveness of mitigation strategies (if they are needed). An indirect mitigation technique is for pumping operators to assess and communicate risk to local communities; there is a growing need to teach earthquake preparedness in communities where risk has increased due to induced earthquakes. Effective risk communication makes use of the concept that people will act when they know what to do, think that it will be effective, and know someone who has done it. I also suggest that it is time for a national strategy, in which resources may be pooled for a faster implemented, more unified, and tactical approach, rather than patchwork state-based solutions.

My work in this and the two previous chapters sets ups a statistical method of quantifying potential earthquake hazard in a way that can be applied to understand the range of possible seismicity. Being able to assess short-term probability of the largest acceptable earthquake is a powerful tool for an operator and a community. As I have outlined, using science will help to better constrain induced seismicity hazards, ultimately leading to a reduction in epistemic uncertainty so more tactical and educated decisions can be made. If induced earthquakes persist,

increased monitoring and data availability will allow for localized testing of the efficacy of different mitigation techniques.

Chapter 4 Figures

PROBABILITY

CONSEQUENCE	Very Likely	Somewhat Likely	Unlikely	Somewhat Unlikely	Very Unlikely
1 MMI > VIII PGA > ~0.34g	High	High	High	Medium	Low
2 MMI : VI - VII PGA > ~0.092g	High	High	Medium	Low	Very Low
3 MMI: V-VI PGA > ~0.039g	Medium	Medium	Low	Very Low	Very Low
4 MMI: II-V PGA < ~0.039g	Low	Very Low	Very Low	Very Low	Very Low

Figure 4.1

Generic risk matrix for induced earthquakes. Risk is equivalent to the hazard (here, given as a probability) times the consequence of the event (Nygaard et al. 2013).

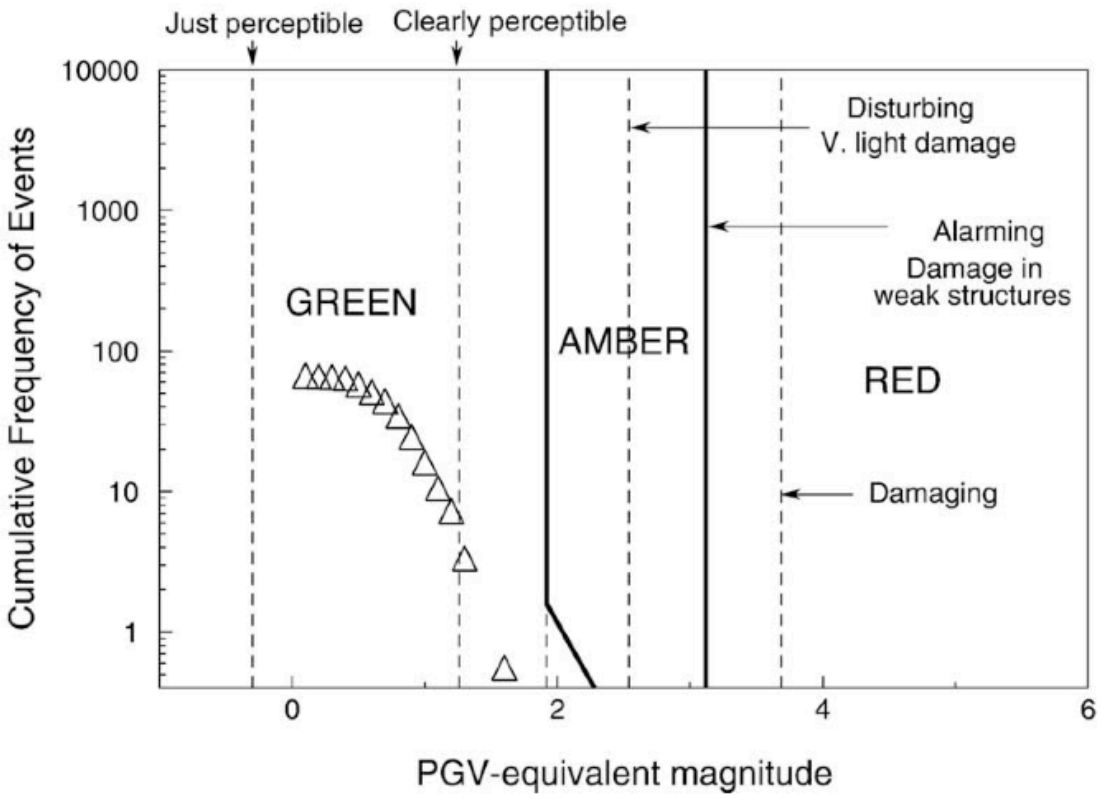

Figure 4.2

Traffic Light Protocol divisions for an energy production project in El Salvador, created by Bommer et al. (2006).

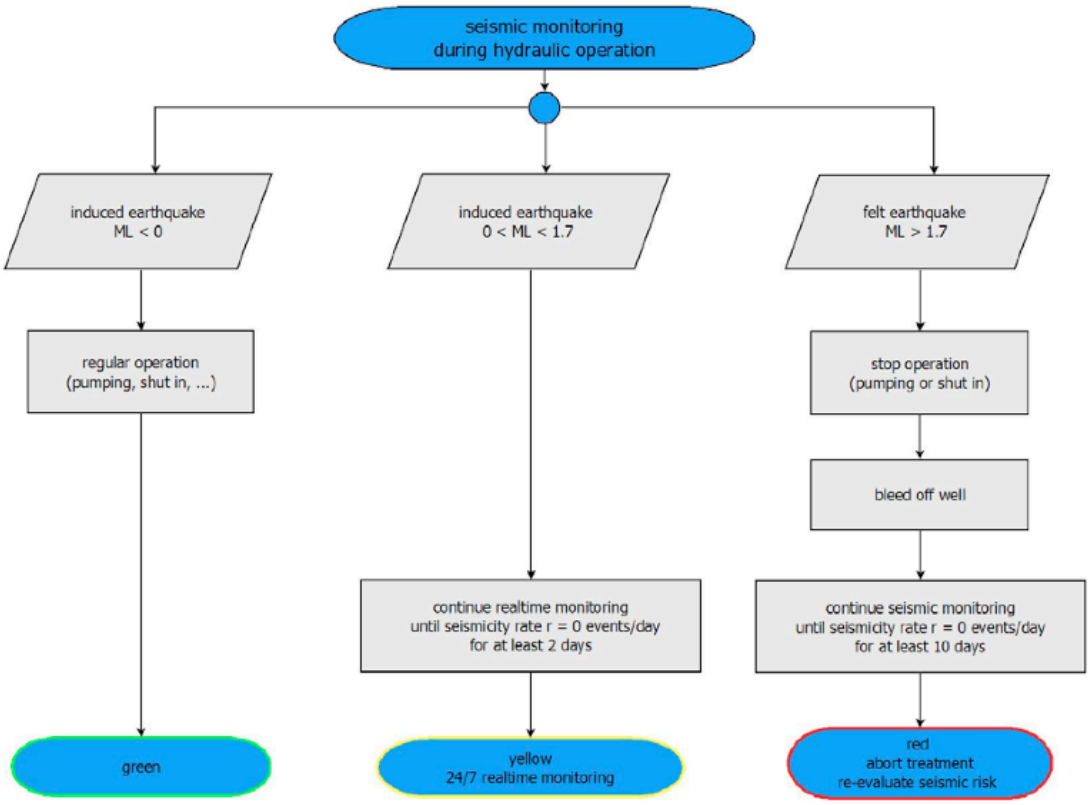

Figure 4.3

A proposed Traffic Light Protocol for stimulation in the Bowland Shale, UK. The "red light" threshold of *M*1.7 is based on an expected post-injection magnitude increase of up to *M*0.9; based on a German code, *M*2.6 is the lowest magnitude at which an earthquake could potentially cause material damage to structures (de Pater and Baisch 2011).

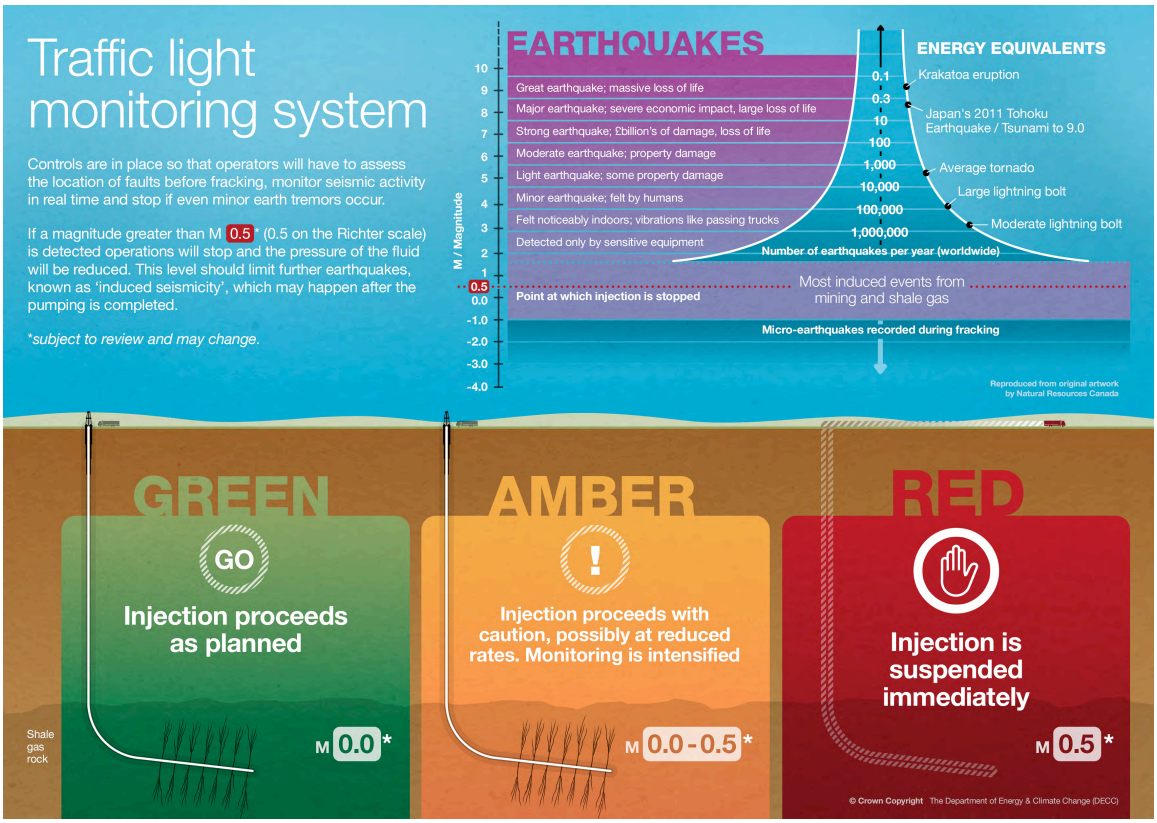

Figure 4.4

The UK government has released a report indicating the maximum allowable earthquake at *M*0.5, for proposed shale gas wells stimulation. This infographic was developed to convey the steps that would be taken as certain magnitude levels were reached (https://www.gov.uk/government/publications/traffic-light-monitoring-system-shale-gas-and-fracking).

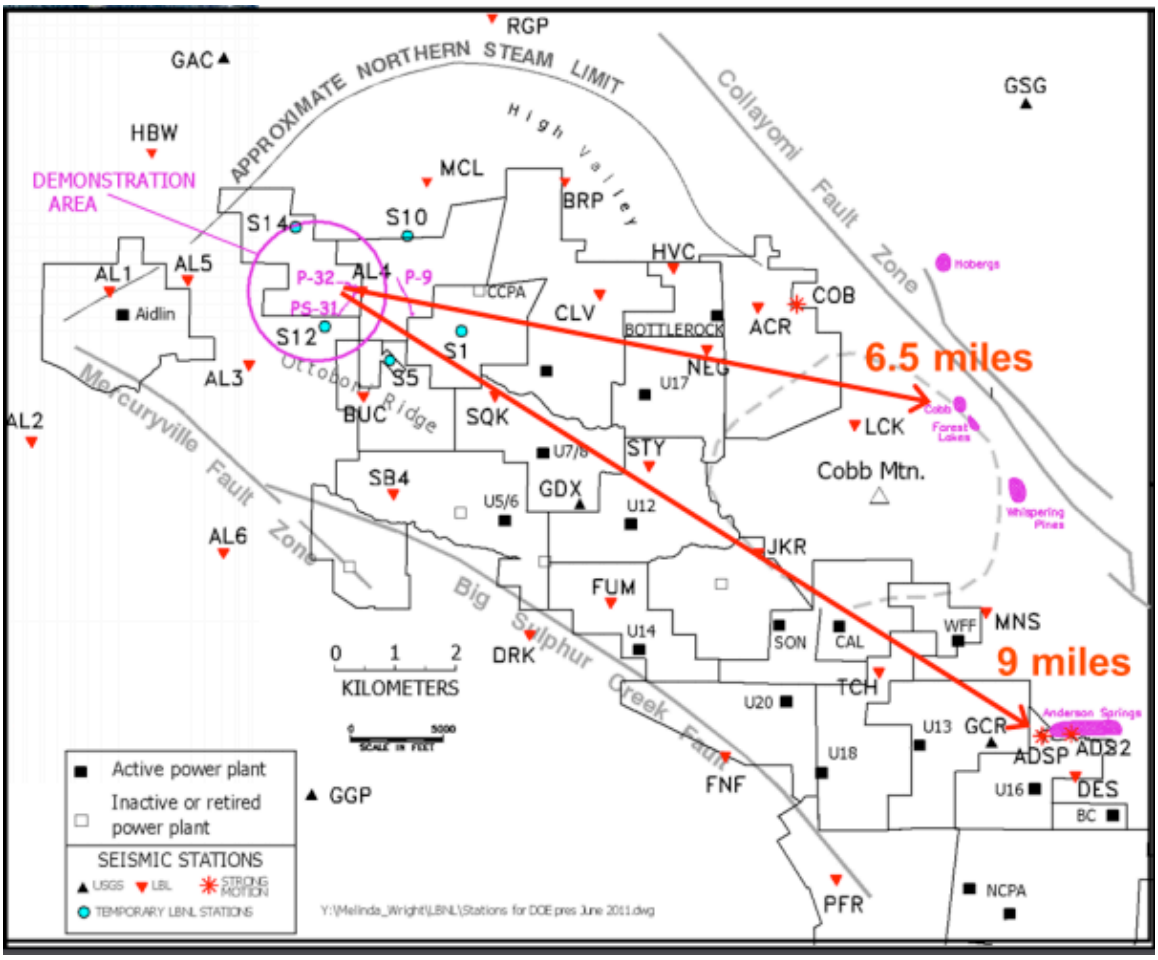

Figure 4.5

Enhanced Geothermal Systems (EGS) wells located in the northwest of The Geysers geothermal field reservoir. Distances to nearby towns of Cobb and Anderson Springs are noted (Hartline 2013). Printed with permission from Calpine.

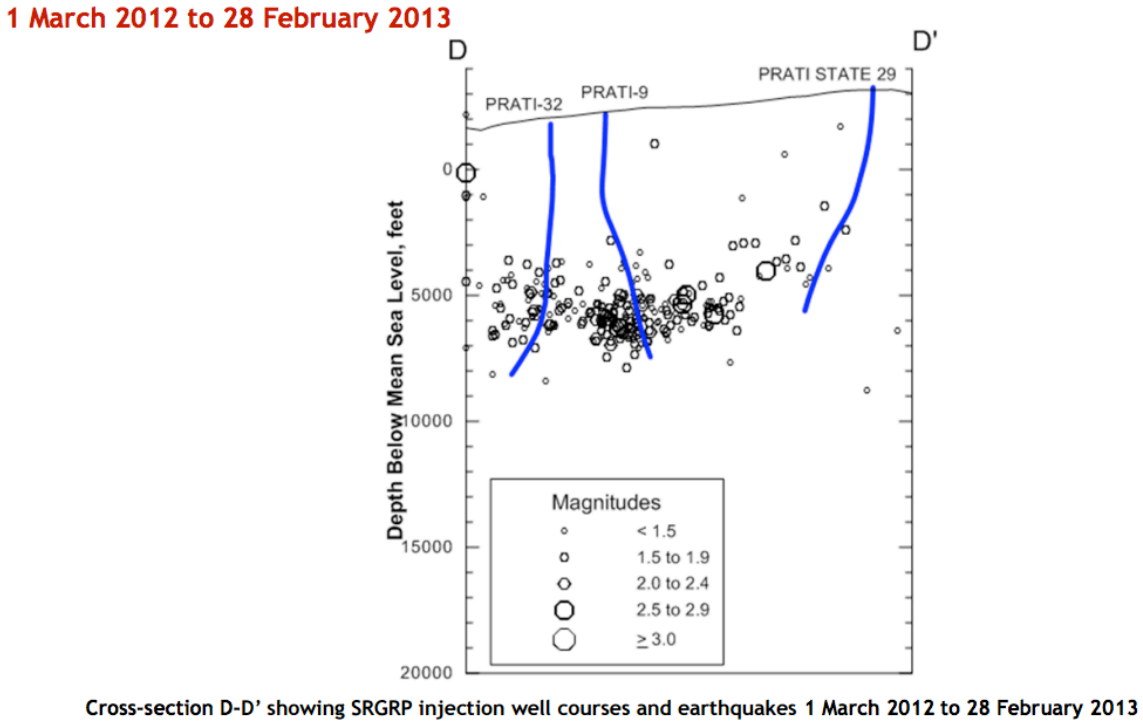

Figure 4.6

Cross-section view of a seismicity cloud forming around EGS test wells in The Geysers northwest region (Hartline 2013). Printed with permission from Calpine.

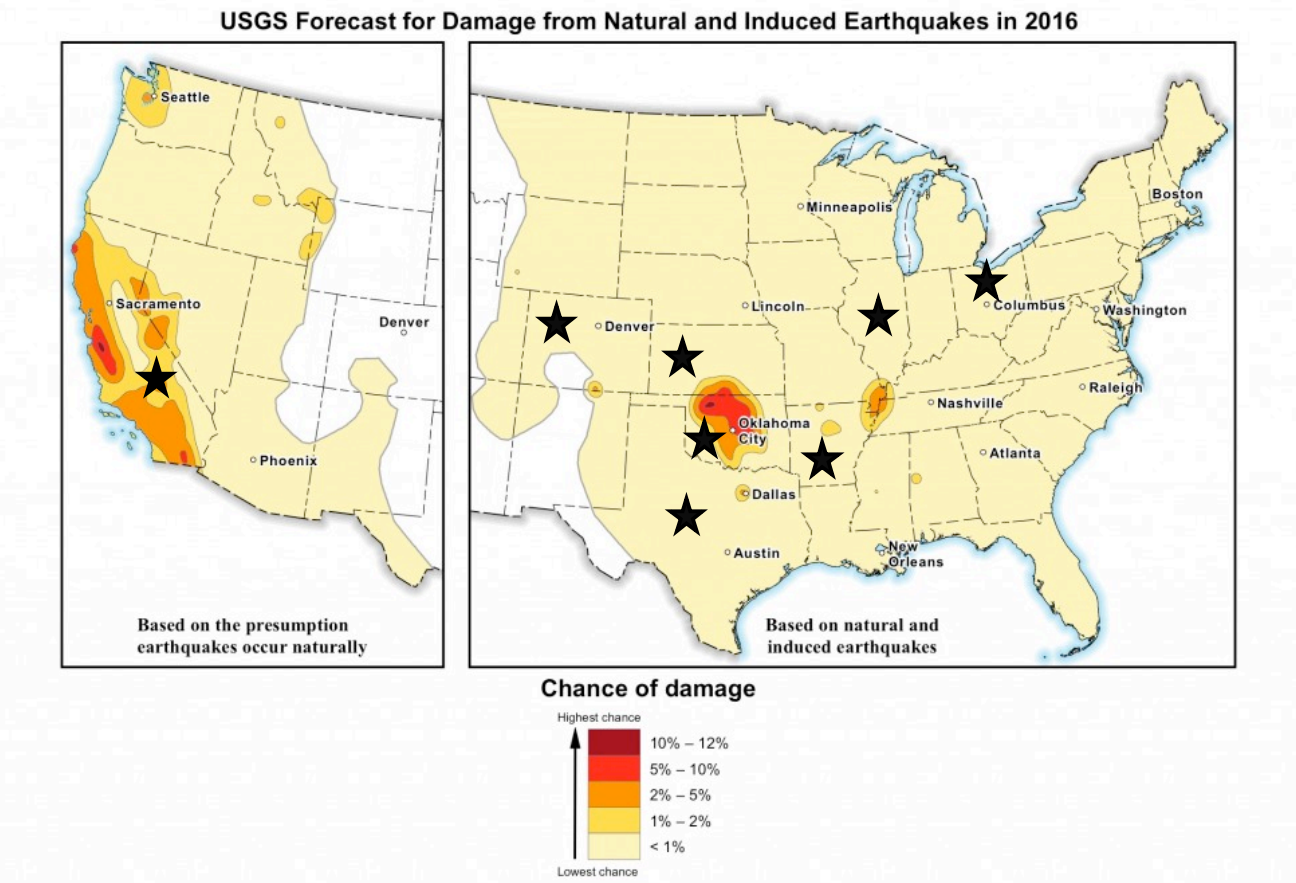

Figure 4.7

Recent U.S. Geological Survey one-year National Seismic Hazard Map, which includes induced earthquakes (modified from Petersen et al. 2016). Hotter colors indicated regions with heightened probability of experiencing damage from an earthquake in the 1-year period following the release of the map. Black stars indicate states with recent legislation governing energy practices for the purpose of earthquake mitigation, as discussed in this chapter.

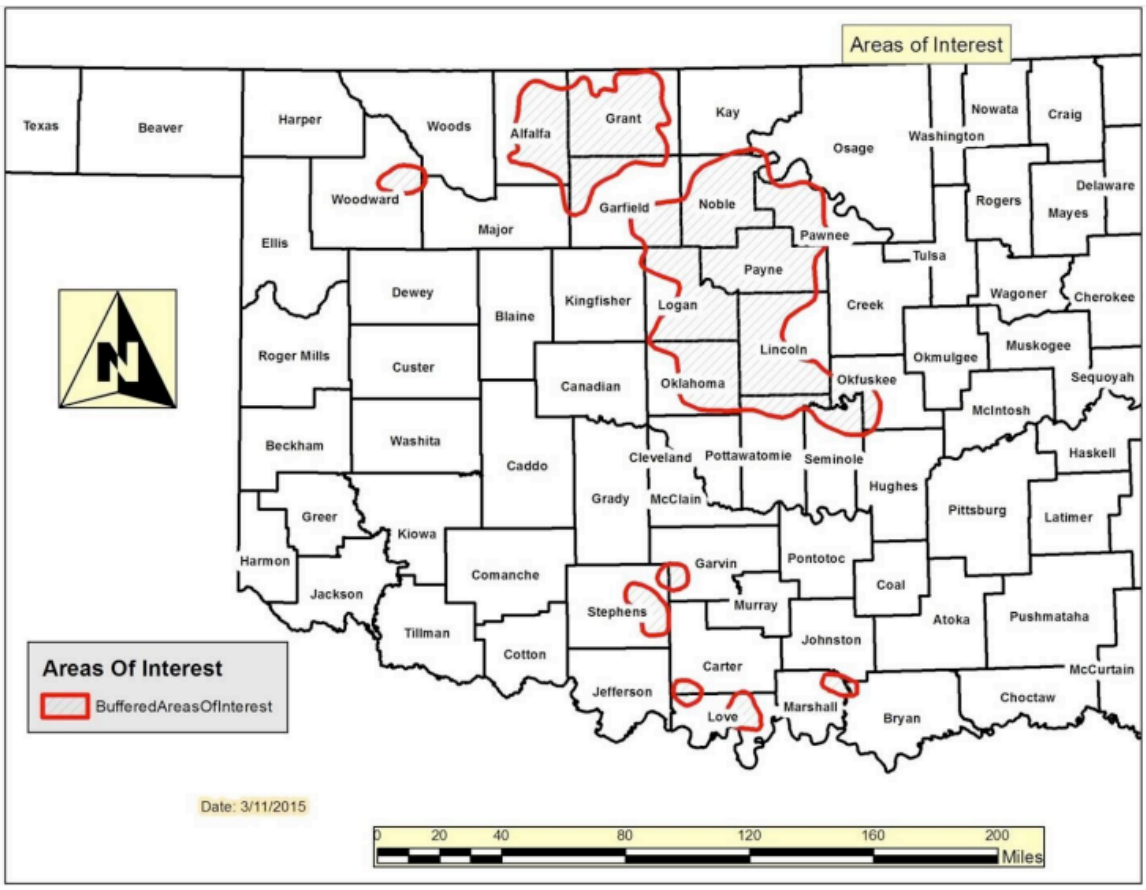

Figure 4.8

Oklahoma Area of Interest (AOI) map, designating regions around the state with increase seismicity rates. AOIs include "swarms" which contain "at least two events with epicenters within .25 miles of one another with at least one event with a magnitude 3.0 or higher." An AOI is a 10 km area centered on the swarm. This particular map was released in a March 25, 2015 media advisory from the Oklahoma Corporation Commission (http://www.occeweb.com/News/2015/03-25-15%20Media%20Advisory%20-%20TL%20and%20related%20documents.pdf).

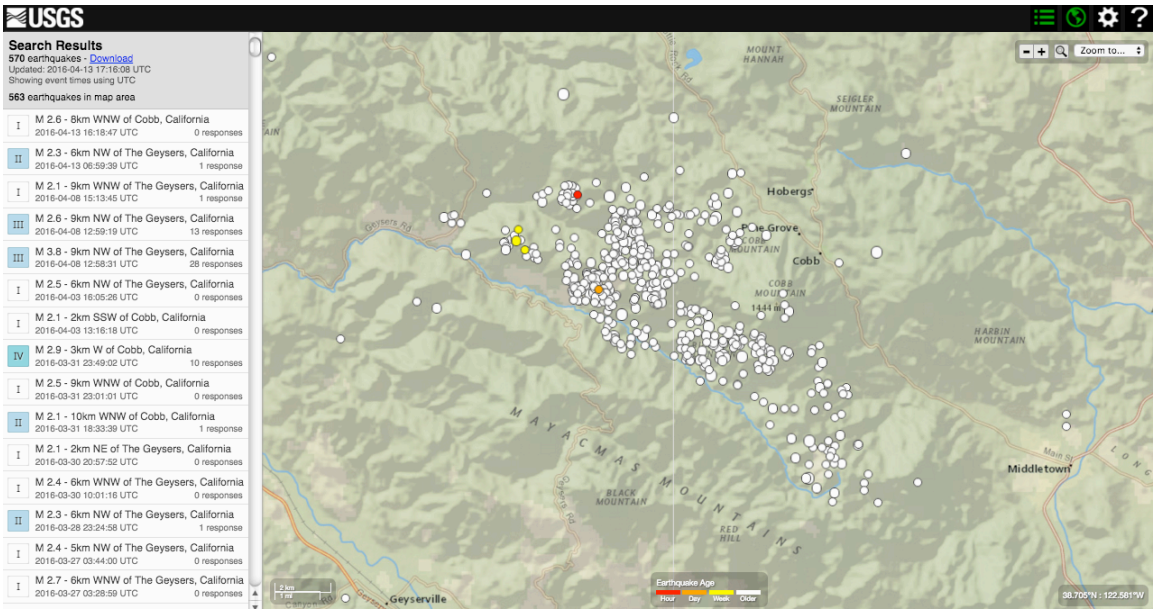

Figure 4.9

December 2000 to April 2016 earthquakes near the Geysers Geothermal Field, with USGS Did You Feel It? information at left (http://earthquake.usgs.gov/data/dyfi/).

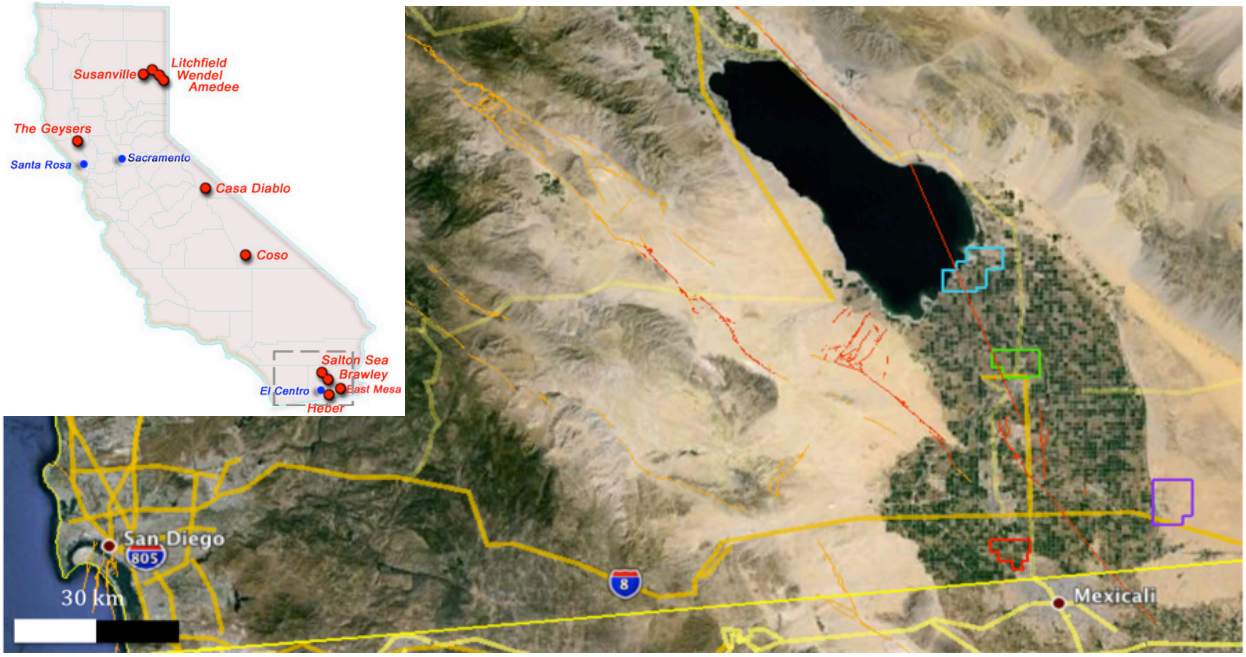

Figure 4.10

The four major Imperial Valley geothermal fields (Salton Sea, Brawley, Heber, and East Mesa) are all within 20 km of mapped traces of the San Andreas Fault system (the Brawley Seismic Zone passes through some of the fields). All four fields are within 12 km of a recent $M \geq 6.2$ earthquake (Google Earth Image) (Inset: http://www.conservation.ca.gov/dog/geothermal/manual/Pages/production.aspx).

4.10 References cited

(AOGC Rule H) Arkansas Oil and Gas Commission, General Rule H—Class II Wells, Rule H-1: Class II Disposal and Class II Commercial Disposal Well Permit Application Procedures, Section(s).

Baisch, S., D. Carbon, U. Dannwolf, B. Delacou, M. Devaux, F. Dunand, R. Jung, M. Koller, C. Martin, and M. Sartori, 2009. Deep Heat Mining Basel: Seismic Risk Analysis, SERIANEX Group. Departement für Wirtschaft, Soziales und Umwelt des Kantons Basel-Stadt, Basel

Baturan, D., S. Karimi, and E. Yenier, 2016, Challenges and Strategies for Monitoring Induced Seismicity, Presented at the Seismological Society of America Annual Meeting, April 20-22, Reno, NV.

Bommer, J.J., S. Oates, J.M. Cepeda, C. Lindholm, J. Bird, R. Torres, G. Marroquin, J. Rivas, 2006, Control of hazard due to seismicity induced by a hot fractured rock geothermal project. Eng. Geol. Vol. 83, p. 287–306, http://dx.doi.org/ 10.1016/j.enggeo.2005.11.002.

Bommer, J., H. Crowley, and R. Pinho, 2015, A risk-mitigation approach to the management of induced seismicity, J Seismol., vol. 19, p. 623–646.

Borque, L., 2015, Demographic Characteristics, Sources of Information, and Preparedness for Earthquakes in California, Earthquake Spectra, vol. 31, issue 4, p. 1909-1930, http://dx.doi.org/10.1193/013014EQS024M.

Carson E. and J. Kreilis, 2016, California Leak Exposes Risks Of Increasing Reliance On Natural Gas, Policy Brief, January 25, 2016, EnerKnol, Inc., EnerKnol Research | Fossil Fuels.

COGCC (Colorado Oil and Gas Conservation Commission), 2011, COGCC Underground Injection Control and Seismicity in Colorado, January 19, Denver, CO: Department of Natural Resources. Available at http://cogcc.state.co.us/Library/InducedSeismicityReview.pdf.

Conley, S. G. Franco, I. Faloona, D.R. Blake, J. Peischl, and T.B. Ryerson, 2016, Methane emissions from the 2015 Aliso Canyon blowout in Los Angeles, CA, Science, vol. 351, issue 6285, p. 1317-1320, DOI: 10.1126/science.aaf2348.

Cypser, D.A., 1996, Colorado Law and Induced Seismicity, available at: http://www.darlenecypser.com/induceq/ColoradoLawandInducedSeismicity.html.

Cypser, D.A. and S.D. Davis, 1994, Liability for induced earthquakes. J. Envtl. L. & Litig., vol. 9, p. 551-589.

de Pater, C. J., and S. Baisch, 2011, Geomechanical study of Bowland Shale seismicity: Synthesis Report, Department of Energy and Climate Change, report 71.

Department of Energy and Climate Change (DECC), 2015, Onshore oil and gas exploration in the UK: regulation and best practice, England, www.gov.uk/decc.

Ellsworth, W.L., 2013, Injection-induced earthquakes, Science, vol. 341, is. 6142, p. 1225942 1-7.

Ellsworth, W.L., A.L. Llenos, A.F. McGarr, A.J. Michael, J.L. Rubinstein, C.S. Mueller, M.D. Petersen, and E. Calais, 2015, Increasing seismicity in the U. S. midcontinent: Implications for earthquake hazard, The Leading Edge, vol. 34, no. 6, p.618-626.

(EPA) U.S. Environmental Protection Agency, 2014, Minimizing and Managing Potential Impacts of Induced-Seismicity from Class II Disposal Wells: Practical Approaches.

Evans, M., N. Hastings and B. Peacock, 1993, Statistical Distributions, Second Edition, New York: John Wiley & Sons, Inc., ISBN–0-471-55951-2.

Finley, P., 2015, Bringing Down the House: The Regulation and Potential Liability of Induced Earthquakes, LSU Journal of Energy Law and Resources, vol. 4, issue 1, p. 111-142, http://digitalcommons.law.lsu.edu/jelr/vol4/iss1/10.

Folger, P. & M. Tiemann, 2014, Human-Induced Earthquakes from Deep-Well Injection: A Brief Overview, Congressional Resarch Service, 7-5700.

Giardini, D., 2009, Geothermal quake risks must be faced, Nature, vol. 462, p. 848-849

Goebel, T., 2015, A comparison of seismicity rates and fluid-injection operations in Oklahoma and California: Implications for crustal stresses, The Leading Edge, vol. 34, no. 6.

Green C.A., P. Styles, and B.J. Baptie, 2012, Preese Hall shale gas fracturing: review and recommendations for induced seismic mitigation. Report to DECC, available for download: https://www.gov.uk/government/uploads/system/uploads/attachment_data/file/48330/5055-preese-hall-shale-gas-fracturing-review-and-recomm.pdf.

Häring, M.O., U. Schanz, F. Ladner, & B.C. Dyer, 2008, Characterisation of the Basel 1 enhanced geothermal system, Geothermics, vol. 37, p. 469–495.

Hartline, C., 2013, Calpine Corporation presentation to the Seismic Monitoring Advisory Committee Meeting (SMAC), http://www.geysers.com/media/Calpine%20May%2013,%202013%20SMAC.pdf, Geothermal Visitors Center Middletown, California, May 13.

Hartline, C., 2014, Calpine Corporation presentation to the Seismic Monitoring Advisory Committee Meeting (SMAC), http://www.geysers.com/media/Calpine%20

Corporation's%20Nov%2017%202014%20Presentation.pdf, Geothermal Visitors Center Middletown, California, November 17.

Hydraulic Fracturing Regulatory Act, S.B. 1715, 98th Illinois Gen. Assem., Reg. Sess. (Ill. 2013).

Healy, J.H., W.W. Rubey, and D.T. Griggs, 1968, The Denver earthquakes. Science, vol. 161, no. 3848, p. 1301-1310.

Inman, M., 2016, Can fracking power Europe?, Nature, vol. 531, p. 22-24, doi:10.1038/531022a.

ISO, 1989, Evaluation of Human Exposure to Whole-Body Vibration: Part 2, Continuous and Shock-Induced Vibrations in Buildings ISO 2631-2:1997, International Organization for Standardization.

Kansas Corporation Commission, 2015, Order Reducing Saltwater Injection Rates, March 19, http://estar.kcc.ks.gov/estar/ViewFile.aspx/15-770%20Order.pdf?Id=ea831b2c-f398-4a05-9986-97f4cb45fe46.

Kansas Seismic Action Plan, 2014, Kansas Department of Health and Environment, Kansas Corporation Commission, Kansas Geological Survey, Kansas Seismic Action Plan, September 26, 2014, http://kcc.ks.gov/induced_seismicity/state_of_kansas_seismic_action_plan_9_26_14_v2_1_21_15.pdf.

Keranen, K.M., H.M. Savage, G.A. Abers, and E.S. Cochran, 2013, Potentially induced earthquakes in Oklahoma, USA: Links between wastewater injection and the 2011 M_w 5.7 earthquake sequence, Geology, doi: 10.1130/G34045.1.

Keranen, K.M, M. Weingarten, G.A. Abers, B.A. Bekins, and S. Ge, 2014, Sharp increase in central Oklahoma seismicity since 2008 induced by massive wastewater injection, Science, vol. 345, issue 6195, p. 448-451.

Kim, W.-Y., Induced seismicity associated with fluid injection into a deep well in Youngstown, Ohio. J. Geophys. Res. 10.1002/jgrb.50247 (2013).

Kraft, T., Wiemer, S., Deichmann, N., Diehl, T., Edwards, B., Guilhem, A., Haslinger, F., Király, E., Kissling, E., Mignan, A., Plenkers, K., Roten, D., Seif, S., and Woessner, J., 2013, The M_L3.5 induced earthquake sequence at Sankt Gallen, Switzerland. American Geophysical Union, Fall Meeting 2013, abstract #S31F-03.

Lipscy, P.Y., K.E. Kushida, and T. Incerti, 2013, The Fukushima Disaster and Japan's Nuclear Plant Vulnerability in Comparative Perspective, Environ. Sci. Technol., vol. 47, p. 6082−6088, dx.doi.org/10.1021/es4004813.

Llenos, A.L. and A.J. Michael, 2013, Modeling Earthquake Rate Changes in Oklahoma and Arkansas: Possible Signatures of Induced Seismicity. Bulletin of the Seismological Society of America, vol. 103, p. 2850–2861.

Majer, E.L., R. Baria, M. Stark, S. Oates, J. Bommer, B. Smith, and H. Asanuma, 2007, Induced seismicity associated with Enhanced Geothermal Systems, Geothermics, vol. 36, p. 185–222.

Majer, E., J. Nelson, A. Robertson-Tait, J. Savy, and I. Wong, 2012, Protocol for addressing induced seismicity associated with enhanced geothermal systems, U.S. Department of Energy, DOE/EE-0662.

Mayoral Seismic Task Force, 2014, Resilience by Design, technical report, available at http://www.aiasfv.org/temp/R-by-D-report.pdf.

McGarr, A., B. Bekins, N. Burkardt, J. Dewey, P. Earle, W. Ellsworth, S. Ge, S. Hickman, A. Holland, E. Majer, J. Rubinstein, A. Sheehan, 2015, Coping with earthquakes induced by fluid injection, Science, vol. 347, p. 830–831.

Meltzer, A., R. Rudnick, P. Zeitler, A. Levander, G. Humphreys, K. Karlstrom, E. Ekstrom, C. Carlson, T. Dixon, M. Gurnis, P. Shearer, and R.D. van der Hilst, 1999, The USArray Initiative, Geological Society of America TODAY, volume 9, p. 8 – 10.

Mignan, A., D. Landtwing, P. Kästli, B. Mena, and S. Wiemer, 2015, Induced seismicity risk analysis of the 2006 Basel, Switzerland, Enhanced Geothermal System project: Influence of uncertainties on risk mitigation. Geothermics, vol. 53, p. 133–146.

Mills, M. and S. Morrissey, 2015, SB 4 Well Stimulation Treatment Permanent Regulations Finalized, California Environmental Law Blog, http://www.californiaenvironmentallawblog.com/oil-and-gas/sb-4-well-stimulation-treatment-permanent-regulations-finalized/.

Moeck, I., T. Bloch, R. Graf, S. Heuberger, P. Kuhn, H. Naef, M. Sonderegger, S. Uhlig, M. Wolfgramm, 2015, The St. Gallen Project: Development of Fault Controlled Geothermal Systems in Urban Areas, Proceedings World Geothermal Congress 2015, Melbourne, Australia.

National Research Council, 2012, Induced seismicity potential in energy technologies, http://www.nap.edu/catalog/13355/induced-seismicity-potential-in-energy-technologies.

Nygaard, K.J., J. Cardenas, P.P. Krishna, T.K. Ellison, and E.L. Templeton-Barrett, 2013, Technical Consideration Associated with Risk Management of Potential Induced Seismicity in Injection Operations, Production and Development of Hydrocarbon Resources Congress Rosario, Argentina May 21-24, 2013.

OCC, 2015, Oklahoma Corporation Commission, Media Advisory—Ongoing OCC Earthquake Response, press release, March 25, 2015, http://occeweb.com/News/2015/04-21-15STATEMENT-OGS-LINK.pdf.

OCC, 2016a, Oklahoma Corporation Commission, Media Advisory - Regional Earthquake Response Plan for Central Oklahoma and Expansion of the Area of Interest, March 7, 2016, http://www.occeweb.com/News/2016/03-07-16ADVISORY-AOI, VOLUME REDUCTION.pdf.

OCC, 2016b, Oklahoma Corporation Commission, http://occeweb.com/, last accessed April 12, 2016.

OCC Website, Office of the Oklahoma Secretary of Energy and Environment, "Earthquakes in Oklahoma: Oklahoma Corporation Commission," http://earthquakes.ok.gov/what-we-are-doing/oklahoma-corporation-commission/, last accessed April 27, 2016.

Ohio Department of Natural Resources, 2012, Preliminary report on the Northstar 1 Class II injection well and the seismic events in the Youngstown, Ohio area: Ohio Department of Natural Resources, 24 p., https://oilandgas.ohiodnr.gov/portals/oilgas/pdf/UICReport.pdf.

Ohio Oil and Gas Laws, Ohio Department of Natural Resources Division of Oil and Gas Resouces. Summary of Oil and Gas Law in Ohio, Last accessed April 13, 2016, http://oilandgas.ohiodnr.gov/laws-regulations/oil-gas-law-summary.

Oklahoma Geological Survey (OGS), 2015, Oklahoma Geological Survey Statement on Oklahoma Seismicity, April 21, 2015, http://wichita.ogs.ou.edu/documents/OGS_Statement-Earthquakes-4-21-15.pdf.

Petersen, M.D., C.S. Mueller, M.P. Moschetti, S.M. Hoover, A.L. Llenos, W.L. Ellsworth, A.J. Michael, J.L. Rubinstein, A.F. McGarr, and K.S. Rukstales, 2016, 2016 One-year seismic hazard forecast for the Central and Eastern United States from induced and natural earthquakes: U.S. Geological Survey Open-File Report 2016–1035, 52 p., http://dx.doi.org/10.3133/ofr20161035.

Rubinstein, J. L., W.L. Ellsworth, A. McGarr, and H.M. Benz, 2014, The 2001-present induced earthquake sequence in the Raton Basin of northern New Mexico and southern Colorado, Bull. Seismol. Soc. Am. vol. 104, no. 5, p. 2162–2181, doi: 10.1785/0120140009.

SB-4 Oil and gas: well stimulation, 2013, Senate Bill No. 4, California Legislative Information http://leginfo.legislature.ca.gov/faces/billNavClient.xhtml?bill_id=201320140SB4.

Stauffacher, M., N. Muggli, A. Scolobig, and C. Moser, 2015, Framing deep geothermal energy in mass media: the case of Switzerland, Technological Forecasting and Social Change, vol. 98, p. 60-70.

Texas Administrative Code, Statewide Rules 9 and 46, November 14, 2014, http://texreg.sos.state.tx.us/public/readtac$ext.ViewTAC?tac_view=4&ti=16&pt=1&ch=3&rl=Y.

Thompson, M.A., J.M. Lindsay, and J. Gaillard, 2015, Journal of Applied Volcanology, vol. 4, no. 6, 24 p., DOI 10.1186/s13617-015-0023-0.

Tomastik, T., 2013, Ohio's New Class II Regulations and Its Proactive Approach to Seismic Monitoring and Induced Seismicity, ONDR, Division of Oil and Gas Resources Management, presentation given at 2013 UIC Conference, http://www.gwpc.org/sites/default/files/event-sessions/Tomastik_Tom_1.pdf.

van Eck, T., F. Goutbeek, H. Haak, and B. Dost, 2006, Seismic hazard due to small-magnitude, shallow-source induced earth- quakes in The Netherlands: Engineering Geology, vol. 87, p. 105-121, http://dx.doi.org/10.1016/j.enggeo.2006.06.005.

Vinson and Elkins, 2013, Illinois Passes Comprehensive Hydraulic Fracturing Legislation, V&E Shale Insights — Tracking Fracking E-communication, June 24, 2013, http://www.velaw.com/uploadedFiles/VEsite/Resources/IllinoisPassesComprehensiveHydraulicFracturingLegislation.pdf.

Wei, S., J-P. Avouac, K.W. Hudnut, A. Donnellan, J.W. Parker, R.W. Graves, D. Helmberger, E. Fielding, Z. Liu, F. Cappa, and M. Eneva, 2015, The 2012 Brawley swarm triggered by injection-induced aseismic slip, Earth and Planet Science Letters, vol. 422, p.115–125.

Wiemer, S., C. Bachmann, J. Woessner, 2007, Statistical Analysis and Earthquake Probabilities. In: Evaluation of the induced Seismicity in Basel 2006/2007: Locations, Magnitudes, Focal Mechanisms, Statistical Forecasts and Earthquake Scenarios. Report of the Swiss Seismological Service to Geopower Basel AG, Basel, Switzerland, 152 pp.

Wood, M., 2014, Chapter 9: Communicating Actionable Risk, In: Learning and Calamities: Practices, Interpretations, Patterns, pg. 143-158.

Wood M. and D. Glik, 2013, Engaging Californians in a Shared Vision for Resiliency: Practical Lessons Learned from the Great California Shakeout, Report for the California Seismic Safety Commission, available at: http://www.seismic.ca.gov/pub/CSSC_13-02_ShakeOutRecommendations.pdf.

Zoback, M., 2012, Managing the seismic risk posed by wastewater disposal, Earth Magazine, vol. 57, no. 4.

5 Dissertation Conclusions

5.1 Observed and possible maximum magnitudes of induced earthquakes?

In agreement with other results, the largest observed earthquake rarely constrains the maximum possible magnitude. I establish that California geothermal fields follow suit; observed catalogs do not constrain upper magnitude limit. I demonstrate that a limiting magnitude of 10 or greater cannot be rejected at any of the sites I examine, based on the present state of earthquake catalogs. In theory, more of the "earthquake story" will be illuminated over time, and as more earthquakes occur perhaps there will be enough data to constrain a true maximum magnitude ($M_{possmax}$). In the meanwhile, using the present distribution of earthquake magnitudes and frequencies at each field, I put 95% confidence limits on what the largest observed earthquake (M_{obsmax}) will be during a fixed time interval.

Given the commonly accepted hypothesis put forth by McGarr (2014) that earthquake magnitude is limited by injected fluid volume, I demonstrate that the maximum observed earthquakes at Basel and Raton basin (two randomly selected sites from McGarr's work) can be explained by sampling a randomly generated catalog with a very large upper magnitude limit. I have not yet examined other sites in his paper.

Finally, I sum the yearly rates of $M \geq 5$ earthquakes within 10 km of active injection wells at California geothermal fields. As shown in Chapter 2, determining the number and rate of earthquake (specifically, the G-R a- and b-values) can be used to estimate the probability that zero earthquake larger than M will occur in a given time interval (Equation 2.5). In Chapter 4, I calculate the probability one or more earthquakes M or larger will occur within a fixed time interval. Equation 4.1 gives a 64% chance of seeing one $M \geq 5$ earthquake within the 4 years from

2015-2018, and a 95% chance of seeing one within the 12 years from 2015-2026. Alternately, the probability can be chosen first and the time interval then follows from the equation. Choosing P = 64% leads to a time interval of 4 years; 95% leads to 12 years. This information can be used to assess uncertainty of the rate of future earthquakes as function of magnitude.

5.2 Relative contributions of induced earthquakes, and examination of temporal correlation of earthquakes and injection with time

I perform a robust examination of nine California geothermal fields, all of which have monthly injection and production data. I do not focus on identifying individual earthquakes as induced; that level of certainty is often beyond the resolution of the pumping data that are publicly available. Whether an individual earthquake is induced is of importance, however it is not the only story. It is beneficial to explore a larger catalog of events to understand the process of induced earthquakes at a location. In many of California's geothermal fields, background seismicity is substantial, however a component of seismicity exists near the wells that can be connected to pumping activities. When earthquake rate densities (ERDs) are examined within three and ten kilometers from active injection wells, I find higher ERDs near wells at Brawley, Casa Diablo, East Mesa, The Geysers, Salton Sea, and Susanville. I conduct two significance tests: a binomial test, and a moving-window test to determine if earthquakes are randomly distributed in the earthquake catalog. The latter is more rigorous; both The Geysers and Salton Sea geothermal fields have earthquake catalogs where seismicity is clustered in times with injection and production at statistically significant rates.

I contrast pumping data with earthquake occurrence, on a monthly basis. I examine earthquake rates before and after pumping began, as well as if earthquake hypocenter depths change, being

careful to consider changing catalog parameters, such as completeness magnitude, over time. Long-term spatiotemporal records are analyzed, both before and after pumping began; using a lower completeness threshold, I examine data trends since the initiation of pumping. By employing a lower M_c for co-pumping times, changes in seismicity at lower magnitudes may be observed, allowing more complex relationships to emerge from the data. My observations highlight the need for more detailed pumping and seismicity data, as I would likely be able to better scrutinize data trends and more closely resolve the seismic response to pumping parameter alterations. For example, Figures 4.6 show seismicity clustering around wells at The Geysers. If pumping data were sampled more continuously, it would create an opportunity to evaluate individual pumping rate or volume changes and how that correlates with seismicity. This information could allow operators and scientists to arrive at a more detailed understanding of how specific actions impact earthquake occurrence, and could contribute to science-based hazard mitigation practices and regulatory limits.

An objective approach to determining if seismicity has been induced is to use a checklist of criteria. I subject California geothermal fields to a series of questions, designed to determine if earthquakes are likely induced or not. Using these questions as a rubric, I find that most fields are not considered to have induced earthquakes. These specific criteria, however, are biased against areas that are seismically active prior to pumping, since induced earthquakes would not be novel to the area.

I identify which identify which fields display evidence of induced earthquakes, using a linear relationship. The model presented is straightforward: it is a linear combination of two end-member hypotheses; I do not consider influences from water production, net fluid injected into the field, or other factors that may impact earthquake occurrence. In my simple model, The

Geysers and Brawley demonstrate a strong correspondence with injection; Coso and Heber do not. Casa Diablo, East Mesa, and Salton Sea are representative of a combination both end-member hypotheses. The linear model does not account for the potential time delay between injection and seismicity, nor does it include any physical constraints.

Combining the findings from three methods outlined above (spatiotemporal analysis, criteria checklists, and linear relationship of two hypotheses), geothermal fields are classified as having strong, moderate, or weak to no evidence of induced seismicity. Geothermal fields with strong evidence for induced seismicity include Brawley, The Geysers, and Salton Sea. Moderate to strong evidence exists for Casa Diablo, Coso, East Mesa, and Susanville. There is little to no evidence for induced seismicity at Heber and Wendel. Litchfield and Amedee are no longer in operation; therefore they are not included in my analysis. Litchfield operated from 1984-2005, and Amedee was in operation from 1988-2014 (but has only produced for 15 months since the end of 2009). Based on my brief qualitative examination of their production records and earthquake activity, it is likely that both fields did not experience much, if any, induced earthquake activity. In the future, magnitudes thresholds should decrease, allowing for more detailed characterization of uncertainties and future earthquake potential. Where there are significant uncertainties now, better data will be useful. Quantifying the relationship between earthquakes and pumping at Casa Diablo and Coso could benefit from better data, and the release of classified information.

As demonstrated in Chapter 2 of this dissertation, I cannot constrain a maximum possible magnitude for earthquakes at California geothermal fields. However, as shown by others' analyses, an earthquake caused by energy production activities at California geothermal fields could trigger a larger, damaging event on one of many nearby large fault systems. Keranen et al.

(2013) determined that a wastewater-disposal induced earthquake triggered the Prague, Oklahoma *M*5.6 mainshock. Brodsky and Lajoie (2013) suggested that the activities in the Salton Sea geothermal field could eventually trigger seismicity on the San Andreas Fault. It is prudent that science-based protocols be developed regarding allowed geothermal pumping activity (and other energy technologies capable of inducing earthquakes,) near major fault systems.

5.3 Science-based decision making in a high-risk energy production environment

Energy production technologies are changing the earthquake status quo. In 2015, Oklahoma had approximately seven times more $M \geq 3$ earthquakes than California (http://earthquakes.ok.gov/, http://earthquake.usgs.gov). Oklahoma saw 907 of these quakes last year, compared to a previous long-time average of 1.5 year. Simply, much of our country is grossly underequipped to handle their new earthquake hazard. Traditionally, earthquake risk mitigation involves strengthening buildings and preparing for periodic tectonic shaking. With the changing scene in America's earthquake threat (Petersen et al. 2016), a new option has emerged: hazard mitigation.

I summarize current options and techniques mitigating induced earthquake hazard, spanning operational changes, thresholds to limit felt earthquakes, community outreach, and legislation (which I cover in detail). All of these lead to the conclusion that taking mitigating actions quickly is critical to their success, as well as the need to tailor strategies to meet the specific needs of each community. However, baseline requirements should be in place; perhaps minimum national standards should be enacted for operations to continue (such as required seismic monitoring and data reporting).

I develop a toolkit for decision-making, where scientific data and analysis provide the means for induced earthquake hazard mitigation and risk reduction. Using the methods outlined in Chapters

2 and 3, I demonstrate how the probability of a magnitude of concern over a specified time period can be established. Using simple information derived from an earthquake catalog, I have demonstrated that one can define confidence bounds of likely future earthquake behavior (e.g. equations 2.5, 2.6 and 4.1; Figures 2.7 and 2.8; Sections 2.3 and 4.6.4.). These are powerful tools to have in ones arsenal when decisions need to be made about operational continuity or to evaluate mitigating actions. The scientific tools and risk management framework presented in this work allow more information to be gained, effectively reducing the uncertainty in a decision. Some uncertainty is inherent, some reducible with improved data, but it is useful to assess the scale of the inherent uncertainty.

5.4 References cited

Brodsky, E. and L. Lajoie, 2013, Anthropogenic Seismicity Rates and Operational Parameters at the Salton Sea Geothermal Field. Science, vol. 341, p. 543-546.

Keranen, K.M., H.M. Savage, G.A. Abers, and E.S. Cochran, 2013, Potentially induced earthquakes in Oklahoma, USA: Links between wastewater injection and the 2011 M_w 5.7 earthquake sequence, Geology, doi: 10.1130/G34045.1.

Petersen, M.D., C.S. Mueller, M.P. Moschetti, S.M. Hoover, A.L. Llenos, W.L. Ellsworth, A.J. Michael, J.L. Rubinstein, A.F. McGarr, and K.S. Rukstales, 2016, 2016 One-year seismic hazard forecast for the Central and Eastern United States from induced and natural earthquakes: U.S. Geological Survey Open-File Report 2016–1035, 52 p., http://dx.doi.org/10.3133/ofr20161035.

McGarr, A., 2014, Maximum magnitude earthquakes induced by fluid injection, J. Geophys. Res.: Solid Earth, vol. 119. 12pp.